Passage Effects in Paramagnetic Resonance Experiments

By M. WEGER

(Manuscript received February 16, 1960)

An attempt is made to classify theoretically paramagnetic resonance signals of inhomogeneously broadened lines occurring under various experimental conditions. The theoretical predictions are checked experimentally. Special emphasis is given to cases in which T_1 is long, and to cases in which the adiabatic condition $\gamma H_1^2 \gg dH/dt$ is violated.

TABLE OF CONTENTS

I. Introduction 1014
II. Some Symmetry Properties of the Bloch Equations 1015
III. Symmetry Properties of Some Systems Not Obeying the Bloch Equations 1020
IV. Approximate Expressions for χ' and χ'', and for the Loss of Magnetization for a Single Spin Packet 1028
V. Approximate Expressions for χ' and χ'' for an Inhomogeneously Broadened Lines 1030
VI. The Various Passage Cases — Detailed Discussion 1031
6.1 Case 1 — Slow Passage 1033
6.2 Case 2 — Rapid Adiabatic Passage with a Long Time Between Consecutive Field Modulation Cycles 1035
6.3 Case 3 — Rapid Passage with a Long Time Between Consecutive Field Modulation Cycles, the Adiabatic Condition Being Slightly Violated 1040
6.4 Case 4 — Rapid Nonadiabatic Passage with a Long Time Between Consecutive Field Modulation Cycles 1047
6.5 Case 5 — Rapid Adiabatic Passage with a Short Time Between Consecutive Field Modulation Cycles and Very Rapid Field Sweep 1048
6.6 Case 6 — Rapid Adiabatic Passage with a Short Time Between Consecutive Field Modulation Cycles, the Magnetization of the Spin Packets Being Partly Destroyed 1052
6.7 Case 7 — Rapid Adiabatic Passage with a Short Time Between Consecutive Field Modulation Cycles — the Stationary Case 1056
6.8 Case 8 — Rapid Adiabatic Passage with a Short Time Between Consecutive Field Modulation Cycles, the Magnetization of the Spin Packets Being Completely Destroyed 1060
6.9 Case 9 — Rapid Nonadiabatic Passage with a Short Time Between Consecutive Field Modulation Cycles and Very Rapid Field Sweep 1063
6.10 Case 10 — Rapid Nonadiabatic Passage with a Short Time Between Consecutive Field Modulation Cycles — the Stationary Case 1064

6.11 Case 11 — Rapid Nonadiabatic Passage with a Short Time Beween Consecutive Field Modulation Cycles, the Magnetization of the Spin Packets Being Completely Destroyed 1067
6.12 Conditions to Maximize Signal 1070
VII. The Various Passage Cases — Diagrammatic Representations and Additional Experimental Points 1072
VIII. Conclusion 1078
IX. Acknowledgments 1081
X. Notation 1081
Appendix A. χ' and χ'' for a Single Spin Packet, for Long Relaxation Times 1083
Appendix B. χ' and χ'' for an Almost Sudden Passage of an Inhomogeneously Broadened Line, Employing a System with a Bandwidth Narrow Compared with the Line Width 1091
Appendix C. χ' and χ'' for a Nonadiabatic Passage, Nonuniform Rate of Sweep 1096
Appendix D. Superposition of Adiabatic Fast Passage Lines 1103
Appendix E. Second-Order Effects Occurring When a Bridge Is Tuned to Observe χ' or χ'' Signals 1107
Appendix F. A Particular χ' Trace Observed at High Powers 1111
References 1112

I. INTRODUCTION

Shapes of electron spin resonance (ESR) and nuclear magnetic resonance signals, observed under various conditions, have previously been predicted theoretically and confirmed experimentally for a few cases.[1-5]

The purpose of this work is as follows:

i. To understand and predict the shapes of observed traces, as an aim in itself.

ii. To use the shapes of the traces to gain some understanding about the local fields in the sample, mainly to understand to what extent the fields can be considered static, and to what extent they must be considered as dynamic (namely, responsible for forbidden lines, etc.).

iii. To determine various conditions under which the resulting traces may cause misleading determinations of line shapes, relaxation times, etc.

iv. To distinguish true "physical" effects from spurious "passage effects" (like splitting of lines).

The work was performed on single crystals of phosphorus-doped silicon, containing about 1.7×10^{16} donors per cm, at temperatures of 10°, 4.2° and 1.2°K. The ESR line due to the donors was observed at about 9300 mc, employing a standard superheterodyne microwave spectrometer,[6] under various experimental conditions. (Mainly various rates and periods of the modulating magnetic field, and various microwave power levels.) Various traces were predicted theoretically and observed experimentally (or vice versa). No attempt was made to measure the intensities of signals absolutely.

The shapes of the traces under various experimental conditions were predicted theoretically by Portis.[5] It was originally attempted to con-

firm those predictions, but it was soon realized that some additional experimental factors must be taken into account — such as the loss of magnetization during adiabatic fast passage or nonadiabatic conditions. However, the basic results of Portis have been confirmed experimentally.

This work does not attempt to be complete or rigorous, but rather to point out some of the most salient effects of various experimental conditions upon observed electron spin resonance lines.

II. SOME SYMMETRY PROPERTIES OF SYSTEMS OBEYING THE BLOCH EQUATIONS

Some spin systems obey the Bloch equations,[1] which in the rotating frame are:

$$\frac{dS_x}{dt} + \frac{S_x}{T_2} - \gamma H_1 \delta S_y = 0,$$

$$\frac{dS_y}{dt} + \frac{S_y}{T_2} + \gamma H_1 \delta S_x - \gamma H_1 S_z = 0,$$

$$\frac{dS_z}{dt} + \frac{S_z}{T_1} + \gamma H_1 S_y = \frac{S_0}{T_1},$$

where S_x, S_y, S_z are the components of the magnetization in a coordinate system, rotating about an externally applied magnetic field H, with S_z being parallel to H. The angular frequency of this rotation is ω. In these equations, $\delta = (H - H_0)/H_1$, where H_0 is the magnetic field at which the system rotates at an angular frequency ω, and H_1 is the magnetic field along S_x, in the rotating frame; $\gamma = \omega/H_0$ is the gyromagnetic ratio of the spin system ($\gamma \approx 1.7 \times 10^7$ rad/sec/gauss for electrons); and T_1 and T_2 are constants known as relaxation times. Let

$$\chi' \equiv \frac{S_x}{2H_1}, \qquad \chi'' \equiv \frac{S_y}{2H_1}.$$

In this work, it will be assumed that the spin systems considered obey the Bloch equations (these will be called "homogeneously broadened lines" or "spin packets"), or consist of noninteracting subsystems that obey the Bloch equations (these are called "inhomogeneously broadened lines"), unless the contrary is explicitly stated.

The behavior of systems obeying the Bloch equations under the transformation $\delta \rightarrow -\delta$; $(dH/dt \rightarrow -dH/dt)$ has been discussed by Jacobsohn and Wangness.[3] The considerations are as follows:

$$\text{If } \delta \rightarrow -\delta, \qquad S_x \rightarrow -S_x, \qquad S_y \rightarrow S_y, \qquad S_z \rightarrow S_z,$$

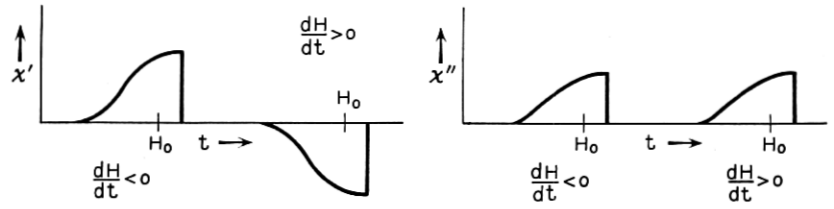

Fig. 1 — Symbolic indication of the parities of χ' and χ'' signals of systems obeying the Bloch equations. Under $dH/dt \rightarrow -dH/dt$, we have: $\chi'(H - H_0) \rightarrow -\chi'(H_0 - H)$; $\chi''(H - H_0) \rightarrow \chi''(H_0 - H)$.

the Bloch equations remain invariant. Therefore, if we start sweeping the magnetic field from an equilibrium state ($S_z = S_0$) not on the line, towards the line, if we reverse the direction of sweep, χ' changes sign, ($\chi' = S_x/2H_1$; $S_x \rightarrow -S_x$), while χ'' does *not* change its sign (since $S_y \rightarrow S_y$, $\chi'' = S_y/2H_1$ — see Fig. 1).

The change in sign of χ' is well known in the "slow passage"† and "adiabatic rapid passage"† cases [see Figs. 2(a) and 2(b)]. The lack of change of sign of χ'' is also well known in the "slow passage" case [see Fig. 2(c).] Actually, if χ'' did change sign, it would mean that power could be extracted from the system.

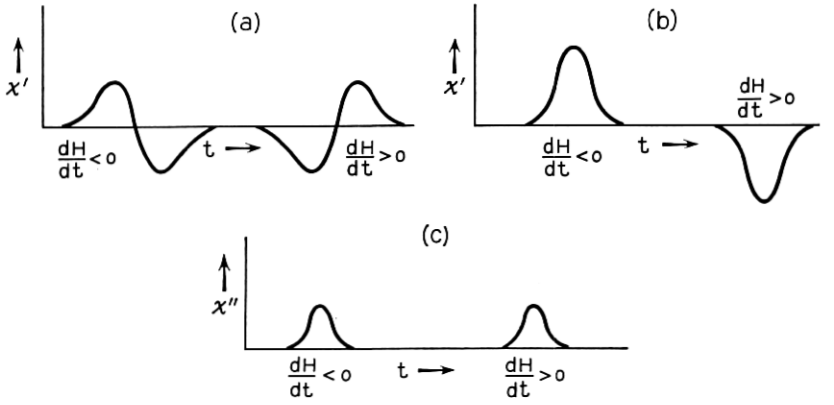

Fig. 2 — The most commonly observed χ' signals of systems obeying the Bloch equations, for (a) slow passage and (b) rapid passage; note the symmetry under $dH/dt \rightarrow -dH/dt$. (c) The most commonly observed χ'' signals of a system obeying the Bloch equations, slow passage.

† The "slow passage" and "adiabatic rapid passage" cases are discussed by Bloch.[1] In the slow passage case, $\dot{\delta} \ll 1/\sqrt{T_1T_2}$, and in the adiabatic rapid passage case, $\dot{\delta} \gg 1/\sqrt{T_1T_2}$, $\gamma H_1 \gg \dot{\delta}$.)

If the χ' and χ'' signals are observed by means of a phase sensitive detector employing magnetic field modulation (Bloch[1]), the symmetry property will be just reversed. This occurs because the magnetic field H is given by

$$H = H_0 + \left(\frac{dH}{dt}\right)_0 t + H_m \cos \omega_m t,$$

where H_0, $(dH/dt)_0$, H_m and ω_m are constants, known as dc field, sweep rate, modulating field and modulation angular frequency, respectively.

Under the transformation $\delta \rightarrow -\delta$,

$$H \rightarrow H_0 - \left(\frac{dH}{dt}\right)_0 t - H_m \cos \omega_m t.$$

The phase of the modulating field with respect to the reference signal $\cos \omega_m t$ is inverted. Thus, if we start sweeping from a relaxed state, the sign of the component of χ' at the modulating frequency (relative to the reference voltage), is the *same* for sweeping in both directions, while the sign of χ'' is reversed.†

$$\text{If } \delta \rightarrow -\delta, \qquad S_x \rightarrow S_x, \qquad S_y \rightarrow -S_y, \qquad S_z \rightarrow -S_z,$$

the Bloch equations also remain invariant.

Thus, if S_z is *inverted* during the passage, on returning, χ' will maintain its sign and χ'' will reverse it.

The opposite sign of χ'' (emission) is not absurd, since the level populations have been inverted and we may have a "maser" effect.

Again, with a phase-sensitive detector (PSD), χ' will invert its sign and χ'' will maintain its sign. For some typical traces, see Figs. 3 and 4. (Some of these shapes will be discussed in more detail later.) Table I shows the parity of χ' and χ'' signals, summarizing these results for systems obeying the Bloch equations.

The preceding symmetry properties apply to both homogeneously and inhomogeneously broadened lines. This point deserves further comment. There is no reason why an assembly of noninteracting subsystems must possess any kind of symmetry under a transformation affecting the magnetic field. There need not be any correlation between subsystems resonating at different magnetic fields. However, often a system con-

† Note that, if the second harmonic signal is observed by applying the second harmonic of the field modulation signal as reference to the phase sensitive detector, then inverting the sign of the field modulation voltage will *not* change the sign of the second harmonic reference voltage. Thus, under the above transformation, the second harmonic signal of χ' is reversed, while that of χ'' is not. The same applies to all even harmonics. The odd ones behave like the fundamental.

sists of "almost" identical subsystems, differing only in the distribution of local magnetic fields. The magnetic fields at which such systems resonate, (at a given frequency) are usually distributed symmetrically about some center. In that case, the symmetry properties just discussed are retained. Therefore, if the observed signals do *not* possess a definite parity, this must be due to one of the following four causes:

Systems *obeying* the Bloch equations, or consisting of noninteracting subsystems obeying them, may possess

i. an asymmetrical envelope of an inhomogeneously broadened line;

ii. partial relaxation between the times the line is traversed in opposite directions (neither $S_z \rightarrow S_z$ nor $S_z \rightarrow -S_z$);

iii. bad experimental adjustment of the equipment — for instance, a mixture of χ' and χ'' signals. (Note that, if the signals are not small, the

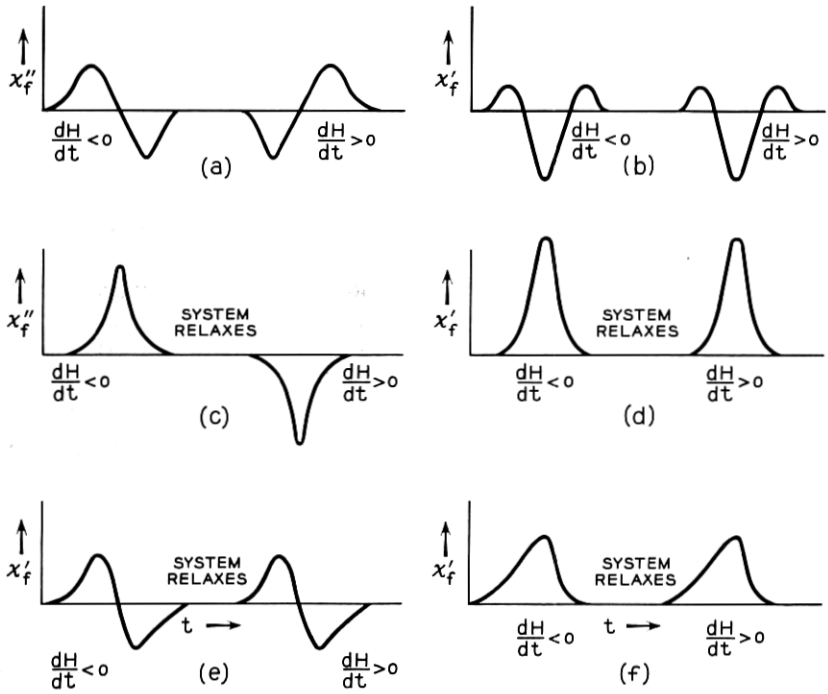

Fig. 3 — Typical traces observed when field modulation and a phase sensitive detector is used: (a) χ''_f, slow passage; (b) χ'_f, slow passage; (c) χ''_f, rapid (non-adiabatic) passage; (d) χ'_f, rapid (adiabatic) passage; (e) χ'_f, rapid passage, very fast weep; (f) χ'_f, a line with spin diffusion (a system *not* obeying the Bloch equations). Note the symmetry under $dH/dt \rightarrow -dH/dt$.

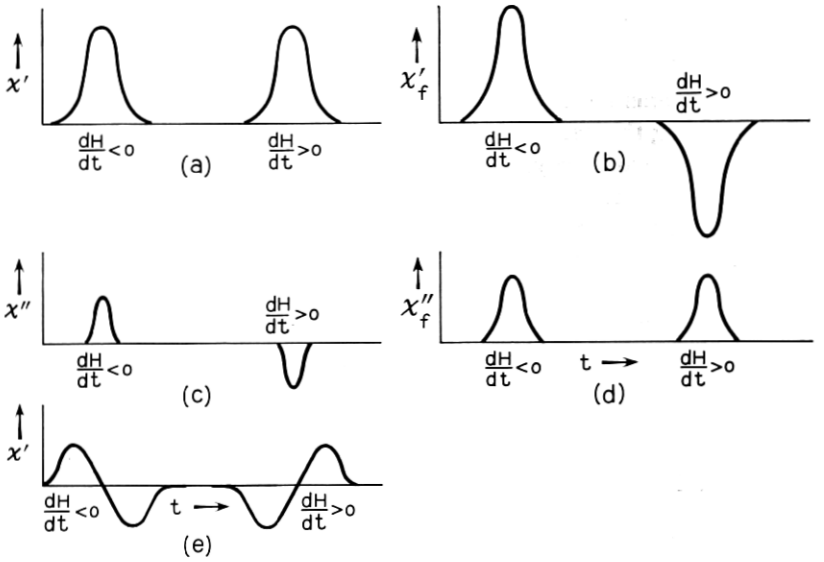

Fig. 4 — Some typical traces observed when the system does *not* relax between consecutive sweeps: (a) χ', *no* phase sensitive detector; (b) χ', *with* P.S.D.; (c) χ'', *no* P.S.D. (rapid, not perfectly adiabatic, passage); (d) χ'', *with* P.S.D.; (e) χ', *with* P.S.D., very rapid sweep. Again, notice the symmetry properties which are *different* from those occurring when the system relaxes between sweeps.

first order bridge theory does not apply; this point will be discussed in Appendix E.)

Systems *not* obeying the Bloch equations may possess

iv. A "genuine" asymmetry.

Some systems of this kind will be discussed in the next section.

TABLE I — PARITY OF χ' AND χ'' SIGNALS UNDER THE TRANSFORMATION $\dfrac{dH_0}{dt} \rightarrow -\dfrac{dH_0}{dt}$

		Direct Signal (and Even Harmonics)	Signal as Detected by Phase Sensitive Detector (and Odd Harmonics)
χ'	System relaxes (between sweeps)	−	+
	System does not relax (between sweeps); adiabatic conditions	+	−
χ''	System relaxes (between sweeps)	+	−
	System does not relax (between sweeps); adiabatic conditions	−	+

III. SYMMETRY PROPERTIES OF SOME SYSTEMS NOT OBEYING THE BLOCH EQUATIONS

Many systems not satisfying the Bloch equations, will still yield signals possessing the parities indicated in Section II.

If H_1 is not small, say, $\gamma H_1 > T_2$, then S_x and S_y relax at different rates; thus, we have two T_2's: The S_y relaxation time T_2 (which equals the zero power T_2) and the S_x relaxation time T_{2e}, which is longer (see Redfield[7]). It is, however, immediately seen that the parities are unaffected by this generalization.

The conditions under which the Bloch equations apply have been discussed by Wangness and Bloch.[8] In essence, they are:

i. The effect of all other spins upon a given spin is equivalent to that of a "bath," in thermodynamical equilibrium.

ii. The "bath" does not heat up.

iii. γH_1, $1/T_1$, $1/T_2 \ll \gamma H_0$, ω^*, where ω^* is the frequency of the local field variations (roughly).

iv. The spin-bath interaction can be expanded in multipoles.

v. Either $s = \frac{1}{2}$,
or $s = 1$, $kT \gg \hbar\omega_0$;
or $s > 1$, $eqQ \ll \hbar\omega_0$;
or $s > 1$, $\omega^* > \omega$, isotropic interaction
(eqQ is the quadrupole interaction).

3.1 *Cross Saturation Within a Line*

Often a line is neither homogeneously broadened nor inhomogeneously broadened, but rather something intermediate: the system consists of subsystems which obey the Bloch equations, except for a (not too strong) interaction among them. Such systems have been discussed by Bloembergen *et al.*[9] Often it may be possible to describe the cross relaxation by means of a diffusion equation like

$$\frac{\partial S_z(H)}{\partial t} = \text{constant} \times \frac{\partial^2 S_z(H)}{\partial H^2},$$

which is linear in S_z and invariant under $H \rightarrow -H$, and thus does not perturb the parity.†

Therefore, one would not expect cross relaxation to destroy the symmetry properties of χ' and χ'' discussed in the preceding section.

† Bloembergen's rate equations are nonlinear, but homogeneous in the occupation numbers (for an n-spin flip), and, for an inhomogeneously broadened line with a symmetrical envelope, they are invariant under $\delta \rightarrow -\delta$. Therefore, the above mentioned parity is maintained.

3.2 *Forbidden Lines*

In a line with cross relaxation, we have diffusion of excitation from one part of the line to the other, which is not explicitly dependent upon the intensity of the microwave magnetic field. In some cases, the rate of diffusion will depend strongly upon the intensity of the applied microwave field, in which case we may say that we have "forbidden lines." One might be tempted to describe such a process with the aid of an equation like

$$\frac{\partial S_z(H)}{\partial t} = \sum_{\delta H} a(\delta H, \gamma H_1)\,[S_z(H + \delta H) - S_z(H)].$$

However, as the following examples will show, this equation may often not describe the system even approximately. Therefore, this case seems to be more complicated and no general discussion will be attempted. Instead, three special examples will be considered. (Another example is given by Bardeen, Slichter and Pines.[10])

3.3 *Example 1*

Consider a system consisting of pairs of electrons and (spin $\frac{1}{2}$) nuclei, with dipolar and contact interaction between them.

Let

s_e = spin of electron,
s_n = spin of nucleus,
μ_e = magnetic moment of electron,
μ_n = magnetic moment of nucleus,
H = magnetic field (in the z-direction),
a = contact interaction,
b = dipolar interaction,
r = electron-nucleus distance.

Then, the Hamiltonian of the system is

$$\mathcal{H} = \frac{\mu_e H s_{z_e}}{s_e} + \frac{\mu_n H s_{z_n}}{s_n} + a(\mathbf{s}_e \cdot \mathbf{s}_n) + b\left(\mathbf{s}_e \cdot \mathbf{s}_n - \frac{3(\mathbf{s}_e \cdot \mathbf{r})(\mathbf{s}_n \cdot \mathbf{r})}{r^2}\right).$$

Let the eigenfunctions of the electron spin corresponding to the eigenvalues $s_z = +\frac{1}{2}$, $s_z = -\frac{1}{2}$, be

$$\left|\uparrow\right> \text{ and } \left|\downarrow\right>,$$

respectively, and those of the nucleus be $|\uparrow>, |\downarrow>$. Then, to the

zeroth order (for $\mu_e H \gg \mu_n H$, a, b), the eigenfunctions of the combined system are

$$\left|\uparrow\uparrow\right>, \quad \left|\uparrow\downarrow\right>, \quad \left|\downarrow\uparrow\right>, \quad \left|\downarrow\downarrow\right>.$$

The energy level diagram is shown in Figs. 5 and 6. Under a variable magnetic field H_1 perpendicular to H, the transitions

$$\left|\uparrow\uparrow\right> \leftrightarrow \left|\downarrow\uparrow\right> \text{ ("line 1")}$$

and

$$\left|\uparrow\downarrow\right> \leftrightarrow \left|\downarrow\downarrow\right> \text{ ("line 2")}$$

are "allowed", i.e., occur even for $a = b = 0$; while the transitions

$$\left|\uparrow\uparrow\right> \leftrightarrow \left|\downarrow\downarrow\right> \text{ ("line 3")}$$

and

$$\left|\uparrow\downarrow\right> \leftrightarrow \left|\downarrow\uparrow\right> \text{ ("line 4")}$$

are forbidden, i.e., occur only if $b \neq 0$. Both forbidden lines need not be of the same intensity. Assume temporarily, for the sake of the argument, that line 4 is strictly forbidden, while line 3 is only partly forbidden.

The populations of the levels at thermal equilibrium will be, approximately $1 + \epsilon$ for

$$\left|\downarrow\downarrow\right> \text{ and } \left|\downarrow\uparrow\right>,$$

and $1 - \epsilon$ for

$$\left|\uparrow\uparrow\right>, \quad \left|\uparrow\downarrow\right>,$$

where $\epsilon = \mu_e H/kT$.

If we sweep from a *low* magnetic field, increasing it, line 3 will be swept first, inverting the populations of the corresponding levels (for adiabatic rapid passage). Then, if no relaxation takes place during the sweep, no more lines will be observed, since for lines 1 and 2, the populations of the "upper" and "lower" levels are equal.

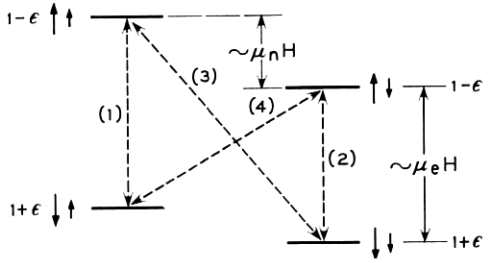

Fig. 5 — Energy-level diagram of an electron-nucleus system in a magnetic field (the nuclear spin is supposed to be $\frac{1}{2}$). Lines (1) and (2) are "allowed," while lines (3), (4) are "forbidden," but not strictly.

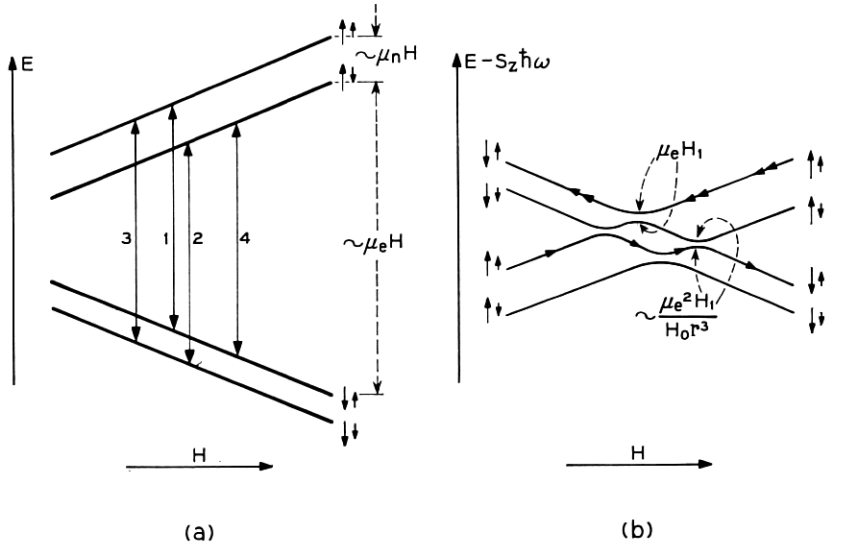

Fig. 6 — The energy levels of an electron and spin half nucleus, as function of the magnetic field for (a) fixed frame and (b) rotating frame. The different behavior of a system in the state $|\uparrow\uparrow>$ under $dH/dt > 0$ and $dH/dt < 0$ can be seen.

If we sweep from a *high* magnetic field, decreasing it, lines 1 and 2 are swept first, yielding signals, and line 3 will then yield a signal too, but of opposite sign, since the populations of its corresponding levels are inverted. Thus, we obtain the signals indicated in Fig. 7.

Obviously, the signals do *not* possess the parity discussed in Section II. Note that an essential assumption for this argument was, that the intensities of lines 3 and 4 are considerably different. An actual calcula-

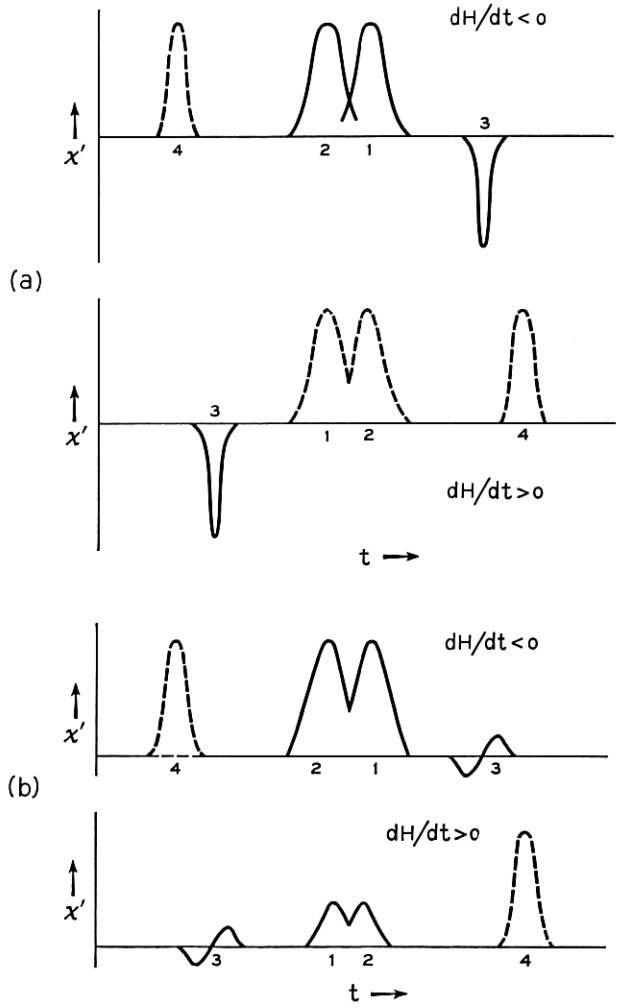

Fig. 7 — (a) The χ' signal expected from the system with energy levels shown in Fig. 5 when *all* transitions (including those of the forbidden lines), are adiabatic; line 4 is assumed to be *strictly* forbidden, while line 3 is not; there is *no* simple symmetry under $dH/dt \rightarrow -dH/dt$. (b) The χ' signal from the system with the energy level diagram shown in Fig. 5, when line 3 is *not* passed adiabatically.

tion indicates, however, that while the lines themselves are of order $[b/(\mu_n H)]^2$ weaker than the allowed ones, the difference between their intensities is of order $[ab/(\mu_e H)^2]^2$, i.e., $[a/(\mu_e H)]^2(\mu_n/\mu_e)^2$ times *less*. Therefore, for all practical purposes this asymmetry may be ignored.

Note that, for $b = 0$ and a microwave field *parallel* to the dc magnetic

field, line 3 is strictly forbidden, while line 4 is not. But line 4 is weak — of order $a^2/(\mu_e H)^2$ weaker than the allowed lines.

3.4 *Example 2*†

Consider a system of pairs of electrons resonating at slightly different frequencies $\omega \pm \Delta\omega$, due to different local fields, with an exchange interaction J between them. Let the eigenfunctions of each electron corresponding to the eigenvalues $m_s = +\frac{1}{2}$, $m_s = -\frac{1}{2}$, be $|\uparrow>$, $|\downarrow>$, respectively. Let $J > \Delta\omega$, $\gamma H_1 > \Delta\omega^2/J$. Then the eigenfunctions of the two-electron system are approximately $|\uparrow\uparrow>$, $|\downarrow\downarrow>$, $|\uparrow\downarrow> + |\downarrow\uparrow>$, $|\uparrow\downarrow> - |\downarrow\uparrow>$; and the energy levels of the system as functions of the magnetic field, in the fixed and rotating frames are shown in Fig. 8.

Assume the system to be at zero temperature. Then, if all passages are adiabatic, the χ' signal is shown in Fig. 9.

The central line will be seen only when we start from $H < H_0$ (or $H > H_0$, depending upon the sign of the exchange integral), with $H_0 = \omega/\gamma$.

Note the following points:

i. The "forbidden" lines at $\omega \pm J/\hbar$ are due to a mixture of the singlet and triplet $S_z = 0$ levels by the difference in local fields at the

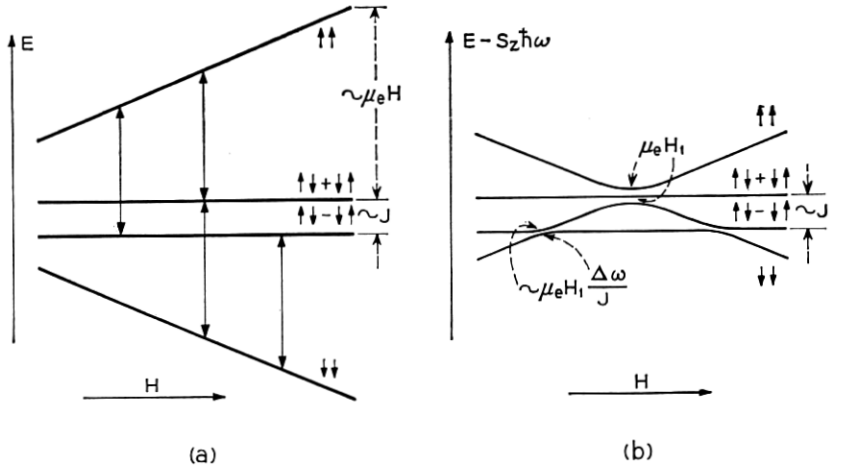

Fig. 8 — Energy levels of a system of two electrons, with a difference in hyperfine interactions of $\hbar\Delta\omega$, and an exchange integral J *strong* compared with the difference in hyperfine interactions: (a) energy levels in a fixed frame; (b) energy levels in a rotating frame. Again, an asymmetry in behavior under $dH/dt < 0$ and $dH/dt > 0$ is expected.

† This system has been treated in detail by P. W. Anderson (private communication).

two sites of the electrons. Therefore, their "intensity" will be reduced (relative to the "allowed" line) by about $(\hbar\Delta\omega/J)^2$. Thus, if $J \gg \hbar\omega$, they are not observed. A similar argument holds for $J \ll \hbar\Delta\omega$.

Thus, only electrons with an exchange interaction satisfying $J \approx \hbar\Delta\omega$ will give rise to the above phenomenon. The exchange interaction depends critically upon the distance between the electrons, thus only electrons at a "critical" distance apart may cause this asymmetry. The probability of finding electrons at this critical distance, in a physically diluted system, may be quite small.

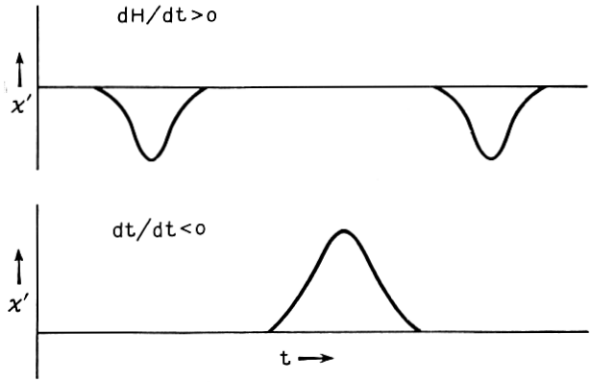

Fig. 9 — Signals expected from the system described in Fig. 8, when the sense of sweep is reversed.

ii. Closer examination of the amplitude of the central line under the various conditions, shows that for $\hbar\omega < kT$, the asymmetry is of order $(\hbar\omega/kT)^2$, not $\hbar\omega/kT$.

Therefore, the above effect is probably of little significance, experimentally.†

3.5 *Example 3*

Consider a system consisting of more than two (nonequidistant) levels, spin *one* particles possessing a quadrupole moment, in a solid. Let the quadrupolar interaction e^2qQ be small compared with μH. Then, the relative populations of the energy levels $S_z = -1$, $S_z = 0$, $S_z = 1$ are approximately $e^{\mu H/kT}$, 1 and $e^{-\mu H/kT}$, respectively. For *positive* eqQ and μ sweeping the magnetic field upward, the intensity of the first line

† However, this effect has been observed experimentally in a phosphorus doped silicon crystal, with impurity concentration of 6.5×10^{16} atoms/cm^3, at 1.2°K.

is proportional to $e^{\mu H/kT} - 1$, and that of the second† to $e^{\mu H/kT} - e^{-\mu H/kT}$, for adiabatic rapid passages neglecting relaxation.

Sweeping downwards, the intensities are $1 - e^{-\mu H/kT}$ and $e^{\mu H/kT} - e^{-\mu H/kT}$, respectively. For $\mu H/kT < 1$, the intensities are, approximately

$$\frac{\mu H}{kT} + \tfrac{1}{2}\left(\frac{\mu H}{kT}\right)^2, \qquad \frac{2\mu H}{kT} \qquad \text{going upwards}$$

and

$$\frac{\mu H}{kT} - \tfrac{1}{2}\left(\frac{\mu H}{kT}\right)^2, \qquad \frac{2\mu H}{kT} \qquad \text{going downwards}$$

indicating an asymmetry of order $(\mu H/kT)^2$.

From the above examples we may conclude that, although it may not be possible to prove the existence of a definite parity of ESR signals under the most general conditions, most physical systems seem to possess it, at least to a good approximation, even if they do not satisfy the the Bloch equations.

We also see the role played by the various conditions given by Bloch, as listed at the beginning of Section III:

i. The possibility of replacing all the interactions of a spin with its surroundings, by a "bath," is necessary, as shown by Examples 1 and 2.

ii. The assumption of a constant bath temperature is probably unnecessary. Heating up of the bath will tend to reduce the signal from those parts of the line swept later, compared to that due to those parts of the line swept earlier. This destroys the symmetry of the line about its center (if it existed in the first place), but not the parity discussed in Section II.

iii. We must have γH_1, $1/T_1$, $1/T_2 \ll \gamma H_0$ in order to observe resonance at all (and, for wide lines, differences in the Boltzman factor at various parts of the line cannot be neglected).

iv. It seems to be always possible to expand the interactions in multipoles. If it is not, the spin system may be broken down to subsystems that do satisfy this condition. These may be interacting, but then i is violated. (For instance, the system of electrons with exchange interaction discussed in ii, may be considered as a system of "singlets" and "triplets," the interaction of which with their environment cannot be expanded in multipoles.)

v. Equidistant levels or a high temperature are necessary, as shown by Example 3.

† Since the population of the level $S_z = 0$ has been changed from "1" to $e^{\mu H/kT}$ by the adiabatic rapid passage through the line $S_z = 1 \leftrightarrow S_z = 0$.

IV. APPROXIMATE EXPRESSIONS FOR χ' AND χ'', AND FOR THE LOSS OF MAGNETIZATION FOR A SINGLE SPIN PACKET

Solutions of the Bloch equations for long relaxation times have been given by Jacobsohn and Wangness[3] and Salpeter.[4]

For an almost sudden transition $\gamma H_1^2 \ll dH/dt$ with constant dH/dt we have, according to Salpeter, for $dH/dt > 0$

$$\chi'(t) = \frac{H_0}{2H_1}\sqrt{\frac{2\gamma H_1^2}{dH/dt}}\,\chi_0 \operatorname{Im}\left[e^{i\gamma(dH/dt)(t^2/2)}\int_{-\infty}^{\sqrt{\frac{\gamma(dH/dt)}{2}}t} e^{-iw^2}\,d\omega\right],$$

$$\chi''(t) = \frac{H_0}{2H_1}\sqrt{\frac{2\gamma H_1^2}{dH/dt}}\,\chi_0 \operatorname{Re}\left[e^{i\gamma(dH/dt)(t^2/2)}\int_{-\infty}^{\sqrt{\frac{\gamma(dH/dt)}{2}}t} e^{-iw^2}\,d\omega\right]$$

For $dH/dt < 0$, χ' inverts sign and χ'' does not. It is assumed that, at $t = 0, H = H_0$ where $\gamma H_0 = \omega$. The loss of magnetization during an almost sudden transition is

$$\frac{\pi\gamma H_1^2}{|dH/dt|}\,|S|.$$

This solution, like the Bloch equations themselves, applies to a single spin packet (or, a homogeneously broadened line). This solution corresponds to the magnetization vector **S** moving on the surface of a sphere, starting from the "north pole," and eventually precessing around it in a circle of radius

$$\sqrt{\frac{2\pi\gamma H_1^2}{dH/dt}}\,|S|.$$

(See A in Fig. 10.) We have three physically distinct regions:

I. $\frac{1}{H_1}\frac{dH}{dt}t \ll 0$ ("before" resonance)†;

II. $\frac{1}{H_1}\frac{dH}{dt}t \approx 0$ ("on" resonance);

III. $\frac{1}{H_1}\frac{dH}{dt}t \gg 0$ ("after" resonance).

In region I, we have small χ' and χ'' signals, of the microwave frequency (approximately); χ'' is considerably smaller than χ'.

In region II, the signals are still of about the microwave frequency, and large; χ' and χ'' are of about the same strength.

† See Fig. 4 of Ref. 4.

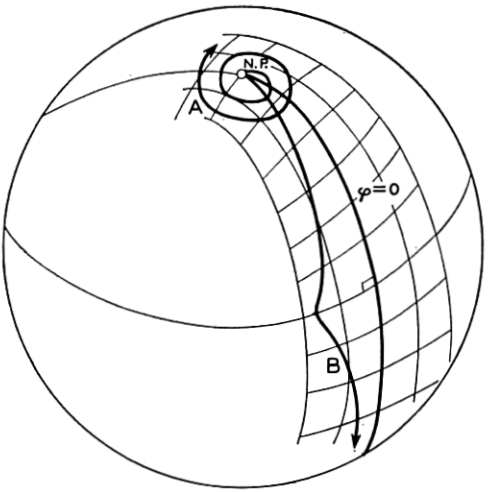

Fig. 10 — Locus of the magnetization vector for almost sudden (A) and almost adiabatic, (B), transitions for infinite relaxation times. (N.P. = North pole; φ = the polar angle.)

In region III, the signals are at a frequency γH, which is *not* the applied microwave frequency. These signals beat with the applied microwave frequency to produce "wiggles."

For an almost adiabatic transition ($\gamma H_1^2 > dH/dt$), we have (again, see Salpeter[4]):

$$\chi' = \pm \frac{1}{\sqrt{1 + \left(\frac{H - H_0}{H_1}\right)^2}} \chi_0 \frac{H_0}{2H_1},$$

$$\chi'' = + \frac{1}{\left[1 + \left(\frac{H - H_0}{H_1}\right)^2\right]^{\frac{1}{2}}} \frac{|dH/dt|}{\gamma H_1^2} \chi_0 \frac{H_0}{2H_1},$$

and the loss of magnetization due to nonadiabaticity is about (see Zener[13]):

$$\exp\left(-\frac{\pi \gamma H_1^2}{|dH/dt|}\right) |S|.$$

Again, this last solution applies to a single spin packet, or a homogeneously broadened line. The loss of magnetization at different values of $\gamma H_1^2/(dH/dt)$ is illustrated roughly in Fig. 11.

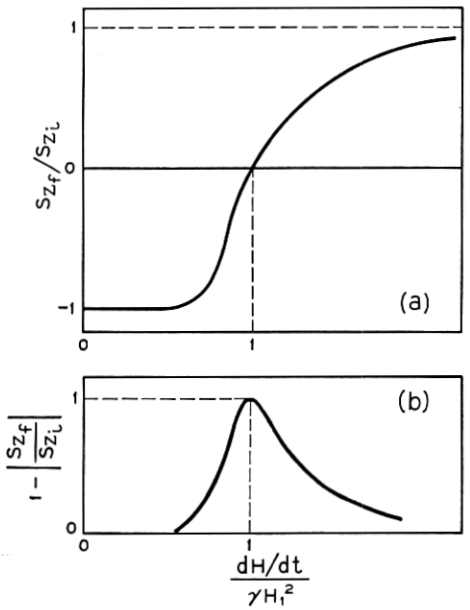

Fig. 11 — Loss of magnetization per passage due to nonadiabaticity (or nonsuddeness), qualitative only. In an adiabatic transition, $S_z \rightarrow -S_z$; in a sudden transition, $S_z \rightarrow S_z$; in both cases, there is no loss of $| S_z |$. In an intermediate transition, there is a loss in $| S_z |$; S_{z_i} and S_{z_f} are the initial and final values of S_z , respectively.

V. APPROXIMATE EXPRESSIONS FOR χ' AND χ'' FOR AN INHOMOGENEOUSLY BROADENED LINE

For an inhomogeneously broadened line for an almost sudden transition, under certain assumptions, χ' and χ'' are calculated in Appendix B. The results are

$$\chi'' = \frac{\pi}{2} H_0 \chi_0 h(H - H_0'),$$

$$\chi' = \tfrac{1}{2} H_0 \chi_0 \frac{dh(H - H_0')}{dH} \Delta H,$$

where $h(H - H_0')$ is the line shape [$\int h(H - H_0')dH = 1$]. These signals are the same as in the nonsaturated case [see Figs. 2(a) and 2(c), and also Fig. 12].

Physically, $S_z \approx S_0$ in *both* the nonsaturated and almost sudden cases. The difference between them is that, in the nonsaturated case,

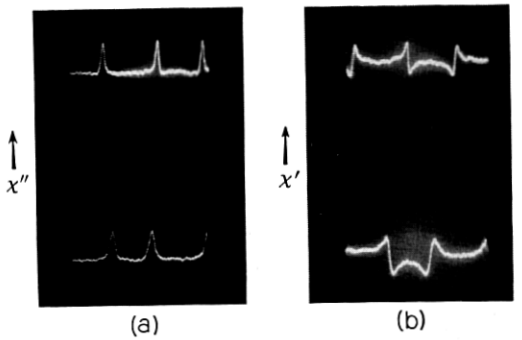

Fig. 12 — (a) χ'' signal of an almost sudden ($dH/dt \gg \gamma H_1^2$) transition of an inhomogeneously broadened line. Although the relaxation times are long, the line behaves as if it were completely relaxed. Data: $H_1 \approx 1/300$ gauss; $T = 1.2°K$ $T_1 \approx 300$ seconds); top trace, $dH/dt \cong 300{,}000$ gauss/second; bottom trace, $dH/dt \cong 100{,}000$ gauss/second. (b) χ' signal of an almost sudden transition, under the same conditions; again, the signal appears unsaturated, although $\gamma H_1 T_1 \approx 10^7$.

the definite phases relationships of the wave function (nondiagonal elements of the density matrix) are destroyed immediately by the relaxation process. In the "almost sudden" case, the relaxation times are long compared with the time in which the line is swept through; thus, these relaxation processes are less effective in destroying the phase relationships. However, the phases of different packets of the inhomogeneously broadened line, "cancel" each other, washing out the difference between it and the nonsaturated case. (However, see Appendix C.)

VI. THE VARIOUS PASSAGE CASES—DETAILED DISCUSSION

In this section, χ' and χ'' signals of an inhomogeneously broadened line will be discussed qualitatively and semiquantitatively. Various experimental conditions will be considered. The individual spin packets will be assumed to satisfy the Bloch equations approximately, and the loss of magnetization due to forbidden lines will be treated only phenomenologically.

The observed χ' and χ'' signals depend upon a variety of variables, which are listed at the end of this paper. To avoid lengthy repetitions, a shorthand notation will be used to describe some of the most frequently occurring relationships among the variables.

In this section, a magnetic field $H = H_0 + (dH_0/dt)t + H_m \cos \omega_m t$ will be postulated. The following terms signify the following relationships:

"Rapid": $\frac{H_1}{dH/dt} \ll \sqrt{T_1T_2}$†	The time each spin packet is swept through, is *short* compared with the mean relaxation time. We have rapid passage conditions, in the Bloch[1] sense.
"Fast": $\omega_m T_1 \gg 1$	The time between successive modulation cycles is *short* compared with T_1. Each spin packet does not relax considerably between successive modulation cycles.
"Slow": $\frac{H_1}{dH/dt} \gg \sqrt{T_1T_2}$	Not rapid, i.e., "slow passage" in the Bloch sense.
"Adiabatic": $\gamma H_1^2 \gg \frac{dH}{dt}$	The passage through the line is sufficiently slow, so that the magnetization vector **S** follows the effective magnetic field $\mathbf{H} - \boldsymbol{\omega}/\gamma + \mathbf{H}_1$ adiabatically (i.e., is parallel or antiparallel to it). Again, see Bloch.[1]
"Nonadiabatic": $\gamma H_1^2 \ll \frac{dH}{dt}$	The passage through the line is so rapid, that the magnetization vector **S** cannot follow the effective field, but stays almost parallel to the dc magnetic field.
"Burnt"	Most of the magnetization S has been destroyed ("burnt out") by the microwave field H_1.
"Stale"	Individual spin packets have reached a stationary state. The magnetization is an almost periodic function of time, with period $\omega_m/2\pi$.
"Fresh"	Most of the contribution to the signal comes from packets which have not yet been swept through many times.
"Scope Trace"	The signal at the output of the IF amplifier (or crystal detector, if no superheterodyne arrangement is used). This may be observed by an oscilloscope, or sometimes, a recorder.
"Recorder Trace"	The signal at the output of the phase sensitive detector.

† T_2 here, and in the following, is essentially T_{2e} of Redfield.[7] For perfect saturation it is approximately T_1. For imperfect saturation it is shorter. The situation $T_2 < H_1/(dH/dt) < \sqrt{T_1T_2}$ corresponds to neither slow nor rapid passage. For $\gamma H_1 T_2 > 1$, we have $T_{2e} \approx T_1$, while for $\gamma H_1 T_2 < 1$, the signal is very weak (under saturation conditions). Therefore, this situation is ignored here.

Only rough estimates of the amplitudes are given, mainly in order to indicate qualitatively the expected effect of variation of the experimental parameters. In general, it will be assumed that $H_1 < H_m$. This restriction, however, is not very severe. If it does not hold, the logarithmic dependence $\log (H_m/H_1)$ (if any) is replaced by a linear dependence H_m/H_1.

The discussion of this section is rather tedious; therefore, the results are summarized in Section VII.

6.1 *Case 1 — Slow Passage*

Physical Description

The time of passage through each individual spin packet, $t \approx H_1/\omega_m H_m$, is long compared with $\sqrt{T_1T_2}$. The system is in equilibrium at any moment.

This case has been treated by Portis,[5] ("Case I") and Portis.[11]

Conditions Under Which This Case Is Observed:

$$\frac{1}{\gamma H_1} \ll \sqrt{T_1T_2} \ll \frac{H_1}{\omega_m H_m}; \qquad H_m \ll \Delta H; \qquad \sqrt{T_1T_2} \ll \frac{H_1}{\omega_m \Delta H}.$$

Note that, for given $\omega_m \Delta H$ and a bounded H_1, this case may apply only for a narrow range of T_1 (if at all). Wider lines, and high modulation frequencies, are unfavorable for this case. [The condition $\sqrt{T_1T_2} \ll H_1/\omega_m \Delta H$ follows, from comparison of the amplitudes in this case, with those of case 2 in Section 6.2. If this condition does not hold, the signal due to the second case predominates.]

Traces and Amplitudes

For slow passage, the solution of the Bloch equation for a single spin packet is[1]

$$\chi' = \tfrac{1}{2}\chi_0 \omega T_2 \frac{(\omega - \omega_0)T_2}{1 + (\gamma H_1)^2 T_1 T_2 + (\omega - \omega_0)^2 T_2^2},$$

$$\chi'' = \tfrac{1}{2}\chi_0 \omega T_2 \frac{1}{1 + (\gamma H_1)^2 T_1 T_2 + (\omega - \omega_0)^2 T_2^2}.$$

Under saturation, $(\gamma H_1)^2 T_1 T_2 \gg 1$. Furthermore, $\omega - \omega_0 \ll \omega$. Thus

$$\chi' \cong \tfrac{1}{2}\chi_0 \omega \frac{\omega - \omega_0}{(\gamma H_1)^2 \dfrac{T_1}{T_2} + (\omega - \omega_0)^2},$$

$$\chi'' \cong \tfrac{1}{2}\chi_0 \frac{\omega}{(\gamma H_1)^2 T_1 + (\omega - \omega_0)^2 T_2}.$$

Now, consider an inhomogeneously broadened line, of shape $h(H - H_0')$ and width ΔH. If $H_1\sqrt{T_1/T_2} \ll \Delta H$, for most spin packets $(\omega - \omega_0)^2 \gg$

$(\gamma H_1)^2(T_1/T_2)$, and the packets for which $(\omega - \omega_0)^2 < \gamma^2 H_1^2(T_1/T_2)$, will give almost equal and opposite contributions to χ'. Then, for the whole line

$$\chi'(H) \approx \tfrac{1}{2}\chi_0 H_0 \int \frac{H - H_0}{H_1^2 \dfrac{T_1}{T_2} + (H - H_0)^2} h(H_0 - H_0')\, dH_0$$

$$\approx \tfrac{1}{2}\chi_0 H_0 \int \frac{1}{(H - H_0)} h(H_0 - H_0')\, dH_0$$

$$= -\chi_0 \int_0^\infty H h(H_0 - H_0') \frac{H_0\, dH_0}{H_0^2 - H^2}.$$

This expression has been given by Portis.[5] Note that the integral does not converge, and must be understood in the sense of its principal part. [The packets for which $(H - H_0)^2 < H_1^2(T_1/T_2)$ will tend to give equal and opposite contributions, which cancel.] For χ'', we cannot make this approximation, because the contributions from $(H - H_0)^2 < H_1^2(T_1/T_2)$ do not cancel, but add up. However, if $\Delta H^2 \gg (\gamma H_1)^2(T_1/T_2)$, $h(H_0 - H_0')$ can be assumed constant and withdrawn outside the integral (for χ' this approximation yields zero, and thus cannot be applied):

$$\chi'' = \frac{\tfrac{1}{2}\chi_0 H_0}{\gamma} \int \frac{h(H_0 - H_0')\, dH_0}{H_1^2 T_1 + (H_0 - H)^2 T_2}$$

$$\approx \frac{\tfrac{1}{2}\chi_0 H_0 h(H_0 - H_0')}{\gamma} \int \frac{dH_0}{H_1^2 T_1 + (H_0 - H)^2 T_2}$$

$$= \frac{\pi}{2} \chi_0 \omega \frac{1}{(\gamma H_1)\sqrt{T_1 T_2}} h(H_0 - H_0')$$

$$= \frac{\pi}{2} \chi_0 \frac{H_0}{H_1} \sqrt{\frac{1}{T_1 T_2}} \frac{h(H_0 - H_0')}{\gamma}.$$

When the field is modulated, $\Delta\chi' = (d\chi'/dH_0)H_m \cos \omega_m t$ for each packet, and signals of different packets must be superimposed:

$$\int \frac{d\chi'(H - H_0')}{dH} h(H_0' - H_0)\, dH_0$$

$$= \frac{d}{dH} \int \chi'(H - H_0) h(H_0' - H_0)\, dH_0$$

$$= \frac{d\chi'(H, H_0')}{dH}.$$

Thus, the recorder trace is proportional to the derivative of the line shape. For

$$h(H_0' - H_0) = \frac{1}{\sqrt{2\pi}\Delta H} e^{-(H_0'-H_0)^2/2\Delta H^2}$$

at the center of the line, the amplitude is

$$-\left(\frac{d\chi'}{dH}\right)_{H=H_0'} \approx \tfrac{1}{2}\chi_0 H \int \frac{1}{H - H_0} \frac{dh(H_0' - H_0)}{dH'} dH_0$$

$$= \tfrac{1}{2}\chi_0 \frac{H}{\Delta H^2}.$$

Thus, the maximum value of the fundamental frequency component of χ', denoted χ_f', is

$$\chi_f' = \frac{1}{2}\left(\frac{H}{\Delta H}\frac{H_m}{\Delta H}\chi_0\right).$$

The same argument also holds for χ'', and we have

$$\chi_f'' = \frac{1}{2}\sqrt{\frac{\pi}{2}}\left(\frac{H_0}{\Delta H}\frac{H_m}{\Delta H}\chi_0\right)\frac{1}{\gamma H_1\sqrt{T_1T_2}}.$$

Experimental Data

A considerable amount of quantitative experimental data applying to this case has been given by Portis.[11] It is not felt necessary to repeat similar data here.

6.2 *Case 2 — Rapid Adiabatic Passage with a Long Time Between Consecutive Field Modulation Cycles*

Physical Description

The time of passage through each individual spin packet is small compared with $\sqrt{T_1T_2}$. Thus, each packet yields an adiabatic rapid passage signal. The time between consecutive sweeps of each packet is long compared with T_1, so that each packet has sufficient time to relax completely.

Conditions Under Which This Case Is Observed:

$$\frac{H_1}{\omega_m H_m} \ll \sqrt{T_1T_2}, \quad \omega_m T_1 \ll 1, \quad \gamma H_1^2 \gg \omega_m H_m, \quad \gamma H_1\sqrt{T_1T_2} \gg 1.$$

Traces

The χ' signal is positive for $dH/dt < 0$, negative for $dH/dt > 0$. Thus, we have the trace shown in Fig. 13 (χ' is practically independent of the rate of change of the magnetic field). The output of the phase-sensitive detector will be proportional to $h(H_0 - H_0')$ [Fig. 3(d)].

The χ'' signal is negligible. If it is present, it may be due to incomplete saturation, partial breakdown of the adiabatic condition or slow passage near the extrema of the modulation cycle. In both cases, the recorder trace will be the derivative of the line shape (since χ'' due to slow passage, or to a breakdown of the adiabatic condition, is inherently of a frequency *twice* the field modulation frequency, and thus not detected by the phase sensitive detector. Only the derivative of the line shape yields a nonvanishing result).

Amplitudes

For each individual spin packet, χ' is proportional to

$$\frac{1}{\sqrt{H_1^2 + (H - H_0)^2}}.$$

For an infinitely wide line,

$$\chi' \propto \int_0^\infty \frac{dH_0}{\sqrt{H_1^2 + (H - H_0)^2}},$$

which is infinite. Therefore, to obtain a finite result, the finite width of

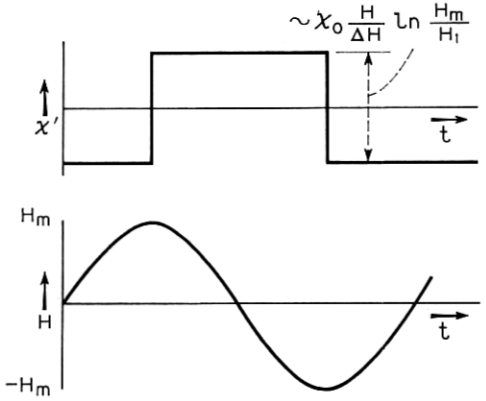

Fig. 13 — Scope trace of χ' signal to be expected in case 2. Ideal conditions are assumed; the field modulation amplitude H_m is small compared with line width ΔH.

the spin packet distribution has to be called upon. This finite width is due to the finite width of the inhomogeneously broadened line itself, and the reduction of the contribution of packets far off resonance due to relaxation. This reduction is difficult to calculate exactly. However, the integral in the expression for χ' above diverges only logarithmically; therefore, variations in the integrand far away from resonance, effect the integral only little. An approximate calculation has been performed by Portis,[5] and his result is

$$\chi_f' = \chi_0 H_0' h(H - H_0') \ln \frac{2H_m\omega_m T_1}{H_1}$$

for $\omega_m H_m \sqrt{T_1 T_2} \gg H_1$ and $T_1 = T_2$. [Portis, Case II(b).] This expression is discussed in Appendix D.

The χ'' amplitude is, for an individual spin packet (for χ'' due to breakdown of the adiabatic condition; see Section IV):

$$\chi'' = \tfrac{1}{2}\chi_0 \frac{H_0}{H_1} \frac{|\gamma H/dt|}{\gamma H_1^2} \frac{1}{\left[1 + \left(\frac{H - H_0}{H_1}\right)^2\right]^{\frac{3}{2}}}.$$

Now,

$$\int_{-\infty}^{\infty} \frac{dH}{\left[1 + \left(\frac{H - H_0}{H_1}\right)^2\right]^{\frac{3}{2}}} = 2H_1 .$$

Thus, superimposing various packets:

$$\chi'' = \chi_0 H_0 \frac{|dH/dt|}{\gamma H_1^2} h(H - H_0') \approx \frac{2}{\pi} \chi_0 H_0 \frac{H_m\omega_m}{\gamma H_1^2} h(H - H_0')$$

$$+ \frac{2}{\pi} \chi_0 H_0 \frac{H_m\omega_m}{\gamma H_1^2} h(H - H_0') \cos 2\omega_m t$$

$$+ \frac{2}{\pi} \chi_0 H_0 \frac{H_m\omega_m}{\gamma H_1^2} \frac{dh(H - H_0')}{dH} H_m \cos \omega_m t .$$

Since the χ'' lines due to an individual spin packet, caused by the breakdown of the adiabatic condition are narrow, neglect of relaxation is justified

Comments

For a sinusoidal field modulation, the passage must be rapid throughout the field sweep and not just in the middle of it. The time between

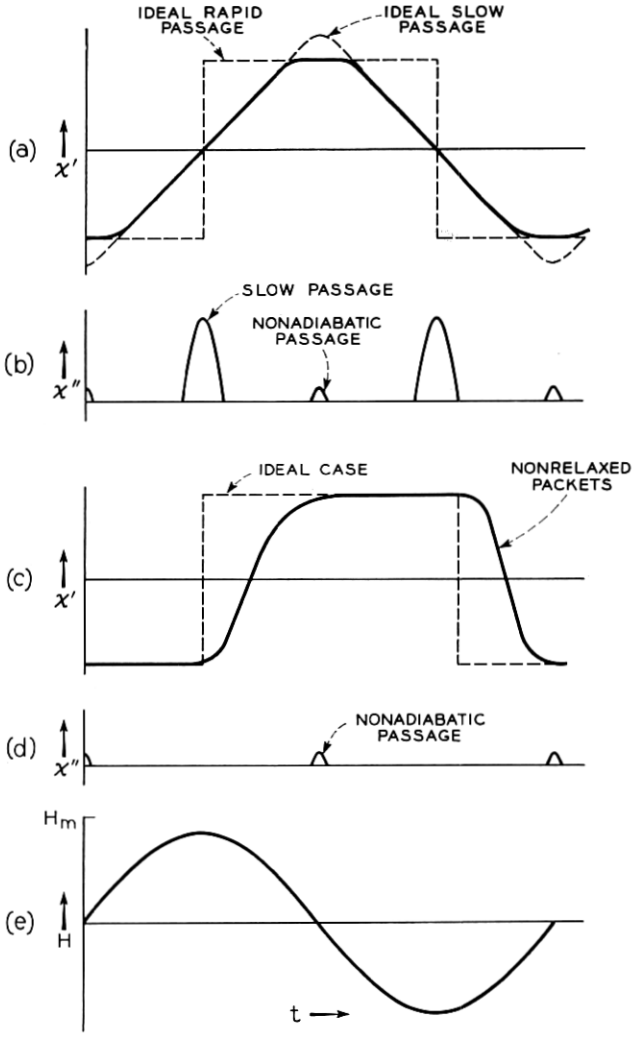

Fig. 14 — Scope traces of χ' signal to be expected when the conditions are not ideal: (a) χ' signal when there is *slow* passage near the extrema of the modulation cycle, where dH/dt is small; (b) χ'' signal when there is slow passage near the extrema of the modulation cycle; there may also be some signal due to imperfect adiabatic conditions, when $|\, dH/dt \,|$ is large; (c) χ' signal when T_1 is not very short compared with the period of the modulating field; spin packets near the extrema of the modulation cycle do not have time to relax completely before being swept over again; (d) χ'' signal under the conditions of (c); (e) the magnetic field modulation cycle.

consecutive sweeps of the same package, must be large compared with T_1 near the extrema of the modulation cycle, too.

These limitations are quite severe. Very often, T_1 will be a little short, and then the passage near the extrema will be slow [Figs. 14(a), (b)], or T_1 will be a little too long, and then the packages near the end will not have sufficient time to relax completely [Figs. 14(c), (d)].

Experimental Data

(*a*) *Fig. 15.*

Data: χ' trace; $H_1 \approx 1/30$ gauss; $H_m = 1$ gauss; $\omega_m = 2\pi \times 1000$ rad/second; $T = 10°$K. Under the same conditions, the χ'' trace was small.

Conditions that are satisfied: H_1, $H_m < \Delta H$; $\gamma H_1 T_1 > 1$; $\gamma H_1^2 > \omega_m H_m$; $\omega_m T_1 < 1$; ($T_2 = T_1 \approx 10^{-5}$ second; $\gamma H_1 T_1 \approx 5$; $\gamma H_1^2 \approx 15000$; $\omega_m H_m \approx 6000$; $\omega_m T_1 \approx 1/20$).

Interpretation: $H_1/(\omega_m H_m) \approx \frac{1}{2} \times 10^{-5}$ second. This is of order T_1. The passage in the *middle* of the modulation cycle is rapid, while at the extrema it is slow. The signal was observed to be just a little less than 90° out-of-phase with the field modulation. This indicates that this is *not* case 1, but rather a (distorted) case 2 [Portis,[5] Case II(b)]. The extrema just commence to flatten [see Fig. 14(a)].

(*b*) *Fig. 16 — Top and Center Traces*

Data: $H_1 \approx 1/100$ guass; $H_m = 1/10$ gauss; $\omega_m = 2\pi \times 1000$ rad/second; $T = 10°$K (top = χ', center = χ'').

Conditions that are satisfied: H_1, $H_m < \Delta H$; $\gamma H_1 T_1 \approx 1$; $\gamma H_1^2 > \omega_m H_m$; $H_1/\omega_m H_m \approx T_1$; ($\gamma H_1^2 \approx 1500$; $\omega_m H_m \approx 600$; $\gamma H_1 T_1 \approx 2$; $H_1/\omega_m H_m \approx T_1$); $T_1 = T_2$.

Interpretation: Here, $\gamma H_1 T_1$ was reduced so that a χ'' signal can be observed at a reasonable amplitude. This, however, causes the conditions of case 2 not to hold very well, and the χ' trace is a little distorted.

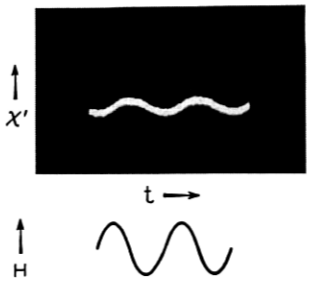

Fig. 15 — Experimental scope trace under the conditions of Fig. 14(a).

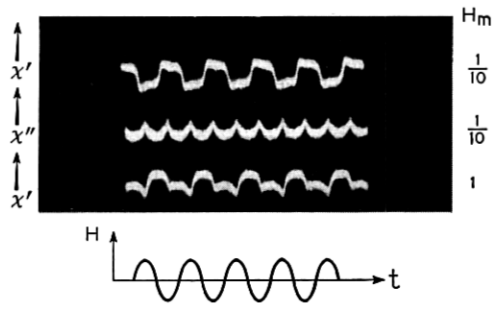

Fig. 16 — Experimental scope traces for case 2. Top trace, χ' signal, almost ideal case "2"; center trace, χ'' signal due to slow passage near the extrema of the modulation cycle; bottom trace, χ' signal, when the adiabatic condition is slightly violated.

(c) *Fig. 17.*

Data: χ'; $H_1 \approx 1/100$ gauss; $dH/dt = 1/10$ gauss/second; over-all sweep: 1.6 gauss; $T = 4.5°\text{K}$; $T_1 \approx 5$ seconds.

Conditions that are satisfied: "H_m", $H_1 < \Delta H$; $\gamma H_1 \sqrt{T_1 T_2} \gg 1$; $\gamma H_1^2 \gg dH/dt$; $H_1/(dH/dt) > \sqrt{T_1 T_2}$.

Interpretation: This is the χ' signal observed at the output of the IF amplifier (no phase sensitive detector). It corresponds to case 2, with a slight amount of case 7 (i.e., incomplete relaxation between successive field sweeps) intermixed [see Fig. 14(c)].

6.3 *Case 3 — Rapid Passage with a Long Time Between Consecutive Field Modulation Cycles, the Adiabatic Condition Being Slightly Violated*

Physical Description

The conditions under which case 2 holds are quite severe, and it may be quite often impossible to satisfy them with the experimental equipment at hand, and it will be necessary to violate some of these conditions.

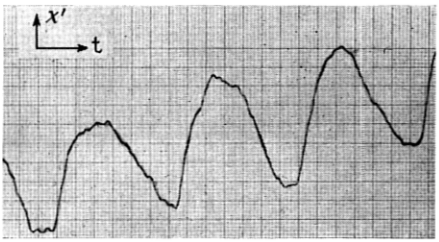

Fig. 17 — χ' signal for rapid adiabatic passage, when T_1 is not very small compared with the field modulation cycle. Compare with Fig. 14(c). No phase sensitive detector is used here (therefore, considerable drift is observed).

If the condition $\omega_m H_m < \gamma H_1^2$ is violated, the adiabatic condition will break down near the centers of the modulation cycle. (This case is not of much theoretical significance, but it is experimentally very common.)

The modulation cycle may be subdivided into a number of regions (see Fig. 18):

Region I: $H_1/(dH/dt) > \sqrt{T_1 T_2}$. In this region we have slow passage conditions.

Region II: $1/(\gamma H_1) < H_1/(dH/dt) < \sqrt{T_1 T_2}$. In this region we have adiabatic rapid passage conditions.

Region III: $H_1/(dH/dt) < 1/(\gamma H_1)$. In this region the adiabatic condition is broken.

We have the further possibilities:

i. $T_1 < \sqrt{H_1/(\omega_m^2 H_m)}$. In this case, $t = T_1$ lies in region I.

ii. $\sqrt{H_1/(\omega_m^2 H_m)} < T_1 < \gamma H_1^2/(\omega_m^2 H_m)$. In this case, $t = T_1$ lies in region II.

iii. $\gamma H_1^2/(\omega_m^2 H_m) < T_1$. In this case, $t = T_1$ lies in region III.

Case i: In region I we have slow passage; in region II we have adiabatic rapid passage of fully relaxed packets; and in region III nonadiabatic passage of fully relaxed packets.

Case ii: Even in region II there are some packets which did not have time to relax since last swept by the field. If $T_1 = T_2$, region I is then, naturally, negligibly small (less than one packet wide). In region III, all packets have fully relaxed.

Case iii: The packets in region II have little time to relax. Even some of the packets in region III did not relax.

Generalizing to systems with $T_2 < T_1$ will create additional cases, since one has to distinguish between relaxation of S_z, and of S_x, S_y.

Traces

See Figs. 18 and 19. In the traces of cases ii and iii, region I has been omitted, since it is small. The traces have been drawn for the center of the line. Off center, the derivative of the line shape will yield an additional χ' signal. In addition, there may be "wiggles" in the border between regions II and III.

The traces detected by a phase-sensitive detector are "absorption" curves, at a phase angle of 90° with the modulating field in case i, 0° in case iii, and an intermediate value for case ii. In addition, the χ' signal of region III will tend to produce a "dispersion derivative." (The signals of regions I and II also produce such a signal, but this is weak compared with the "absorption" shaped signal. If region III is *large*, its "dispersion derivative" signal may become comparable, or exceed the

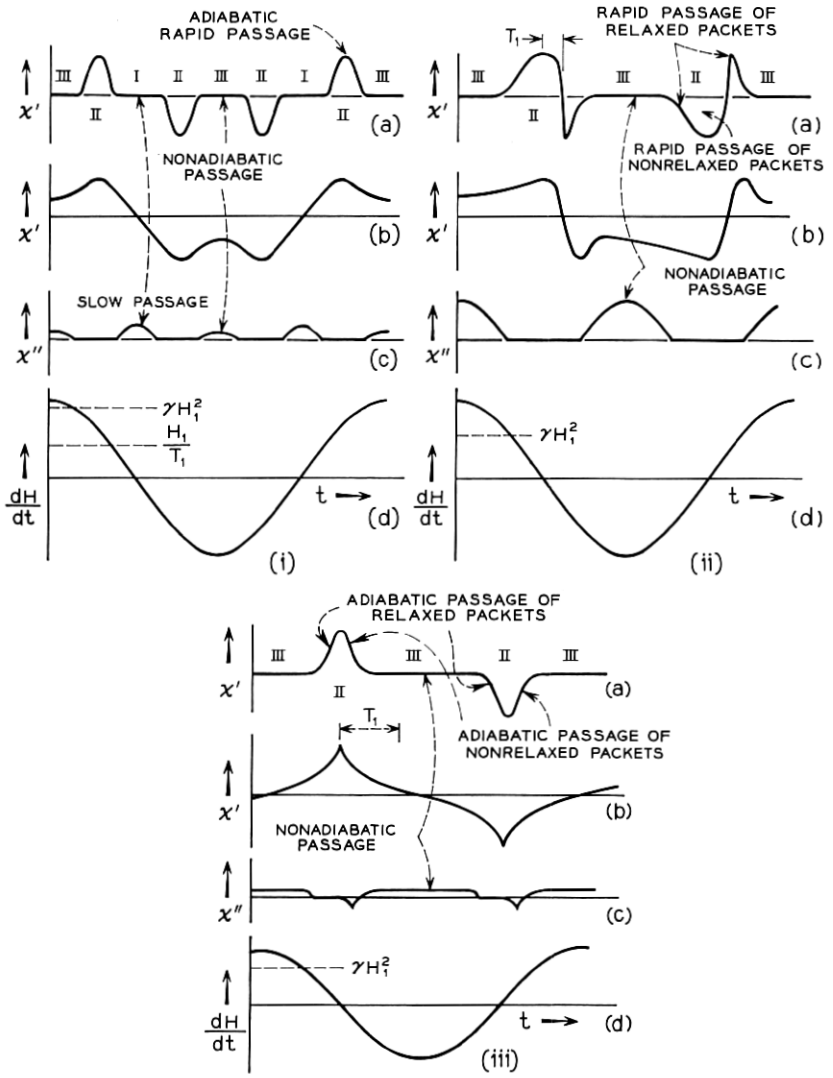

Fig. 18 — Signal to be expected when the adiabatic condition $\gamma H_1^2 \gg dH/dt$ is broken: (i) Short T_1 ; there is slow passage near the extrema of the field modulation cycle, and the spin packets are completely relaxed in the other regions. (ii) Slightly longer T_1 ; some spin packets which are swept through adiabatically, are not relaxed. (iii) Still longer T_1 ; all spin packets which are swept through adiabatically, are not relaxed. In all three sections, (a) is an "idealized" χ' trace, (b) is a more "realistic" χ' trace, (c) is the χ'' trace and (d) is the magnetic field modulation.

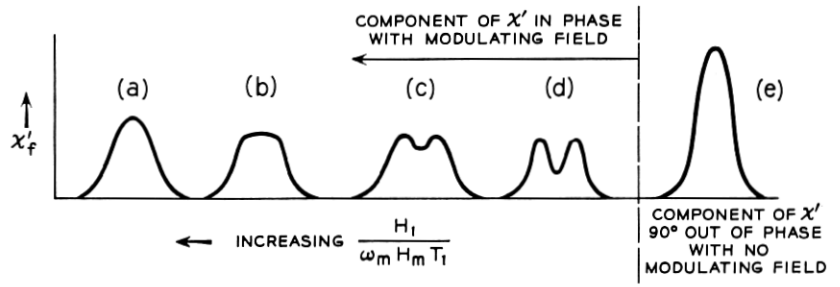

Fig. 19 — Expected recorder traces for rapid (adiabatic or nonadiabatic) passage, with a field modulation period long compared with, or of the same order, as T_1 : (a) large H_1 , small H_m ; (b) and (c) intermediate values of H_1 , H_m ; (d) Small H_1 , large H_m . (These four are the component of χ_f' in-phase with the field modulation.) (e) Component of χ_f' 90° out-of-phase with the field modulation.

"absorption" signal due to region II.) The "dispersion derivative" signal is at 0° with respect to the modulating field, so we may expect χ' traces as shown in Fig. 19.

Note that region III also yields a χ'' signal component at the modulation frequency, proportional to dh/dH; this component (which yields an "absorption derivative" trace) is small.

Amplitudes

I shall not attempt a quantitative treatment of this case. However, if the relative depth of the "notches" of cases i and ii can be measured, and is found to be β, the fundamental frequency component falls down by $(2/\pi)\beta$, for the simplified shape function of Fig. 20.

Case iii is essentially identical with case 10.

Making use of the formula for χ' of case 2:

$$\chi_f' \approx \left(\frac{2}{\pi}\beta\right) \chi_0 H h (H - H_0') \ln \frac{2H_m\omega_m T_1}{H_1}.$$

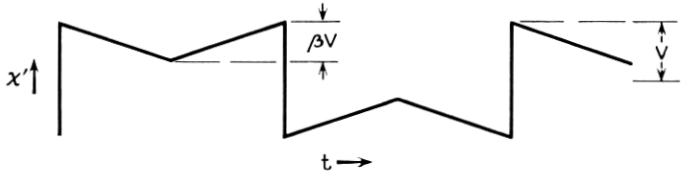

Fig. 20. — An idealized χ' scope trace of case 3, used to estimate the amplitude of the signal.

Experimental Data

(*a*) *Fig. 16 — Bottom Trace*

Data: $H_1 \approx 1/100$ gauss; $H_m = 1$ gauss; $\omega_m = 2\pi \times 1000$ rad/second; $T = 10°\text{K}$.

Conditions that are satisfied: H_m , $H_1 < \Delta H$; $\gamma H_1 T_1 > 1$; $H_1/\omega_m H_m < T_1$; $T_1 = T_2$; ($\gamma H_1 T_1 \approx 2$; $H_1/\omega_m H_m \approx 1/10\ T_1$; $\gamma H_1^2 \approx 1500$; $\omega_m H_m \approx 6000$).

Interpretation: Here, the adiabatic condition begins to be violated. χ' is small for $dH/dt > \gamma H_1^2$ and this causes the 'notches' in the photo [see (i)–(b) in Fig. 18].

The observed trace probably includes a small χ'' component [see (i)–(c) in Fig. 18], which adds up with χ' to yield the observed trace.

(*b*) *Fig. 21.*

Data: χ'; $H_1 \approx 1/100$ gauss; $H_m = 1$ gauss; $\omega_m = 2\pi \times 1000$ rad/second; $T = 10°\text{K}$ [same as in (a) above, except for higher scope gain]; bottom trace: sitting in the center of the line; top and center traces: off the center of the line.

Conditions: the same as in (a).

Interpretation: Since the condition $H_m \ll \Delta H$ is not very well satisfied, a slight admixture proportional to the derivative of the line shape, distorts the shape somewhat. This is particularly evident for the traces off the center of the line.

Synthesis of the observed traces from those due to various cases is shown in Fig. 22.

(*c*) *Fig. 23.*

Data: χ''; $H_1 \approx 1/100$ gauss; $H_m = 1$ gauss; $\omega_m = 2\pi \times 1000$ rad/second; $T = 10°\text{K}$; top and center traces: off the center of the line;

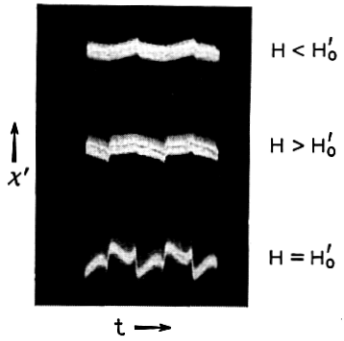

Fig. 21 — χ' scope traces of rapid, nonadiabatic passage of a line, when T_1 is very short compared with the field modulation cycle, at the center of the line (bottom trace), and on both sides of it (top and center traces).

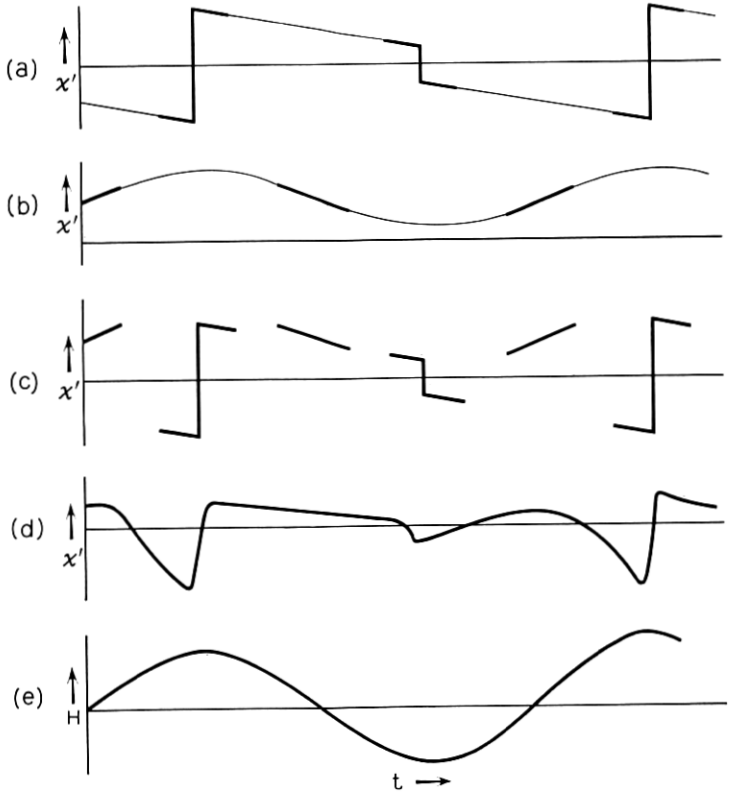

Fig. 22 — Synthesis of the χ' trace observed in Fig. 21: (a) a case 2 signal (adiabatic rapid passage, slow modulation), on the *shoulders* of the line; (b) a case 4 signal (nonadiabatic); (c) synthesis of (a) for the portions of the modulation cycle for which dH/dt is small, and (b) for those for which dH/dt is large; (d) rough shape of the trace expected experimentally; (e) the modulating field.

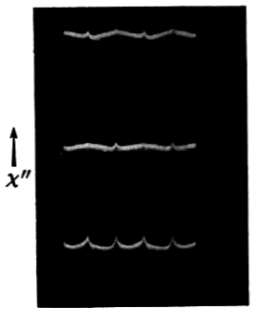

Fig. 23 — χ'' scope traces under the same conditions as those of Fig. 21. We observe slow passage signals, with some component proportional to the derivative of the line shape, due probably to incomplete saturation. ($\gamma H_1 T_1 \approx 2$.)

bottom trace: at the center of the line [*same* as in (b), only χ'' instead of χ']

Interpretation: Again we have mainly case 3 [Fig. 18(i)] with some component due to the derivative of the line shape superposed, off the center of the line.

This admixture may be due to a small component corresponding to cases 4 or 9, or more probably a slight amount of nonsaturation ($\gamma H_1 T_1 \not> 1$). The peaks at the edges may be due to slow passage near the extrema of the modulation cycle.

(*d*) *Fig. 24.*

Data: χ_f' (employing phase-sensitive detection); $H_1 \approx 1/300$ gauss; $H_m = 1$ gauss; $\omega_m = 2\pi \times 1000$ rad/second; $T = 10°$K.

Fig. 24(a) — reference voltage *in phase* with the modulating field;

Fig. 24(b) — reference voltage 90° out of phase with the modulating field.

Conditions satisfied: H_1, $H_m < \Delta H$; $H_1/\omega_m H_m < T_1$ ($H_1/\omega_m H_m \approx 1/30\ T_1$; $\gamma H_1^2 \approx 200$; $\omega_m H_m \approx 6000$; $\gamma H_1 T_1 \approx 1$).

Interpretation: We have case 3 with some admixture of components due to case 4, or nonsaturation. Notice the flat top on the trace of Fig. 24(a) (see Fig. 19).

(*e*) *Fig. 25.*

Data: χ_f' (employing phase-sensitive detection; component in phase with field modulation); $H_1 \approx 1/100$ gauss; $H_m = 1$ gauss; $\omega_m = 2\pi \times 1000$ rad/second; $T = 10°$K.

Conditions satisfied: H_1, $H_m < \Delta H$; $\gamma H_1 T_1 > 1$; $H_1/\omega_m H_m < T_1$; $T_1 = T_2$ ($\gamma H_1 T_1 \approx 2$)

Interpretation: The increased saturation, and more important, the less violent violation of the adiabatic condition, compared with Fig. 24(a), gives a "cleaner" trace (χ', without phase-sensitive detection under the same conditions, is shown in Fig. 21).

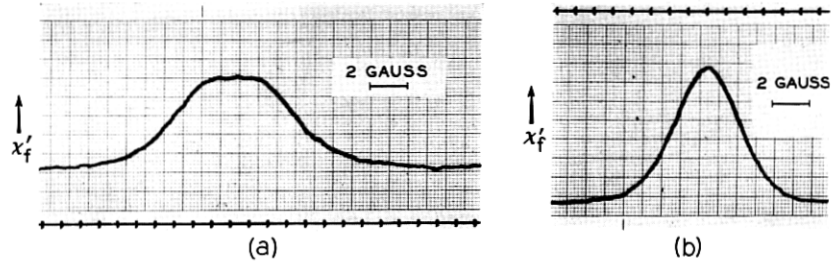

Fig. 24 — (a) χ' for mixture of cases 1 and 2; with P.S.D., 0° phase shift between modulating field and reference voltage [compare with Fig. 19(b)]. (b) Same as (a), but χ' signal 90° out-of-phase with modulating field.

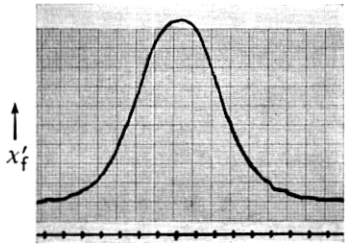

Fig. 25 — The component of χ'_f in-phase with the modulating field, with higher microwave power than that used to obtain Fig. 24(a); the higher power yields a "cleaner" trace [compare with Fig. 19(a)].

6.4 *Case 4 — Rapid Nonadiabatic Passage with a Long Time Between Consecutive Field Modulation Cycles*

Physical Description

The adiabatic condition $\gamma H_1^2 > dH/dt$ is violated throughout the modulation cycle. However, T_1 and T_2 are so short that spin packets are completely relaxed between consecutive sweeps (regions I and II of case iii in Section 6.3 vanish). If T_1 and T_2 are not *very* short, we may neglect relaxation effects, since packets that have relaxed by an appreciable amount, beat with H_1 to produce a signal of a far off frequency. The signal will, therefore, be a "superposition of wiggles," which is not detected by the narrow bandwidth system usually employed, as treated in Section V. (Even if T_1 , T_2 are shorter, their effect will probably not be large. The effect of T_2 is to destroy the phases — but phases of various packets, interfere destructively, as discussed in Section V; T_1 increases S_z , but, for $\gamma H_1^2 \ll dH/dt$, S_z does not fall off much, anyway.)

Conditions Under Which This Case Is Observed:

$$\omega_m T_1 < 1; \qquad \gamma H_1^2 \lll H_m \omega_m ; \qquad H_m < \Delta H; \qquad \gamma H_1 \sqrt{T_1 T_2} \gg 1.$$

Note that the condition $\gamma H_1^2 \ll H_m \omega_m$ requires a very small H_1 , while saturation requires that it be not too small. Thus, this case may be difficult to achieve practically. A wider line makes it possible to increase H_m , and thus, makes the observation of this case easier.

Traces

For oscilloscope traces, see Fig. 26.

The output of the phase-sensitive detector will consist of a "dispersion derivative" line for χ' and a "absorption derivative" for χ''.

Amplitudes

As discussed in Section 3.5, χ' and χ'' for the extreme nonadiabatic case are the *same* as for the nonsaturated case. Therefore, the line shapes and amplitudes will be the same here as in the nonsaturated case, (although T_1 , T_2 may be quite large):

$$\chi_f' \approx \tfrac{1}{2} \frac{H}{\Delta H} \chi_0 \frac{H_m}{\Delta H},$$

$$\chi_f'' \approx \tfrac{1}{2} \frac{H}{\Delta H} \chi_0 \frac{H_m}{\Delta H}.$$

6.5 *Case 5 — Rapid Adiabatic Passage with a Short Time Between Consecutive Field Modulation Cycles and Very Rapid Field Sweep*

Physical Description

In this case, each spin package yields an adiabatic rapid passage signal. The time between consecutive modulation cycles is small compared with T_1 . In addition, the conditions are such that the packages do not lose much of their magnetization during the whole process. [$H = H_0 + (dH_0/dt)\ t + H_m \cos \omega_m t$. If dH_0/dt is sufficiently large, this may be the case.]

This case has been treated by Portis,[5] and called "Case IV" by him.

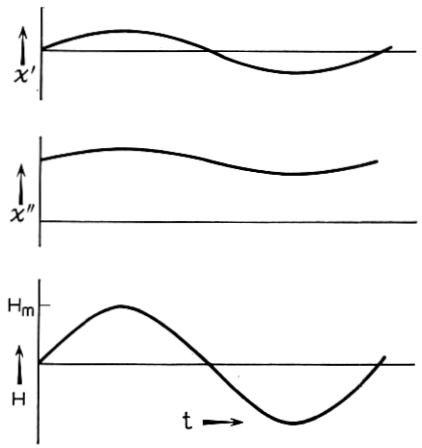

Fig. 26 — Expected scope trace of signal of case 4 (spin packets are completely relaxed; χ'' signal *off* the center of the line).

Conditions Under Which This Case Applies:

$$\omega_m T_1 \gg 1; \qquad \gamma H_1^2 \gg H_m \omega_m ; \qquad \gamma H_1 \sqrt{T_1 T_2} \gg 1.$$

In addition, assume that a fraction α of the line is "burnt" during each passage. Then, the average of the magnetization, (and signals) of N passages will be

$$\frac{1}{N}[1 + (1 - \alpha) + (1 - \alpha)^2 + \cdots] = \frac{1 - (1 - \alpha)^N}{\alpha N} \approx \frac{1 - e^{-\alpha N}}{\alpha N}.$$

The number of times each packet is swept over is

$$N = \frac{2H_m}{dH_0/dt}\left(2\frac{\omega_m}{2\pi}\right).$$

Thus, for little burnout, we must have; $\alpha N \ll 1$, or $[H_m \omega_m/(dH/dt)]\alpha \ll 1$.

The amplitude of the signal in this case will be about $H_m/\Delta H$ weaker than in case 6. Therefore, the above condition is a little too soft, and we must have

$$\frac{H_m \omega_m}{dH_0/dt}\alpha \ll \frac{H_m}{\Delta H}, \qquad \frac{\Delta H \omega_m}{dH_0/dt}\alpha \ll 1.$$

The loss of magnetization during rapid passage, α, also depends very much upon the sample used. If the loss is mainly due to relaxation between consecutive modulation cycles, $\alpha \approx 1/(\omega_m T_1)$, as postulated by Portis.[5]†

Traces

Each spin packet yields the traces shown in Fig. 27 (χ'' is due to non-perfect adiabaticity). Notice that the various packets will combine to produce a χ' signal that is approximately constant and a sinusoidal χ'' signal ($\chi'' \propto dH/dt \approx \omega_m H_m \sin \omega_m t$ for each packet). The derivative of the line shape will yield variations in the χ' signal, and thus a component of the signal at the modulation frequency (Fig. 28). Thus the recorder traces are as shown in Fig. 29. The χ' signal is of "absorption derivative" shape, and χ'' of "absorption" shape. However, the parities are as discussed in Section II.

Amplitudes

The amplitude of the χ' trace depends quite critically upon α, which is a rather indefinite quantity. It depends upon the rate at which a spin

† For the sample employed in this experiment, the loss was found to be due mainly to nonadiabatic passage, and to forbidden lines (Section 3.3).

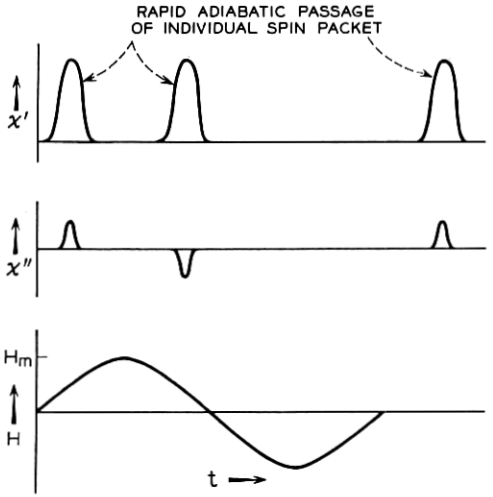

Fig. 27 — Signals from one spin packet, case 5; the spins do *not* relax between consecutive field modulation cycles, so χ' does not change sign, while χ'', which is due to nonperfect adiabaticity, changes sign.

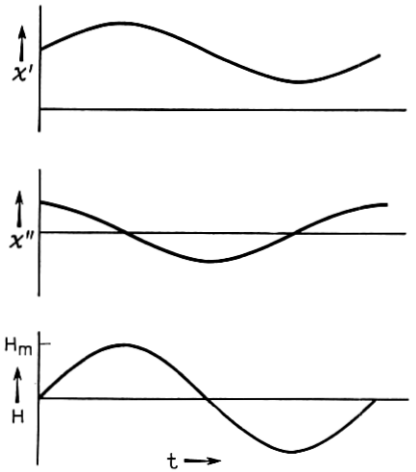

Fig. 28 — Scope traces of signal of case 5 (combination of the signals due to the individual spin packets, Fig. 27). Although χ' is large, its component at the field modulation frequency is small, and due to the derivative of the line shape.

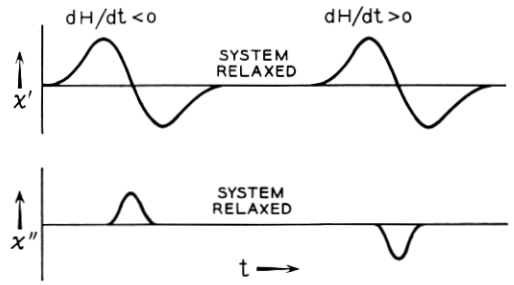

Fig. 29 — Expected recorder traces of signal of case 5.

packet is swept through, which varies with time due to the linear field sweep, dH_0/dt. It also depends upon the environment of each spin — and in an inhomogeneously broadened line, different packets will have different environments and different α's. Thus, only order of magnitude estimates of α, and of the amplitude, can be given.

In the limit when $\alpha N \ll 1$, the signal has been calculated by Portis.† Quoting his results, (with slightly changed notation):

$$\chi'(H) = \mp \tfrac{1}{2}\chi_0 H \int_0^\infty \frac{h(H_0 - H_0')}{\sqrt{(1+\delta^2)}} \frac{dH_0}{\gamma H_1} \approx \mp \frac{1}{2\sqrt{2\pi}} \chi_0 \frac{H}{\Delta H} \ln \frac{2\Delta H}{H_1}$$

for a gaussian line, with $H_1 \ll \Delta H$. Modulating the field, the component at the field modulation frequency is

$$\chi'\left(H_0' \pm \frac{\Delta H}{\sqrt{2}}\right) \approx \frac{1}{\sqrt{2\pi}} \chi_0 \frac{H_0}{\Delta H} \frac{H_m}{\Delta H} \ln \frac{2\Delta H}{H_1} \cos \omega_m t.$$

To include losses due to partial relaxation, multiply this value by

$$\frac{1 - e^{-\alpha N}}{\alpha N},$$

where α is the loss of magnetization per passage and

$$N = \frac{2}{\pi} \frac{H_m \omega_m}{dH_0/dt}.$$

The χ'' signal is calculated as in case 2, but, since the magnetization vector changes sign with dH/dt, χ'' changes sign too, and we have, neglecting burnout,

$$\chi'' = \chi_0 H \frac{H_m \omega_m \sin \omega_m t}{\alpha H_1^2} h(H - H_0').$$

† Ref. 5, p. 17.

Including burnout, we must multiply this result by $(1 - \alpha)^{N/2} \approx e^{-\alpha N/2}$, since the packets in the *middle* of the modulating cycle give most of the contribution to the χ'' signal, and these have been swept over $N/2$ times only (i.e., instead of an average over-all packets, I have calculated here the amplitude of the middle packet only).

Note that, if $\omega_m H_m/(\gamma H_1^2)$ is *not* very small, it is difficult to get the 'nonburnt' case, since there is considerable burnout due to nonadiabaticity. If it is small, χ'' is small.

Experimental Data

See Fig. 30 (noting that there are *two* distinct lines on this trace).

Data: χ_f' (employing phase sensitive detection); $H_1 \approx 1/300$ gauss; $H_m = 1/20$ gauss; $\omega_m = 2\pi \times 100$ rad/second; $T = 1.2°$K. sweep rate: 8 gauss/second.

Conditions satisfied: H_1 , $H_m \ll \Delta H$; $\gamma H_1 T_1 \gg 1$; $\gamma H_1^2 > \omega_m H_m$. Number of times each packet is swept:

$$\frac{2H_m}{dH/dt}\left(\frac{2\omega_m}{2\pi}\right) = 2.5$$

Loss of magnetization per passage: $\alpha \approx 0.1$ (roughly); $\gamma H_1^2 \approx 200$; $\omega_m H_m \approx 30$.

Interpretation: The recorder trace agrees quite well with the theoretically expected trace on Fig. 29.† Also, consecutive traces have someferent shapes and amplitudes. This will be discussed in Section 6.6.

6.6 *Case 6 — Rapid Adiabatic Passage with a Short Time Between Consecutive Field Modulation Cycles, the Magnetization of the Spin Packets Being Partly Destroyed*

Physical Description

Each spin packet yields a rapid passage adiabatic signal. However, there is relatively more burnout than in case 5, and the burnout cannot

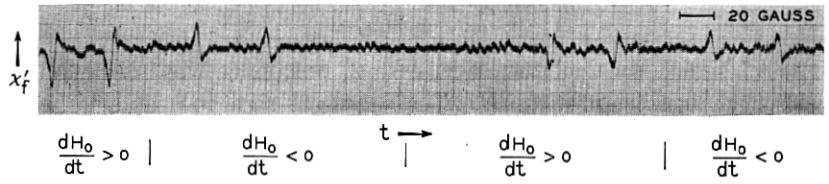

Fig. 30 — Experimental recorder trace of case 5 (compare with Fig. 29).

† Note that the system does *not* relax between consecutive sweeps, since T_1 is much larger than the time between sweeps.

be assumed just to reduce the amplitude of the signal without affecting its shape.

This case is an intermediate one and of little theoretical significance in itself. However, it is important to understand the processes occurring here. Let

$$H = \begin{cases} H_0 + H_m & t < 0 \\ H_0 + H_m \cos \omega_m t & t > 0 \end{cases}$$

(H_0 is at the center of the line.) Consider $\chi'(t)$ (see Fig. 31).

For $t \leqq 0$, $\chi'(t) = 0$, since we have the slow passage case, and are (say) at the center of the line.

For $0 < t < 1/\omega_m$ (say), we have a very fast rise of χ', since we have rapid passage through nonburnt packets. This is region I in Fig. 31.

For slightly larger t, we have a *constant* χ', independent of the sign of dH/dt. Since *both* dH/dt and S_z reverse their sign, χ' maintains its sign. This is region II.

Eventually, spin packets will burn out, either because of loss of magnetization *during* passage, or T_1 relaxation of "inverted" spins, between passages. The spins are partly burnt out in region III

Finally, a stationary state is reached, in which the burnout per passage is replaced by means of the T_1 relaxation, between passages (region IV).

Operation in regions I or II yields case 5. Operation in region IV yields case 7. Operation under conditions all regions contribute, but I, II, III contribute more than IV, yields case 8. Operation under conditions at which region III is important, yields this case, 6.

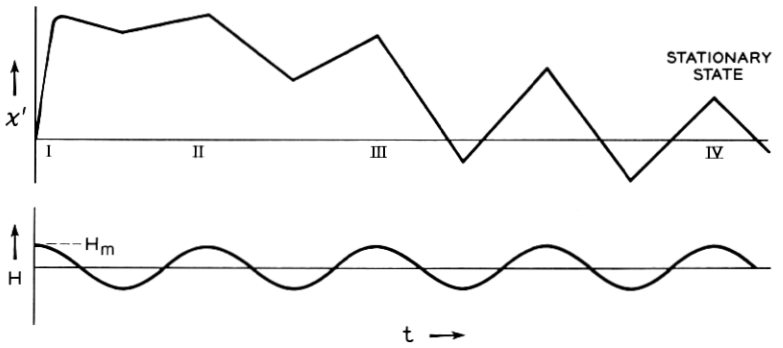

Fig. 31 — Transient χ' trace, for illustration of case 6: χ' is first large and constant; eventually, spin packets "burn out"; χ' decreases, but its component at the field modulation frequency may increase.

Conditions Under Which This Case Is Observed:

$\gamma H_1\sqrt{T_1T_2} \gg 1$; $\gamma H_1^2 \gg H_m\omega_m$; $\omega_m T_1 \gg 1$; $H_m \gg 1$; $N\alpha \approx 1 (N \equiv 2H_m/(dH_0/dt)2\omega_m/2\pi$; α: loss of magnetization per passage).

Traces

The χ' signal will be approximately as shown in Fig. 32(a). The χ'' signal will be as in case 5, but somewhat smaller, since, for packets in the middle of the modulation cycle, for which dH/dt is large and therefor χ'' (due to nonideal adiabaticity) should be appreciable, the magnetization is smaller.

Near the extrema of the modulation cycle we may have slow passage conditions and a corresponding χ'', which is, however, mostly at the second harmonic of the field modulation frequency. Thus, the output of

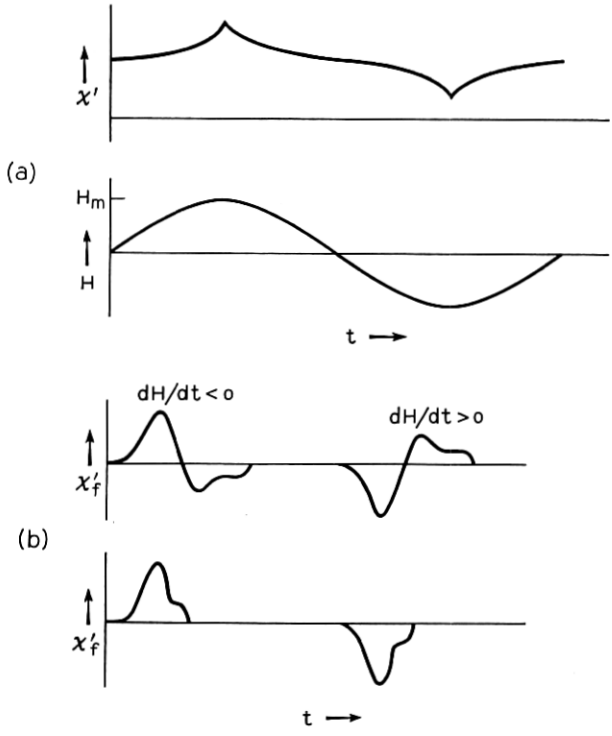

Fig. 32 — (a) Expected scope trace of case 6: spin packets just commence to "burn out"; χ' is large, but its component at the field modulation frequency is small. (b) Expected recorder traces of hybrids of case 5 with cases 6, 7, or 8.

the phase-sensitive detector is of "absorption" shape, 0° phase shift with field modulation for χ' and small for χ''.

A mixture of case 5 will distort the χ' signal and yield traces as shown in Fig. 32(b).

Amplitudes

Amplitudes are difficult to estimate, since the rate of burnout will be different for different spins and different parts of the field modulation cycle.

If the loss of magnetization is mainly due to T_1 relaxation between sweeps, the rate of burnout is about $1/T_1$, as discussed by Feher.†

The amplitude of the χ' signal will then be about that of case 7 (discussed below), but it may be larger or smaller.

If the burnout is mainly due to T_1 relaxation, the magnetization vectors at one extremum of the modulation cycle (dH/dt = maximum) will burn out fastest, and those at the other one will burn out slowly. Thus, a transient condition may develop in which the signal is *stronger* than in case 7.

If the spins at the extrema burn out fastest (since dH/dt is small there and "T_2" processes are therefore more effective) the signal will tend to be weaker than in case 7.

Therefore, attempting to give some general expression for the amplitude is not of much use here.

Comment

The mixture of cases 5 and 6 (and possibly 7 and 8) yields the peculiar trace shown in Fig. 32(b). If, due to different environments, different spins lose different amounts of their magnetization per passage, the fast-burning spins will tend to create case 6 (or 8), i.e., an "absorption" shape, while the slow burning ones tend to create case 5 (nonburnt absorption line derivative). Thus, after starting from equilibrium, the *first* trace may look more like an "absorption" line, and consecutive ones, more like "absorption derivative" (see Fig. 30).

Experimental Data

See Fig. 33.

Data: χ', $H_1 = 1/1000$ gauss; $dH/dt = \frac{1}{2}$ gauss/second. Over-all sweep: 1 gauss; $T = 4.5°$K.

† Ref. 12, p. 1242.

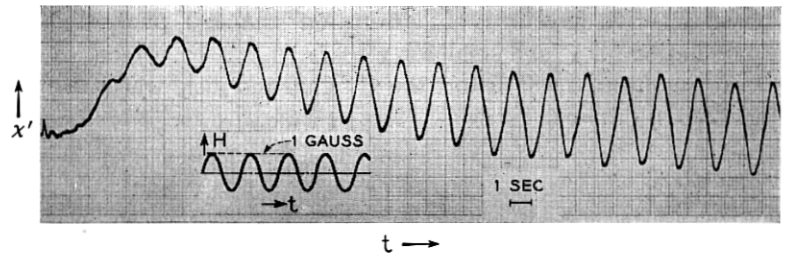

Fig. 33 — Transient χ' signal; this trace verifies experimentally the theoretically predicted trace of Fig. 31.

Conditions satisfied: H_1, $\delta H \ll \Delta H$; $\gamma H_1 T_1 \gg 1$; $\gamma H_1^2 \gg dH/dt$; "ω_m"$T_1 \gg 1$; ($\gamma H_1^2 \approx 20$; $\gamma H_1 T_1 \approx \frac{1}{2} \times 10^6$). Repetition rate: $\frac{1}{2}$ sec^{-1}; $T_1 \approx 5$ seconds.

Interpretation: This trace coincides with the theoretically predicted trace of Fig. 31.

6.7 *Case 7 — Rapid Adiabatic Passage with a Short Time Between Consecutive Field Modulation Cycles — the Stationary Case*

Physical Description

Each spin packet yields an adiabatic rapid passage signal. However, the packets are in stationary state, which depends upon T_1 and the loss of magnetization per passage, but *not* upon dH_0/dt which is assumed to be so small as to let the stationary state be established. This case has essentially been discussed by Portis[5] [his Case III(b)] and Feher.[12]†

Conditions Under Which This Case Is Observed:

$$\gamma H_1 \sqrt{T_1 T_2} \gg 1; \qquad \gamma H_1^2 \geqq H_m \omega_m ; \qquad \omega_m T_1 \gg 1; \qquad H_m \gg H_1 .$$

In addition, the signal due to this case must be strong compared to that of cases 6 and 8, which compete with it. This requires: $dH_0/dt \ll H_m/T_1$ (see sections on amplitudes).

Traces

The spin packets, resonating at $H \approx H_0 - H_m$, are most of the time in a field *above* their resonant field. Therefore, their S_z will be positive for $H > H_0$, and thus negative for $H < H_0$.

† See Feher,[12] p. 1241–1242.

Thus, for $dH/dt < 0$, we get a positive χ', and for $dH/dt > 0$ a negative one. For packets resonating near $H \approx H_0 + H_m$ signs are reversed.

Packets resonating at $H \approx H_0$ are about half the time in a field above their resonant field, and half the time in a lower field. Therefore, their magnetization is small. We thus have the traces shown in Fig. 34.

Amplitudes

Let the fractional loss of magnetization during each passage be α. Then [as in Equation (33) of Feher[12]],

$$-S_N = [S_{N-1}e^{-t_1/T_1} - S_0(1 - e^{-t_1/T_1})](1 - \alpha),$$
$$-S_{N+1} = [S_N e^{-t_2/T_1} + S_0(1 - e^{-t_2/T_1})](1 - \alpha),$$

where S_N is the magnetization after the Nth sweep, and S_0 is the equilibrium magnetization.

In the stationary state:

$$\begin{aligned} S_{N-1} = S_{N+1} &= -[S_N e^{-t_2/T_1} + S_0(1 - e^{-t_2/T_1})](1 - \alpha) \\ &= e^{-t_2/T_1}[S_{N-1}e^{-t_1/T_1} - S_0(1 - e^{-t_1/T_1})](1 - \alpha)^2 \\ &\quad + S_0(1 - e^{-t_2/T_1})(1 - \alpha), \end{aligned}$$

$$S_{N-1} = \frac{e^{-t_2/T_1}(2 - \alpha) - e^{-(t_1+t_2)/T_1}(1 - \alpha) - 1}{1 - (1 - \alpha)^2 e^{-(t_1+t_2)/T_1}}(1 - \alpha)S_0,$$

$$S_N = \frac{e^{-t_1/T_1}(2 - \alpha) - e^{-(t_1+t_2)/T_1}(1 - \alpha) - 1}{1 - (1 - \alpha)^2 e^{-(t_1+t_2)/T_1}}(1 - \alpha)S_0.$$

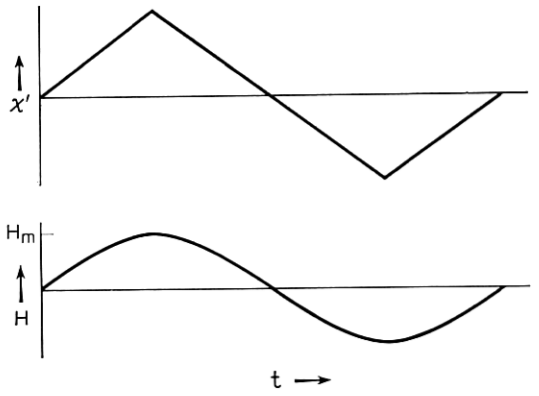

Fig. 34 — Scope trace of signal of case 7: a stationary state is established; the spin packets at the center of the field modulation cycle are burnt out, while those at the extrema yield an adiabatic rapid passage signal.

For $T_1 \gg t_1 + t_2$:

$$S_{N-1} \approx \frac{-(2-\alpha)\frac{t_2}{T_1} + (1-\alpha)\frac{t_1+t_2}{T_1}}{[1-(1-\alpha)^2] + (1-\alpha)^2\frac{t_1+t_2}{T_1}}(1-\alpha)S_0\,,$$

$$S_N \approx \frac{-(2-\alpha)\frac{t_1}{T_1} + (1-\alpha)\frac{t_1+t_2}{T_1}}{[1-(1-\alpha)^2] + (1-\alpha)^2\frac{t_1+t_2}{T_1}}(1-\alpha)S_0\,.$$

If, furthermore, $\alpha \ll 1$, then:

$$S_{N-1} = \frac{\frac{t_1-t_2}{T_1}}{2\alpha + \frac{t_1+t_2}{T_1}}S_0\,,$$

$$S_N = \frac{\frac{t_2-t_1}{T_1}}{2\alpha + \frac{t_1+t_2}{T_1}}S_0\,.$$

S_N , S_{N+1} are then still linear functions of $t_1 - t_2$, as is the case when $\alpha = 0$. For $t_2 = 0$, say,

$$S_N = -S_{N-1} = \frac{\frac{2\pi}{\omega_m T_1}}{2\alpha + \frac{2\pi}{\omega_m T_1}}S_0 = \frac{S_0}{1 + \frac{\alpha\omega_m T_1}{\pi}}\,.$$

The approximate number of cycles required to achieve equilibrium can be estimated as follows.

If $\alpha\omega_m T_1/\pi \ll 1$, the approach to equilibrium will be governed mainly by T_1 . The loss of magnetization during "rapid passage" can be neglected. The rate of establishment of the "stationary" state will be about T_1^{-1}, as discussed in Feher's work.[12]

If $\alpha\omega_m T_1/\pi \gg 1$, during each cycle a spin packet is reduced by $(1-\alpha)^2$. Thus, $(1-\alpha)^{2m} \approx \pi/\alpha\omega_m T_1$, where m is the number of cycles to reach equilibrium. If $\alpha \ll 1$, then $(1-\alpha)^{2m} \approx e^{-2\alpha m}$, and $m \approx 1/(2a)\ \ln\ [\pi/(\alpha\omega_m T_1/\pi)]$.

Numerical examples (corresponding to conditions of the present experiments):

(a): $\alpha = 0.1$; $\omega_m = 2\pi \times 1000$ rad/second; $T_1 = 100$ seconds; $(\alpha\omega_m T_1)/\pi = 2000$; $m \approx 5(\log 2000) \approx 50$ cycles.

(b): $\alpha = 0.5$; $\omega_m = 2\pi \times 100$ rad/second; $T_1 = 5$ seconds; $(\alpha\omega_m T_1)/\pi = 500$; $4^m = 500$; $m \approx 5$ cycles.

[Packets near the center do not yield exactly zero signal, since when $S_z < 0$ relaxation is slightly faster than when $S_z > 0$. If we let $t_1 = t_2$,

$$S_N = S_{N+1} \approx -\frac{\alpha\dfrac{t_1 + t_2}{2T_1} + \frac{1}{4}\left(\dfrac{t_1 + t_2}{T_1}\right)^2}{2\alpha + \dfrac{t_1 + t_2}{T_1}} S_0,$$

and the signal due to these packets is of the second order. Spin packets at the center of the modulation cycle have been discussed in detail by Salpeter.[4]]

Using the result $S_N \approx \pi S_0/(\alpha\omega_m T_1)$, we have

$$\chi_f' \approx \frac{\chi_0 H_0}{\alpha\omega_m T_1} h(H_0' - H_0) \ln \frac{10H_m}{H_1}.$$

(χ'' is small).

This approximate result is derived as follows. The signal due to each packet is

$$\chi' = \frac{S_0}{2H_1} \frac{\pi}{\alpha\omega_m T_1},$$

where H' is the field at which the spin packet resonates and H_0 is the magnetic field at the instant at which the modulation field is zero. Superimposing the signals of the various packets,

$$\chi' \propto \int_{H_0 - H_m}^{H_0 + H_m} \frac{\dfrac{H_0 - H'}{H_m}}{\sqrt{1 + \left(\dfrac{H - H'}{H_1}\right)^2}} dH'$$

if the signal due to packets with $H' > H_0 + H_m$ or $H' < H_0 - H_m$ can be neglected (it can, if $H_m \gg H_1$). This expression has its maximum when $H = H_0 + H_m$. For it, the integral is

$$\frac{H_1}{H_m} \int_{H_0 - H_m}^{H_0 + H_m} \frac{H_0 - H'}{\sqrt{H_1^2 + (H_0 + H_m - H')^2}} dH' \approx H_1 \log \frac{4eH_m}{H_1}.$$

Now, since $S_0 = \chi_0 H h(H - H_0')$, we have, approximately,

$$\chi_f'(H) \approx \chi_0 H \frac{h(H - H_0')}{\alpha\omega_m T_1} \ln \frac{10H_m}{H_1}.$$

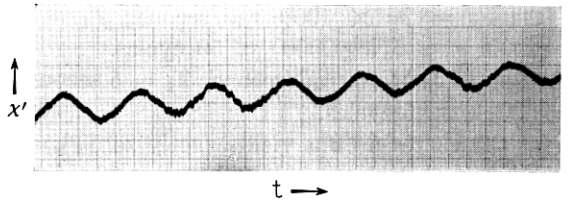

Fig. 35 — χ' of case 7 (no phase sensitive detector used.) Compare with Fig. 34.

Experimental Data

See Fig. 35.

Data: χ'; *no* phase-sensitive detection; $H_1 \approx 1/100$ gauss; "H_m" = 0.8 gauss; dH/dt = 0.8 gauss/second; T = 4.5°K (triangular sweep).

Interpretation: This trace corresponds to Fig. 34.

6.8 *Case 8 — Rapid Adiabatic Passage with a Short Time Between Consecutive Field Modulation Cycles, the Magnetization of the Spin Packets Being Completely Destroyed*

Physical Description

In this case, the loss of magnetization per sweep is large, or T_1 is

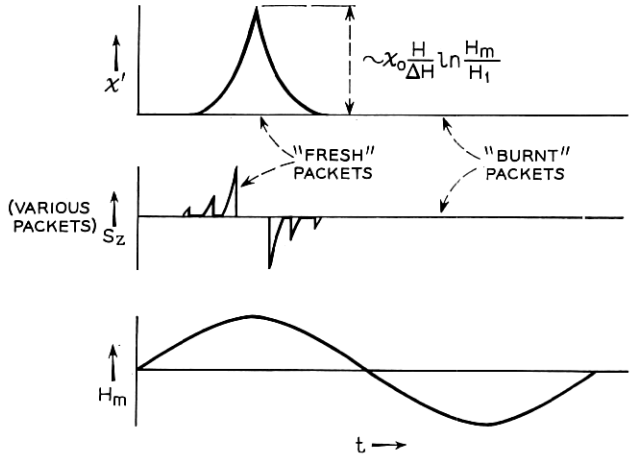

Fig. 36 — The contribution of the various spin packets to a "case 8" signal: spin packets near the extremum of the field modulation cycle have not been swept many times, and thus are not "burnt out"; packets further removed from the extremum are partly, or completely, burnt.

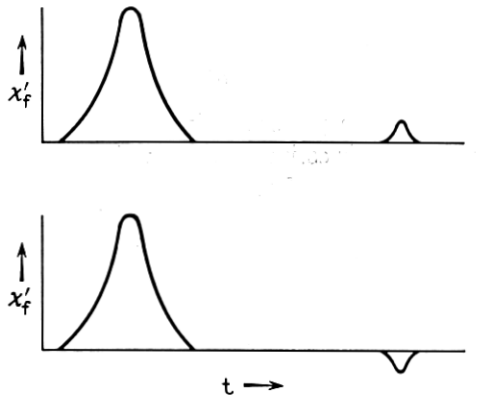

Fig. 37 — Expected recorder traces of case 8 signals: the line is burnt while sweeping through, consecutive sweeps yield weaker lines; their sign depends upon T_1, the time between consecutive sweeps, and the extent to which the line is "burnt out."

long, and the line burns out rather completely, and fast. Most signal is due to "fresh" packets covered by the advancing, modulated field.

Conditions Under Which This Case Is Observed:

$\gamma H_1\sqrt{T_1T_2} \gg 1$; $\gamma H_1^2 \geqq \omega_m H_m$; $\omega_m T_1 \gg 1$; $H_m \gg H_1$; $\alpha\omega_m \Delta H \gg dH_0/dt \gg H_m/T_1$; (the last condition ensures that the signal due to this case exceeds those of cases 5 and 7).

Traces

Since only the packets near the advancing extremum of the modulation cycle are not burnt, the χ' trace is as shown in Fig. 36. The output of the phase-sensitive detector is an "absorption" signal. When we sweep the line again after a time short compared with T_1, it is *saturated* and we get little response (Fig. 37). The χ'' signal again is small. It may be due to slow passage near the extremum, or nonadiabaticity; however, it is *not* at the second harmonic of the field modulation frequency.

Amplitudes

The χ' amplitude is

$$\chi_f' \approx \chi_0 H_0 h(H - H_0') \frac{dH_0}{dt} \frac{2\pi}{\alpha\omega_m} \ln\left(\frac{2\pi \frac{dH_0}{dt}}{\alpha\omega_m H_1}\right)$$

if the loss of magnetization per sweep is constant. (However, this is a very bad assumption.) This estimate is derived as follows:

If the burnout per cycle is α, after N passages of a packet its magnetization will be down by $(1 - \alpha)^N \approx e^{-\alpha N}$. Thus, the shape of the magnetization versus t curve, for a given modulation cycle, is approximately as shown in Fig. 38:

$$\chi_{\text{peak}}' \approx \chi_0 H h(H - H_0') \int_{-\infty}^{\infty} \frac{e^{-\left|\frac{\alpha\omega_m H'}{dH_0/dt\,\pi}\right|}}{\sqrt{1 + \left(\frac{H - H'}{H_1}\right)^2}} \frac{dH'}{H_1}$$

$$\approx 2\chi_0 H h(H - H_0') \ln\left(\frac{2\pi \frac{dH_0}{dt}}{\alpha\omega_m H_1}\right).$$

If the width of the distribution is small, the component of χ' at the field modulation frequency is about $(1/\pi)\chi_{\text{peak}}' \times$ (width of distribution). Or, about

$$\chi_f' \approx \frac{dH_0}{dt} \frac{2}{\alpha\omega_m H_m} (\chi_0 H) h(H - H_0') \ln\left(\frac{2\pi \frac{dH_0}{dt}}{\alpha\omega_m H_1}\right)$$

for $H_m \alpha\omega_m \gg dH_0/dt$.

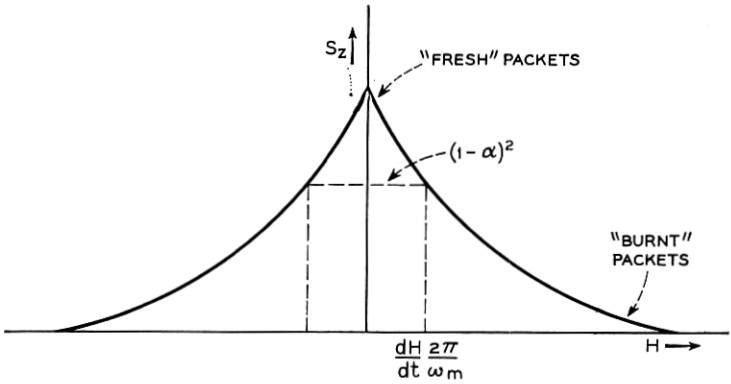

Fig. 38 — Magnetization in the range of one modulation cycle, case 8 (or 11): spin packets at the extremum of the field modulation cycle are not burnt out, while those removed from it are.

However, if the width becomes larger, there is no longer the linear dependence of χ' on dH_0/dt. In addition, α can by no means be considered constant. For $H_m \alpha \omega_m \approx dH_0/dt$, the width of the distribution will be of order H_m, and we may expect a signal of the order $\chi'_{\text{peak}} H_m$, or, very roughly, $\chi' \approx (\chi_0 H) h(H - H'_0) \ln H_m/H_1$.

Some experimental data concerning the dependence of χ' upon dH_0/dt and H_m are given in Section 6.12.

Experimental Data

See Fig. 39.

Data: $H_1 \approx 1/300$ gauss; $\omega_m = 2\pi \times 100$ rad/second; $H_m = 0.3$ gauss; $dH_0/dt = 3.2$ gauss/second; $T = 1.2°$K. Top trace is χ''; center and bottom traces are χ' with opposite values of dH_0/dt.

Conditions satisfied: $H_1, H_m \ll \Delta H$; $\gamma H_1 \sqrt{T_1 T_2} \gg 1$; $\gamma H_1^2 \geqq \omega_m H_m$; $\omega_m T_1 \gg 1$ ($\gamma H_1^2 \approx 200$; $\omega_m H_m \approx 200$).

Interpretation: These photographs correspond to the predicted traces of Fig. 36. The χ'' trace is weak and may be a spurious χ' signal (i.e., the bottom trace, weaker and inverted).

6.9 *Case 9 — Rapid Nonadiabatic Passage with a Short Time Between Consecutive Field Modulation Cycles and Very Rapid Field Sweep*

Physical Description

In this case, each packet is traversed very rapidly, so that the passage

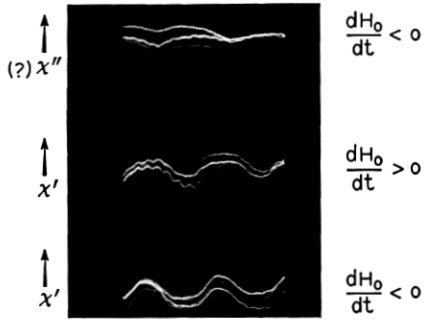

Fig. 39 — Experimental scope traces corresponding to case 8 (compare with Fig. 36): the χ'' trace is probably a spurious χ' signal; the signal here is weak, so the signal-to-noise ratio is not good.

is not adiabatic, and the burnout is small. The signal will be the superposition of "wiggles" treated in Section V.

If $T_2 \ll 1/\omega_m$,† the packets are initially aligned along the z-axis, and we may use the results of Section V straightforwardly. If T_2 is longer, there will be some "wiggles," but these will be rapidly averaged out by the limited bandwidth of the system. (For a more detailed treatment, see Appendix C.)

The χ'' signal is proportional to $h(H - H_0')$, so the component at the field modulation frequency is proportional to the derivative of the line shape and, similarly, that of χ' is roughly proportional to the second derivative of the line shape.

In the moderately nonadiabatic case, in the region for which $\gamma H_1^2 \approx dH/dt$, there is immediate burnout, and a "nonburnt" case is probably impossible.

Conditions Under Which This Case Is Observed:

$\gamma H_1^2 \lll \omega_m H_m$; $\gamma H_1 \sqrt{T_1 T_2} > 1$; $(\gamma H_1^2/(dH_0/dt)).(H_1/H_m) \lll 1$ (little burnout).

Traces

See Figs. 3(a) and 3(b).

Amplitudes

As in case 4,

$$\chi' \cong \frac{1}{2}\frac{H}{\Delta H}\chi_0\frac{H_m}{\Delta H}; \qquad \chi'' \cong \frac{1}{2}\frac{H}{\Delta H}\chi_0\frac{H_m}{\Delta H}.$$

This case requires an extremely low H_1 and fast sweep. Both these factors contribute to the degradation of the signal-to-noise ratio.

6.10 *Case 10 — Rapid Nonadiabatic Passage with a Short Time Between Consecutive Field Modulation Cycles — the Stationary Case*

Physical Description

Each packet is passed almost suddenly. Equilibrium conditions have time to establish (very small dH_0/dt).

Note that if the passage is nonadiabatic, **S** is not inverted. All packages will have the same times to relax in the same direction.

† Here, T_2 is not T_{2e} (as at beginning of Section VI), but the zero of field T_2 .

The fractional amount of magnetization cut off during a nonadiabatic passage is $\pi[\gamma H_1^2/(dH/dt)]$ (Section III). Thus, during those parts of the field modulation cycle in which the field varies fast, less will be cut off (see Fig. 40).

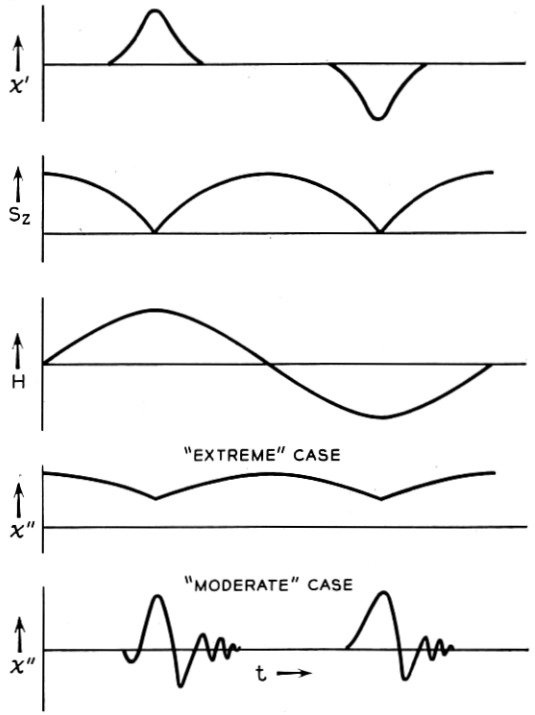

Fig. 40 — Expected scope traces of case 10: χ' depends critically upon *variations* of S_z ; these may be due to "burnout," or the derivative of the line shape; here, variations due to burnout are postulated.

The χ' signal has a sign depending on

$$\frac{dH}{dt}\frac{d\,|S|}{dH},$$

so that it will be as shown in Fig. 40, while χ'', which is proportional to $|S|$, will be mainly at the second harmonic frequency.

Conditions Under Which This Case Is Observed:

$\gamma H_1^2 \ll \omega_m H_m$; $\gamma H_1\sqrt{T_1T_2} \gg 1$; $\omega_m T_1(\gamma H_1^2/\omega_m H_m)$ not too large; $dH_0/dt \ll \omega_m H_m$; $H_m \ll \Delta H$.

(If this last condition is not fulfilled, we shall often have case 9, or a mixture of cases 9 and 10.)

Traces

See Fig. 40. In the moderate nonadiabatic case, the signal from the adiabatic portions near the extrema of the modulation cycle, may overwhelm that of the nonadiabatic ones.

Amplitudes

In the "moderate" nonadiabatic case (γH_1^2 is smaller than $\omega_m H_m$, but not very much), the amplitude will be about the same as in case 7. The reason for this is that, at the extrema of the modulation cycle, $dH/dt \ll \omega_m H_m$, so that we may have $dH/dt < \gamma H_1^2$ there, and the adiabatic condition fulfilled — and these regions yield most of the contribution to the χ' signal.

In the "extreme" nonadiabatic case ($\gamma H_1^2 \lll \omega_m H_m$), let $\alpha = \pi[\gamma H_1^2/(dH/dt)]$, and use the formula in Section 6.7:

$$S_N = \frac{S_0}{\frac{\alpha\omega_m T_1}{\pi} + 1} \approx \frac{\pi S_0}{\alpha\omega_m T_1} = \frac{|\, dH/dt \,|\, S_0}{\gamma H_1^2 \omega_m T_1}.$$

Differentiating with respect to H,

$$\frac{dS_N}{dH} = \frac{d^2H/dt^2}{(dH/dt)\gamma H_1^2 \omega_m T_1}\chi_0 H = \pm\cot\omega_m t \frac{\chi_0 H}{\gamma H_1^2 T_1}$$

since

$$H = H_0 + H_m \cos\omega_m t.$$

Note that this relation holds only for $dH/dt > \gamma H_1^2$, or

$$\omega_m H_m |\sin\omega_m t| > \gamma H_1^2, \quad |\sin\omega_m t| > \frac{\gamma H_1^2}{\omega_m H_m}.$$

From the result of Section V,

$$\chi = \tfrac{1}{2} H \chi_0 \frac{d\text{“}h\text{”}}{dH}\Delta H,$$

where "h" may be any "line shape" — here it is the "shape" due to the burnout of spin packets — and

$$\frac{d\text{“}h\text{”}}{dH} = h(H - H_0')\cot\omega_m t \frac{1}{\gamma H_1^2 T},$$

where $h(H - H_0')$ (without quotation marks) is the true line shape. Thus,

$$\chi' = \tfrac{1}{2}H\chi_0 h(H - H_0') \cot \omega_m t \left(\frac{1}{\gamma H_1^2 T_1}\right) \times \text{width of distribution.}$$

The width of the magnetization distribution will be of order H_m (see Fig. 40), so that

$$\chi' \approx \tfrac{1}{2}H\chi_0 h(H - H_0') \cot \omega_m t \left(\frac{1}{\gamma H_1^2 T_1}\right) H_m ,$$

and the component at the modulation frequency is roughly

$$\chi_f' = \tfrac{1}{2}H\chi_0 h(H - H_0') \frac{H_m}{H_1} \frac{1}{\gamma H_1 T_1} \int_{\gamma H_1^2/(\omega_m H_m}^{\pi/2} \cot \omega_m t \cos \omega_m t \, d(\omega_m t)$$

$$= \tfrac{1}{2}H\chi_0 h(H - H_0') \frac{H_m}{H_1} \frac{1}{\gamma H_1 T_1} \ln\left(\frac{2\omega_m H_m}{e\gamma H_1^2}\right).$$

Here, χ'' is approximately that of the nonburnt case, multiplied by $\pi/(\alpha\omega_m T_1)$:

$$\chi'' \approx \chi_0 H h(H - H_0') \frac{\pi}{\gamma\omega_m T_1} \frac{H_m}{\Delta H}.$$

Comment

If γH_1^2 is very small compared with $\omega_m H_m$, we have little burnout even near the extrema of the modulation cycle. If γH_1^2 is of the order $\omega_m H_m$ (or slightly smaller), the passage near the extrema of the modulation cycle is adiabatic, and this case does not apply either. Therefore, this case is difficult to create experimentally.

6.11 *Case 11 — Rapid Nonadiabatic Passage with a Short Time Between Consecutive Field Modulation Cycles, the Magnetization of the Spin Packets Being Completely Destroyed*

Physical Description

In this case, the adiabatic condition $\gamma H_1^2 > dH/dt$ is violated. In addition, the magnetization is destroyed during the passage, and most of the contribution to the signal comes from spin packets that have not been swept over many times. The general considerations concerning the "stale" case 10, apply here too.

Again, we must distinguish between the "moderately" nonadiabatic case, in which the passage near the extrema of the modulating field is

adiabatic, and the extreme nonadiabatic case in which γH_1 is *very* small compared with $\omega_m H_m$.

The moderate nonadiabatic case is essentially the same as case 8, the adiabatic fresh case. This case applies, if the width of the nonburnt region (Fig. 38) is limited by the adiabatic condition $dH/dt = \gamma H_1^2$, or if it is narrower. Since the burnout α is a very indefinite quantity, a theoretical estimate is very unreliable. However, the width of the burnt region can *very* easily be determined from the oscilloscope trace.

The extreme nonadiabatic case is much more difficult to treat. It should be noted that, near the extrema of the modulation cycle, dH/dt is extremely nonuniform, and it is not always clear whether solutions obtained assuming *constant* dH/dt apply here. Some of the considerations are given in Appendix C.

Conditions Under Which This Case Is Observed:

$\gamma H_1^2 < \omega_m H_m$; $\gamma H_1 \sqrt{T_1 T_2} \gg 1$; $\omega_m T_1 \gg 1$; $\gamma H_1^2/\omega_m H_m$ not too small compared with unity (otherwise we have case 9) $(dH_0/dt)/\omega_m H_m$ not too small compared with unity (otherwise we have case 9 or 10).

Traces

For the extreme nonadiabatic case, see Appendix C. For the moderately nonadiabatic case, the traces are exactly the same as for case 8 (Figs. 36 and 37).

Amplitudes

For the moderate case, the amplitudes are the same as for case 8. The signal of the extreme case is difficult to estimate. For some considerations, see Appendix C.

Experimental Data

(*a*) *Fig. 41(a).*

Data: χ' Signal; $H_1 \approx 1/100$ gauss; $\omega_m = 2\pi \times 1000$ rad/second; $H_m = 1$ gauss. Sweep rate: 1 gauss/second; $T = 1.2$°K. Top trace: light off, opposite signs of dH_0/dt; center and bottom traces: light shining on the sample, relaxing it (see Feher[12]).

Conditions satisfied: $\gamma H_1 T_1 \gg 1$; $\omega_m T_1 \gg 1$; $\omega_m H_m > \gamma H_1^2$. Number of times each packet is swept through: about 4000 ($\gamma H_1^2 \approx 2000$; $\omega_m H_m \approx 6000$).

Interpretation: This is a "moderately" nonadiabatic case; i.e., $\gamma H_1^2 <$

$\omega_m H_m$ but not $\gamma H_1^2 \lll \omega_m H_m$. At the extrema of the modulation cycle, the adiabatic condition is satisfied, and thus the trace of this case is indistinguishable from case 8 (see Fig. 39).

(*b*) *Fig. 41(b)*.

Data: $H_1 \approx 1/1000$ gauss; $\omega_m = 2\pi \times 1000$ rad/second; $H_m = 1/10$

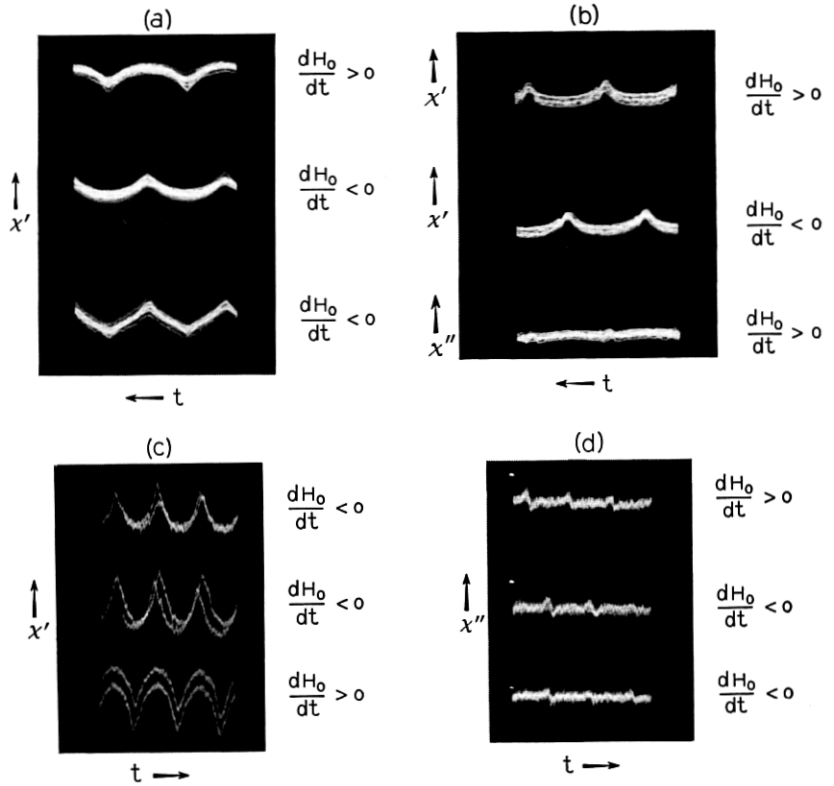

Fig. 41 — (a) Top and center traces: experimental scope χ' trace corresponding to a "moderate" case 11; ($\omega_m H_m > \gamma H_1^2$, but, only the spin packets near the extrema of the modulation cycle are not "burnt," and for these $dH/dt < \gamma H_1^2$); this case is very similar to case 8 — compare with Figs. 36 and 39. Bottom trace: corresponds (essentially) to case 7 (see Fig. 34) indicating that light reduces T_1, but it is still long compared with a field modulation cycle. (b) Experimental scope χ' and χ'' traces of an 'extreme' case 11 ($\gamma H_1^2 \ll \omega_m H_m$); the 'wiggles' are an indication of the nonadiabatic conditions near the extremum of the modulation cycle, where dH/dt is small. (c) χ' scope trace corresponding to case 11, the conditions being very similar to those of (a); however, a lower power reduced losses due to forbidden lines ($\gamma H_1^2/\omega_m H_m$ is the same). Data: $H_1 \approx 1/300$ gauss; $H_m = 1/10$ gauss; $\omega_m = 2\pi \times 1000$ rad/second; $T = 1.2$°K. Top trace: light shining on the sample; center and bottom traces: no light shining on the sample; opposite signs of dH_0/dt. (d) χ'' scope trace corresponding to case 11. Data: $H_1 \approx 1/300$ gauss; $\omega_m = 2\pi \times 1000$ rad/second; $T = 1.2$°K. Top and center traces: light shining on the sample opposite senses of dH_0/dt; bottom trace: no light shining on sample.

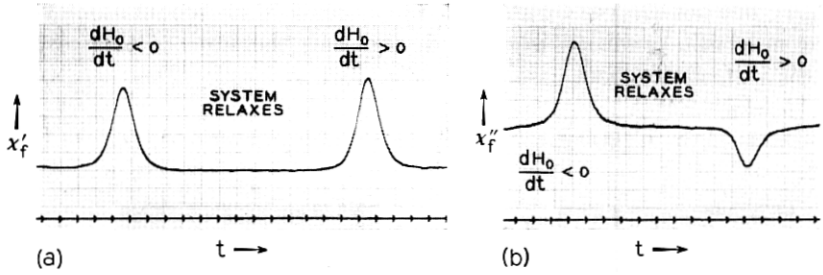

Fig. 42 — (a) χ_f' for case 11, with P.S.D. (compare with Fig. 37); the magnetization was completely burnt out after one passage, so the sample was completely relaxed between consecutive sweeps. (b) χ_f'' for case 11, with P.S.D. Note the different parity of the χ' and χ'' traces.

gauss. Sweep rate: 8 gauss/second; $T = 1.2°$K. Top trace: χ', $dH_0/dt > 0$; center trace: χ', $dH_0/dt < 0$; bottom trace: χ''.

Conditions satisfied: $\gamma H_1 T_1 \gg 1$; $\omega_m T_1 \gg 1$; $\gamma H_1^2 \ll \omega_m H_m$. Number of times each spin packet is swept: about 50 ($\gamma H_1^2 \approx 20$; $\omega_m H_m \approx 600$)

Interpretation: Here the adiabatic condition is more strongly violated, and the "wiggles" can be seen. Also, the reduced H_m reduces the beat frequency between spin packets, which are a fraction of the field modulation cycle out of tune and the microwave signal. This, too, makes the wiggles more easily observable.

(c) *Fig. 42.*

Data: $H_1 \approx 1/1000$ gauss; $H_m = 1/10$ gauss; $\omega_m = 2\pi \times 1000$ rad/second; $T = 1.2°$K. Fig. 42(a): χ_f'; Fig. 42(b): χ_f''. The χ_f' and χ_f'' signals are *not* to the same scale — the gain of the system is 10 db higher for the χ_f'' measurement than for the χ_f' measurement.

Interpretation: These data correspond to Figs. 3(c), 3(d) and 25. There is a slight admixture of χ_f' signal in the χ_f'' trace, due to imperfect adjustment of the bridge. We have a "moderate" nonadiabatic case.

6.12 *Conditions to Maximize Signal*

An experiment was carried out to determine the dependence of the amplitude of the χ_f' signal upon H_1, H_m and dH_0/dt, for cases 9, 11 and neighboring ones.

The 11 cases treated in this section are idealizations, and usually we shall have a case intermediate between them. Thus, quantitative agreement with the formulas given in this section cannot be expected. However, there seems to be qualitative agreement with the theory. The results of the experiments are shown in Fig. 43.

From the dependence of the observed signal strength upon H_1 and H_m it is clearly seen that in order to obtain a strong signal, the adiabatic condition $\gamma H_1^2 > dH/dt$ should be violated, but not by too much (say, roughly $3 < (dH/dt)/\gamma H_1^2 < 10$).

If it is not violated, we do not have much burnout, and thus have cases 5 or 6, which yield quite low signals. If the adiabatic condition is

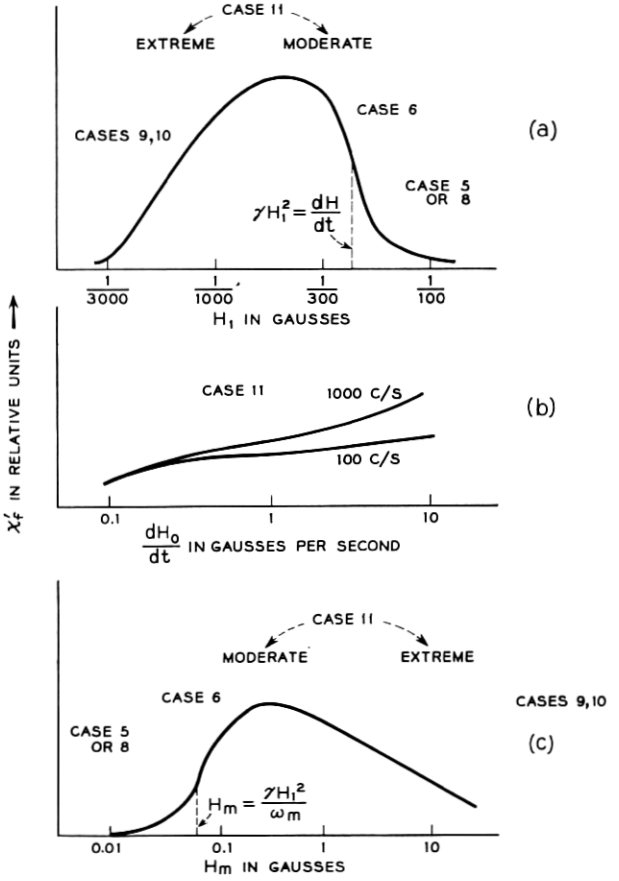

Fig. 43 — Dependence of amplitude of χ'_f signal (as detected by phase sensitive detector) upon H_1, H_m, dH_0/dt, for case 11: (a) Dependence upon H_1. Data: $H_m = 1/10$ gauss; $\omega_m = 2\pi \times 100$ rad/second; $dH_0/dt = 2$ gauss/second; $T = 1.2°K$; concentration, 3.2×10^{15} phosphorus atoms/cc. (b) Dependence upon dH_0/dt. Data: $H_1 = 1/300$ gauss; $H_m = 1/10$ gauss; $T = 1.2°K$; concentration, 3.2×10^{15} phosphorus atoms/cc. (c) Dependence upon H_m. Data: $H_1 \approx 1/300$ gauss; $\omega_m = 2\pi \times 100$ rad/second; $dH_0/dt = \frac{1}{2}$ gauss/second; $T = 1.2°K$; concentration, 3.2×10^{15} phosphorus atoms/cc.

violated too much, we again do not have much burnout, since we have an almost sudden transition (see Fig. 11). We then approach case 9 and case 10, which again yield weak signals.

The dependence of the signal strength upon dH_0/dt is weak. This is due to the fact that, when the burnout is due mainly to the breakdown of the adiabatic condition, the width H' of the unburnt region is given by

$$\left(\frac{dH}{dt}\right)_{H=H'} \approx \gamma H_1^2,$$

and this is independent of dH_0/dt. Of course, when we reduce dH_0/dt, we shall eventually reach a stage when H' becomes smaller, and then χ_f' falls faster when dH_0/dt drops (see formula under *Amplitudes* in Section 6.8).

At 1000 cps the adiabatic condition was well violated, while at 100 cps we have $\gamma H_1^2 \approx dH/dt$. Thus, the burnout at 100 cps is not so efficient, and the 1000-cps signal is stronger, particularly at high dH_0/dt.

When a quantitative agreement between theory and experiment is desired, the following effect must be taken into account. Much of the loss of magnetization at high powers may be due to forbidden lines. This loss does not occur when $\gamma H = \omega$, but at different fields. Thus, one must distinguish between losses occurring "within" the field modulation cycle (at which a given spin packet is swept), i.e., at a field satisfying $| H - \omega/\gamma | < H_m$ and losses occurring "outside" the field modulation cycle, ($| H - \omega/\gamma | > H_m$). The first affect both the amplitude and the "passage case", while the later affect the amplitude only.

Note that the "moderate" case 11 is characterized by a broad maximum in the dependence of χ_f' upon H_1 and H_m, and only slight dependence upon dH_0/dt. This makes it easy to obtain this case by experimentally adjusting H, H_m and dH_0/dt simply for maximum signal.

However, for reliable determination of fine details of line shapes, it is recommended to see to it that $\omega_m H_m/\gamma H_1^2 \approx$ 3–10 and that dH_0/dt is large enough.

VII. THE VARIOUS PASSAGE CASES — DIAGRAMMATIC REPRESENTATIONS AND ADDITIONAL EXPERIMENTAL POINTS

In this section, we attempt to present some hints that may be of aid in the experimental identification of "passage" cases. The section contains a number of diagrams, suggestions and experimental data.

Table II indicates the logical relationship of the various cases, and scope and recorder traces to be expected.

TABLE II — LOGICAL RELATIONSHIP OF THE VARIOUS PASSAGE CASES

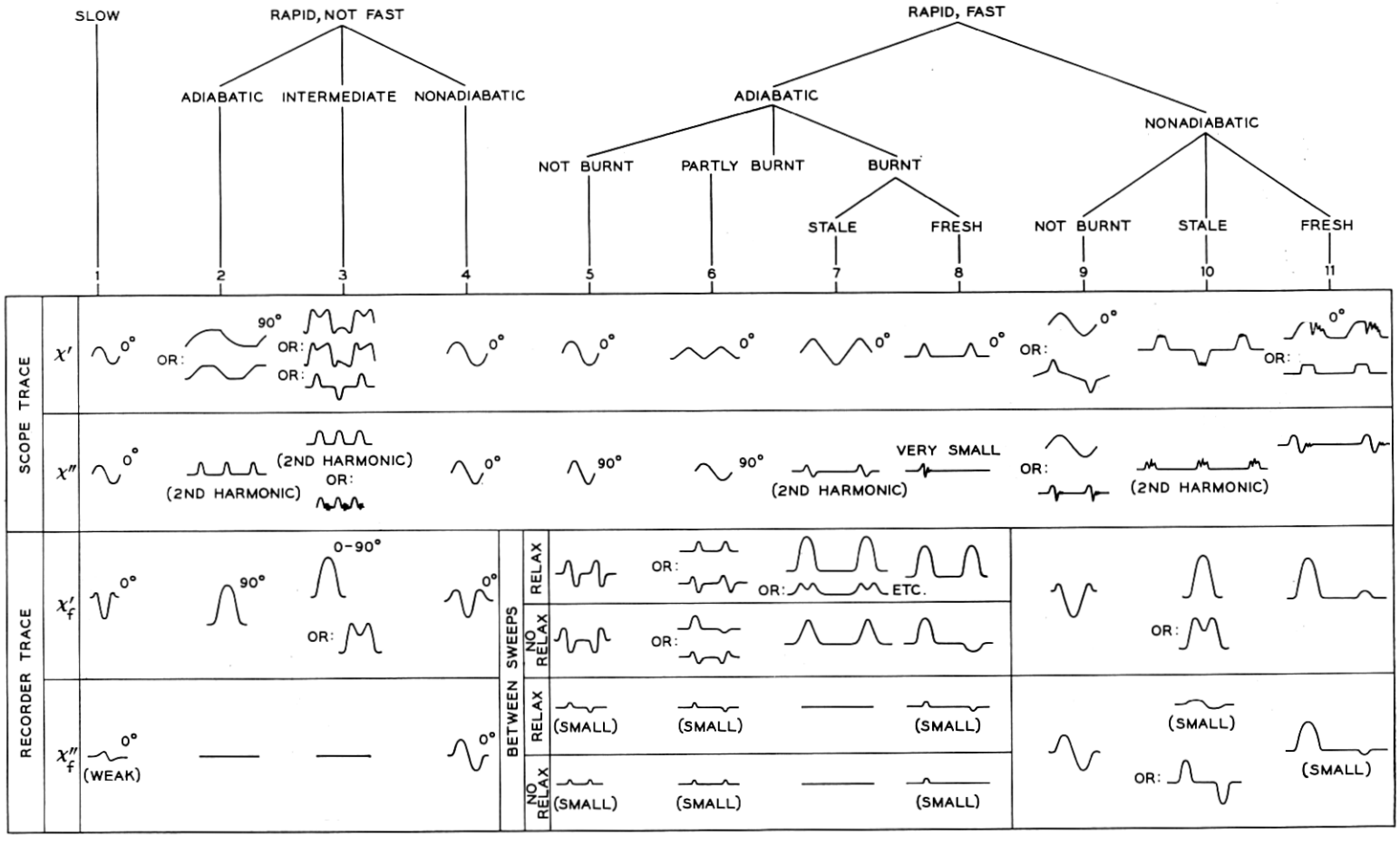

TABLE III — PASSAGE CASES TO BE EXPECTED AT VARIOUS VALUES OF H_1 AND T_1

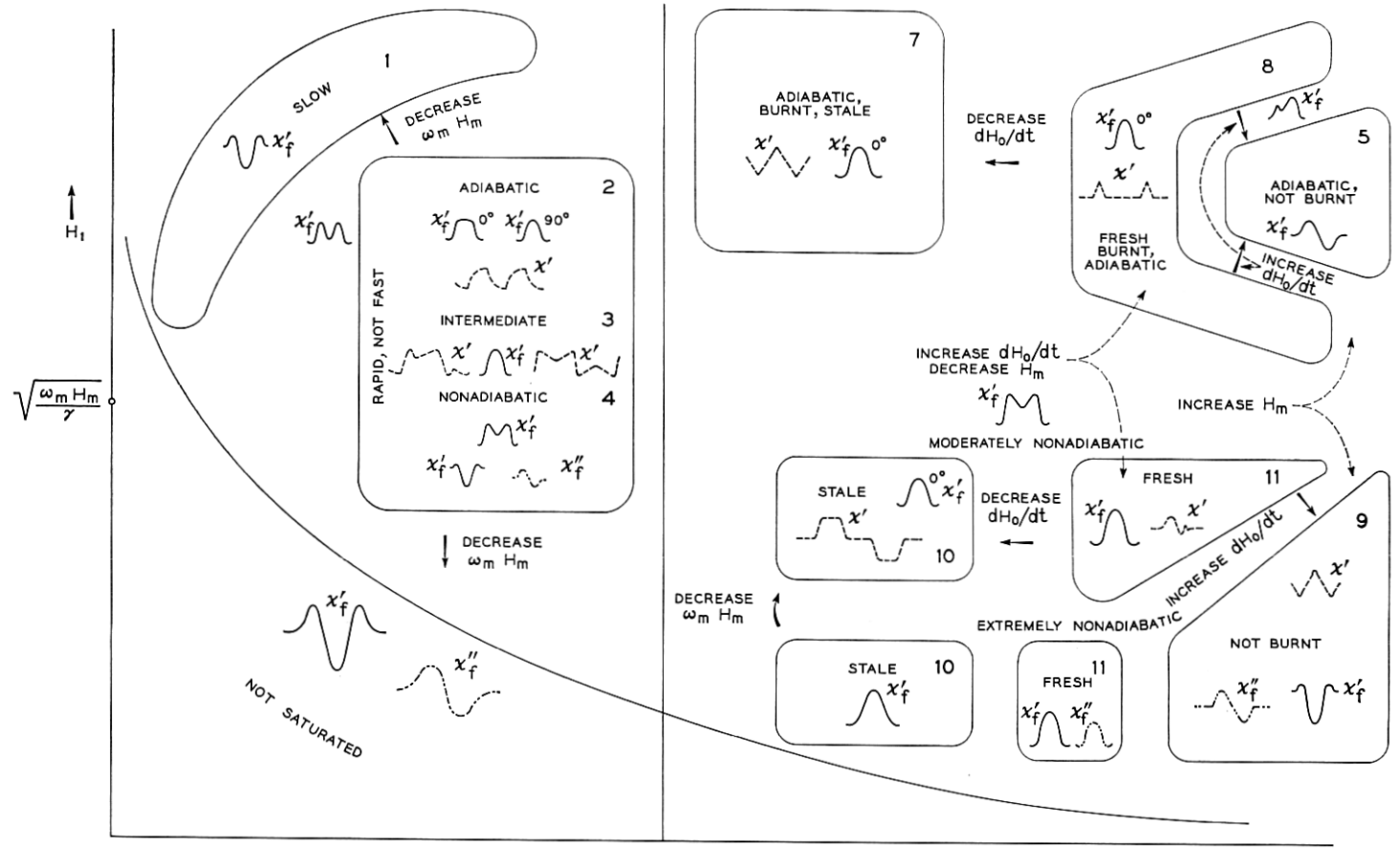

Table III indicates roughly the case to be expected for a given microwave magnetic field H_1 and relaxation time T_1, and the effect of various variations of the parameters upon the shape of the experimental traces.

Table IV indicates roughly the conditions under which each case is to be expected, and approximate values of the amplitudes of the χ_f' and χ_f'' signals.

Experimental Identification of the Passage Case

If nothing is known *a priori*, it is recommended that the scope trace be observed. This trace is obtained by connecting the output of the IF amplifier to the Y amplifier of the oscilloscope. Thermal noise can be reduced by an RC filter. Low-frequency noise often proves much more troublesome and may be reduced as follows: The scope is operated at a *low* time base frequency (about 10 cps) and a high X gain, so that a cycle or two of the modulating field are displayed on the scope screen. Then, successive cycles (which will be displaced vertically from each other, due to low-frequency noise), will be distinguishable and the noise will not wash out the signal.†

On the scope trace, "wiggles" and other sorts of oscillations indicate nonadiabatic conditions.‡ See Fig. 41(b) for a typical picture. "Fresh" cases are also very easily identified (by lack of symmetry between the positive and negative extrema of the modulating field.) "Fresh" cases can also be identified by the reduction of amplitude of successive recorder traces (if the time between them is short compared with T_1.)

Cases 2, 7 and 8 (or 11), which are most common, are particularly easy to identify by the scope trace. Note that the sweep dH_0/dt must be *on*, since the case occurring depends on dH_0/dt, and altering it may yield a different case. The parameters (H_m, H_1, dH_0/dt) may be changed and the effect upon the scope trace yields further information.

Since many different cases possess similar recorder traces (as a matter of fact, χ' traces are either of "absorption" or "dispersion derivative" shapes, or a combination of these two, commonly), extreme care should be exercised in trying to identify a case (or measure T_1, say) using recorder traces *only*.

If H_1 can be estimated, the passage case occurring can be determined approximately, and resort to scope traces can perhaps be avoided. A *direct* method to estimate H_1 is to photograph adiabatic rapid passage

† The appearance of such traces can be seen in Figs. 39, 41(c), and others. Due to the phosphorescense of the CRT screen, a number of preceding traces can be seen too, but these are easy to distinguish from the last trace.

‡ For these to be observed, T_2 must be sufficiently long.

TABLE IV — CONDITIONS UNDER WHICH THE VARIOUS PASSAGE CASES APPLY AND APPROXIMATE SIGNAL AMPLITUDES

Conditions			Case Number	x_f'	x_f''
$\omega_m T_1 \ll 1$	$\gamma H_1^2 > \omega_m H_m$	$T_1 < \dfrac{H_1}{\omega_m \Delta H}$	1	$\chi_0 \dfrac{H_0}{\Delta H} \dfrac{H_m}{\Delta H}$	$\chi_0 \dfrac{H_0}{\Delta H} \dfrac{1}{H_1\sqrt{T_1 T_2}} \dfrac{H_m}{\Delta H}$
		$T_1 > \dfrac{H_1}{\omega_m H_m}$	2	$\chi_0 \dfrac{H_0}{\Delta H} \ln \dfrac{H_m \omega_m T_1}{H_1}$	$\chi_0 \dfrac{H_0}{\Delta H} \dfrac{H_m}{\Delta H} \dfrac{H_m}{H_1} \dfrac{\omega_m}{\gamma H_1}$
	$\gamma H_1^2 < \omega_m H_m$		3	$\chi_0 \dfrac{H_0}{\Delta H} \ln \dfrac{H_m \omega_m T_1}{H_1}$	
	$\gamma H_1^2 \ll \omega_m H_m$		4	$\dfrac{1}{2} \dfrac{H_0}{\Delta H} \chi_0 \dfrac{H_m}{\Delta H}$	$\dfrac{1}{2} \dfrac{H_0}{\Delta H} \chi_0 \dfrac{H_m}{\Delta H}$
	$\gamma H_1^2 > \omega_m H_m$	$\dfrac{\omega_m H_m}{dH_0/dt} \alpha \ll 1$	5	$\chi_0 \dfrac{H_0}{\Delta H} \dfrac{H_m}{\Delta H} \ln \dfrac{2\Delta H}{H_1}$	$\chi_0 \dfrac{H_0}{\Delta H} \dfrac{H_m \omega_m}{\gamma H_1^2}$
		$\dfrac{\omega_m H_m}{dH_0/dt} \alpha \approx 1$	6		small
		$\dfrac{dH_0}{dt} \ll \dfrac{H_m}{T_1}$	7	$\chi_0 \dfrac{H_0}{\Delta H} \dfrac{\ln \dfrac{H_m}{H_1}}{\alpha \omega_m T_1}$	small

$\omega_1 T_1 \gg 1$		$\dfrac{H_m}{T_1} \ll \dfrac{dH_0}{dt} \ll \alpha\omega_m \Delta H$	8	$(\chi_0 H_0/\Delta H) \ln H_m/H_1$ or $\chi_0 \dfrac{H_0}{H} \dfrac{dH_0/dt}{\alpha\omega_m} \ln \dfrac{dH_0/dt}{\alpha\omega_m H_1}$	small
	$\gamma H_1^2 < \omega_m H_m$	$\dfrac{\gamma H_1^2}{dH_0/dt} \dfrac{H_1}{H_m} \lll 1$	9	$\dfrac{1}{2} \dfrac{H_0}{\Delta H} \chi_0 \dfrac{H_m}{\Delta H}$	$\dfrac{1}{2} \dfrac{H_0}{\Delta H} \chi_0 \dfrac{H_m}{\Delta H}$
		$\dfrac{dH_0}{dt} \ll \omega_m H_m$ $\omega_m T_1 \dfrac{H_1^2}{\omega_m H_m} \leqq 1$	10	$\chi_0 H_0 \dfrac{H_m}{\Delta H} \dfrac{\ln \omega_m H_m/\gamma H_1^2}{\gamma H_1^2 T_1}$	$\chi_0 \dfrac{H_0}{\Delta H} \dfrac{H_m}{\Delta H} \dfrac{\pi}{\alpha\omega_m T_1}$
		$\dfrac{dH_0}{dt} \approx \omega_m H_m$ $\omega_m T_1 \dfrac{H_1^2}{\omega_m H_m} > 1$	11	$\chi_0 \dfrac{H_0}{\Delta H} \ln \dfrac{H_m}{H_1}$ or $\chi_0 \dfrac{H_0}{\Delta H} \dfrac{dH_0/dt}{\alpha\omega_m} \ln \dfrac{dH_0/dt}{\alpha\omega_m H_1}$	small

χ' and χ'' transients (if T_1 is large). The ratio of χ'' to χ' peaks is

$$\frac{\frac{dH}{dt}}{\gamma H_1^2} \frac{1}{\ln \frac{2\Delta H}{H_1}}$$

if $\Delta H < (dH/dt)T_1$; otherwise, the ratio is

$$\frac{\frac{dH}{dt}}{\gamma H_1^2} \frac{1}{\ln \frac{2\frac{dH}{dt}T_1}{H_1}}$$

(see Section 6.2, and Appendix D.) From this relation, H_1 can be determined (H_1 occurs under the logarithm too, but there its effect is not large, and a crude approximation will do.)

These photographs can be obtained by letting $H_m > \Delta H$, (say $H_m = 5\Delta H$), switching H_1 off, letting the system relax, switching H_1 on and letting the voltage that switches H_1 on, trigger the scope (switched to "one-shot" operation).

Another way is to set H_m to an extreme position ($+$ or $-$) off the line, letting the line relax, and then switching the modulating field "on."

If T_1 is short (but not too short), it is possible to avoid the use of transients and use steady-state operation. Then, amplitudes can be read from the scope directly, without use of a camera. Of course, H_1 must be in the right range ($\gamma H_1^2 > dH/dt$, but not $\gamma H_1^2 \gg dH/dt$). Since $H_m \gg \Delta H$, dH/dt equals $\omega_m H_m$; thus, γH_1^2 can be determined quite accurately.

If signals at twice the modulation frequency can be detected, χ'' signals due to slow passage near the extrema of the modulation cycle, or due to nonadiabaticity in the middle of the modulation cycle, can be observed. Also, "fresh" cases yield strong second harmonic signals, while "stale" and "nonburnt" cases yield weak second harmonic signals, as illustrated in Fig. 44.

It has been observed experimentally that, if the conditions are adjusted for maximum amplitude, the passage conditions often correspond to case 11.

VIII. CONCLUSION

Abragam[16] states that "If the line is inhomogeneously broadened with a width ΔH, and the modulation and the scanning are defined by

a law $H = H_0(t) + H_m \cos \Omega t$, no less than seven parameters having the dimensions of frequency may be introduced to discuss the shape and the size of the signals observed; namely, $1/T_1$, $1/T_2$, $\gamma \Delta H$, γH_1, γH_m, Ω, $(1/H_1)(dH_0/dt)$. The shape of the signals depends considerably on the relative values of these parameters and may become very complicated. They can, in practice, be analyzed mathematically using Bloch equations, and a considerable literature exists on this subject. However, there is nothing fundamental in the complications of these shapes, and the rather negative conclusion to be drawn from their analysis is the following: whenever the methods of observation are such that a complicated mathematical treatment is required to establish a relationship between the data (signals) and the physical nature of the system studied, the methods of observation are inadequate and must be changed, whenever possible."

The aim of this work is *not* to suggest using the complicated expressions given here to determine T_1, T_2, etc. The expressions are at best of qualitative value. This work attempts rather

i. to determine whether the seven parameters are sufficient to determine the signals (i.e., to determine whether the physical system studied can be described to a sufficient accuracy by the Bloch equations), and

ii. to determine whether line shapes, relative amplitudes, etc., can be determined in a reliable way under certain (complicated) relationships

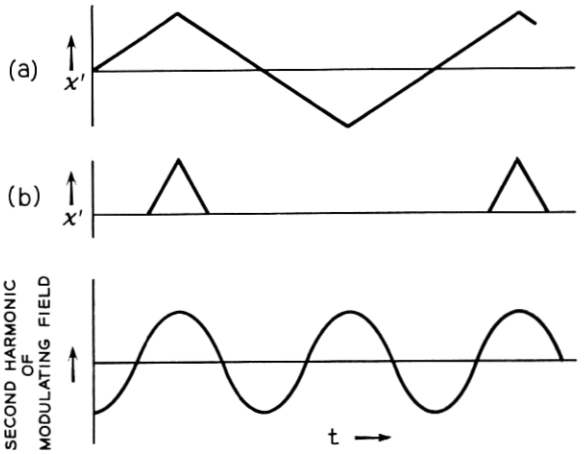

Fig. 44 — Demonstration of the strong harmonic content of "fresh" signals: (a) χ' of case 7 (stale); (b) χ' of case 8 (fresh). Note that the "stale" signal possesses only odd harmonics of the magnetic field modulation frequency, while the "fresh" signal possesses a strong second harmonic component.

between the variables (under conditions that insure a good signal-to-noise ratio) and, if they can, to determine the right conditions for this purpose.

Concerning i, it was found that forbidden lines had a drastic effect upon the signals observed here. With other samples, spin diffusion processes might become very important. Therefore, inhomogeneously broad-

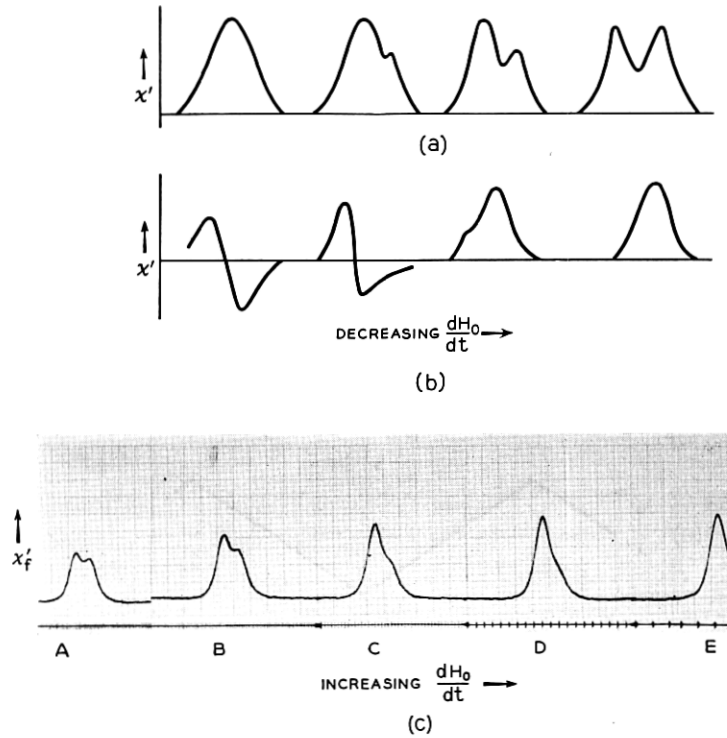

Fig. 45 — Expected and observed recorder χ'_f signals of various hybrid cases: (a) Transition from case 11 to case 10 (or 9) upon reduction of dH_0/dt. Note that, in the "fresh" cases, the line is shifted by an amount H_m , due to the fact that the *leading* edge of the field modulation cycle yields the signal; in the "stale" and "unburnt" cases, the line is broadened, but not shifted. Thus, for $H_m/\Delta H$ not very small, a hybrid between a "fresh" and "nonfresh" case will yield an unsymmetrical line; increasing $\omega_m H_m/\gamma H_1^2$ will *reduce* the burnout and tend to produce case 9; increasing $H_m/\Delta H$ has the same effect. Therefore, increasing H_m has a very large effect in producing "splitting" of a line. (b) Transition from case 5 to case 8 (or 7) upon decrease of dH_0/dt. (c) Experimental change of shape of χ' trace upon increase of dH_0/dt. Data: $H_1 \approx 1/300$ gauss; $H_m = 1$ gauss; $\omega_m = 2\pi \times 1000$ rad/second; $T = 1.2°K$; $dH_0/dt \approx 1/10$ gauss/second (A), 1/5 gauss/second (B), 2/5 gauss/second (C), 1 gauss/second (D) and 2 gauss/second (E).

ened lines can be described by the Bloch equations only under very specialized conditions.

Concerning ii, it appears that conditions can be found under which an undistorted line can be observed, with a good signal-to-noise ratio, for *any* T_1. For short T_1's, nonsaturated conditions can be maintained. For very long values of T_1, slightly nonadiabatic conditions should be maintained, and a linear field sweep that is fast enough to avoid any traces of line splitting (see Fig. 45). This set of conditions is discussed in Section 6.12. The amplitude of the signal under these conditions depends upon the external variables H_m, ω_m, dH_0/dt and H_1, but very little upon T_1 and T_2, if they are sufficiently long.

Experiments to check this were carried out, and will be reported elsewhere. It is concluded that the "moderate nonadiabatic" case 11 is quite reliable in determination of relative intensities of different lines and fine details of line shapes.

IX. ACKNOWLEDGMENTS

This work was carried out under the supervision and with the constant help of G. Feher. In many of the experiments the writer was assisted by E. Gere. The writer also profited from discussions with W. Blumberg, and suggestions made by P. W. Anderson.

X. NOTATION

$a \equiv$ Hyperfine interaction (except in Appendix C).
$b \equiv$ Dipolar interaction between an electron and a nucleus.
$H \equiv$ Magnetic field in the z-direction at any instant.
$H_0' \equiv$ Magnetic field at the center of an inhomogeneously broadened line.
$H_0 \equiv$ Magnetic field at the center of a spin packet, or at the center of the field modulation cycle.
$H' \equiv$ The width (on the H scale) of a nonsaturated spin packet distribution.
$H_1 \equiv$ Component of rotating magnetic field, perpendicular to the z-direction.
$H_m \equiv$ Peak modulating magnetic field (in the z-direction).
$\Delta H \equiv$ Width of inhomogeneously broadened line (defined as the second moment of the line).
$dH/dt \equiv$ Instantaneous value of time derivative of the magnetic field.
$dH_0/dt \equiv$ Magnetic field sweep (assumed constant).

$h(H - H_0')$ ≡ Shape function of inhomogeneously broadened line, normalized to unity: $\int_{-\infty}^{\infty} h(H - H_0')\, dH = 1$.

$\mathbf{i}, \mathbf{j}, \mathbf{k}$ ≡ Unit vectors along the coordinate axes.

J ≡ Exchange integral.

k ≡ $(1/H_1)(dH/dt)$, assumed constant or slowly varying.

k ≡ Boltzman's constant.

N ≡ Number of field modulation cycles.

s_e ≡ Electron spin.

s_n ≡ Nuclear spin.

$\mathbf{S}$ ≡ Magnetization vector.

S_x, S_y, S_z ≡ Components of magnetization vector.

$|S|$ ≡ Absolute value of magnetization vector.

S_0 ≡ Equilibrium value of magnetization vector.

S_N ≡ Absolute value of magnetization vector after N field modulation cycles.

t ≡ Time.

T_1 ≡ Longitudinal relaxation time.

T_2 ≡ Transverse relaxation time.

T ≡ Period of modulating field.

T ≡ Temperature.

u, w, p, q, x ≡ Dimensionless integration variables.

x, y, z ≡ Cartesian coordinates in space, or $z = x + iy$ coordinates in the complex plane.

α ≡ Fractional loss of magnetization during rapid passage (except in Appendix E).

γ ≡ Gyromagnetic ratio.

δ ≡ $H - H_0/H_1$.

ϵ ≡ $\mu_e H/kT$.

θ, φ ≡ Spherical coordinates.

μ_e ≡ Magnetic moment of electron.

μ_n ≡ Magnetic moment of nucleus.

χ' ≡ $S_x/2H_1$.

χ_f ≡ Component of χ' at magnetic field modulation frequency.

χ'' ≡ $S_y/2H_1$.

χ_f'' ≡ Component of χ'' at magnetic field modulation frequency.

ω ≡ Microwave angular frequency.

ω_m ≡ Angular frequency of magnetic field modulation.

$\Delta\omega$ ≡ Difference in resonant angular frequencies of two electrons.

$\Delta\omega_{sys}$ ≡ Bandwidth of system.

APPENDIX A

χ' and χ'' for a Single Spin Packet, for Long Relaxation Times

A.1 Approximations for Long Relaxation Times

The Bloch equations are three equations in three variables, S_x, S_y, S_z and thus are difficult to solve. They can be solved relatively easily, if one variable can be eliminated. The "conventional" method is to eliminate S_z. For a sudden passage, we let S_z be a constant and for an adiabatic passage: $S_z = (\delta/\sqrt{1+\delta^2})S_0$, say. Once we know S_z, then S_x and S_y can be combined to one complex variable $S_x + iS_y$, and we have one linear first-order differential equation with one complex variable, which is integrable by quadratures.†

However, in a region intermediate between adiabatic and sudden passages, particularly for the transient solution, this method does not work.

If T_1, T_2 are long, the Bloch equations are in the rotating frame,

$$\frac{\partial S}{\partial t} = -\gamma H_1 \sqrt{1+\delta^2}\left[\frac{\mathbf{i} + \delta\mathbf{k}}{\sqrt{1+\delta^2}} \times \mathbf{S}\right];$$

i.e., $|S|$ is a constant and S moves on the surface of a sphere. Thus, S can be described by *two* variables — say, the spherical coordinates θ and φ, and the third variable is eliminated. But if we write the Bloch equations in terms of spherical coordinates, they are practically unmanageable.

However, a *portion* of the surface of a sphere can be covered quite accurately by a rectangular coordinate system. In the sudden case, S is limited to a region in the vicinity of the "north pole." In the adiabatic case, it is limited to a narrow strip from the north pole to the south pole along the $\varphi = 0°$ longitude. Even if $\gamma H_1^2 = dH/dt$, S will be in the "northern" hemisphere, which can reasonably well be covered by a cartesian net.

Thus, in any case the relevant portions of the sphere can be covered by a rectangular net. Using these coordinates, the Bloch equations are *two* linear first-order equations in two variables, which can be combined to *one* in one complex variable, which is soluble by quadratures. This solution, though only approximate for $\gamma H_1^2 \approx dH/dt$ does not break down for any ratio of these parameters. Of course, in the adiabatic and sudden cases it reduces to the well-known solutions.

In the intermediate case, S_x, S_y, S_z can be written down explicitly in terms of a relatively simple integral for which there seems to be no

† A more detailed discussion of this point is given by Salpeter.[4]

tabulated functions, but which may be evaluated numerically quite easily.

The Bloch equations are:

$$\frac{\partial S}{\partial t} = -\gamma H_1 \delta (\mathbf{k} \times \mathbf{S}) - \gamma H_1 (\mathbf{i} \times \mathbf{S})$$

$$= -\gamma H_1 \sqrt{1 + \delta^2} \left(\frac{\mathbf{i} + \delta \mathbf{k}}{\sqrt{1 + \delta^2}} \times S \right)$$

(H_0 in z-axis direction, H_1 in x-axis direction). So, $| S |$ = constant = S_0 and $\mathbf{S}$ moves on the surface of a sphere (see Fig. 46); $\partial \mathbf{S}/\partial t$ is perpendicular to $\mathbf{r}$, where

$$\mathbf{r} = \frac{\mathbf{S}}{S_0} - \frac{\mathbf{i} + \delta \mathbf{k}}{\sqrt{1 + \delta^2}},$$

and is of magnitude $\gamma H_1 \sqrt{1 + \delta^2} \, | \mathbf{r} |$. Note that cot $\theta = -\delta$ (θ = polar angle). Now, in case the adiabatic condition is satisfied, S will move along the $\varphi = 0$ longitude. While, if $\gamma H_1^2 \ll dH/dt$, ("sudden" case), S will remain close to the "north pole." In both cases, a *cartesian* coordinate system can cover those portions of the sphere in which S and the effective field move, and the metric will be closely Euclidean, since the

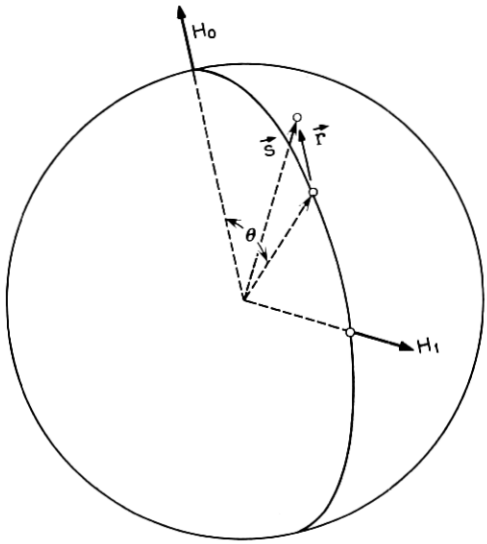

Fig. 46 — Position of magnetization vector in space.

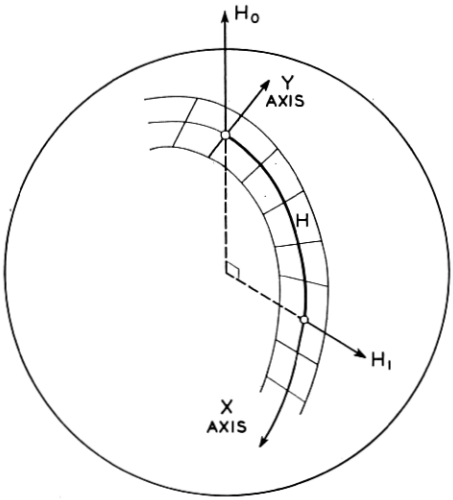

Fig. 47 — Almost-cartesian coordinate net covering a part of a sphere.

regions are "narrow" (see Fig. 47). In this coordinate system,

$$\frac{dx}{dt} = \gamma H_1 \sqrt{1 + \delta^2}\, y,$$

$$\frac{dy}{dt} = -\gamma H_1 \sqrt{1 + \delta^2}\,(x - x_0) \qquad (x_0 = \theta)$$

(see Fig. 48). Now the xy plane can be considered as the complex z plane, with $z = x + iy$. In it,

$$\frac{dz}{dt} = -i\gamma H_1 \sqrt{1 + \delta^2}\, z + i\gamma H_1 \sqrt{1 + \delta^2}\, x_0.$$

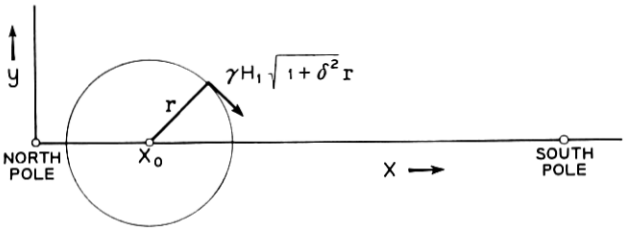

Fig. 48 — Diagram illustrating the differential equation satisfied (approximately) by the magnetization vector.

The differential equation

$$\frac{du}{d\xi} + a(\xi)u = b(\xi)$$

has the general solution:

$$u(\xi) = \exp\left[-\int_{\xi_0}^{\xi} a(\xi')\,d\xi'\right]\int_{\xi_0}^{\xi} b(\xi')\exp\left[\int_{\xi_0}^{\xi} a(\xi'')\,d\xi''\right]d\xi' + u(\xi_0)\exp\left[-\int_{\xi_0}^{\xi} a(\xi')\,d\xi'\right].$$

In our case, at $t = -\infty$, $z = 0$. Assume for simplicity a linear change in δ: $\delta = kt$, with $k = (1/H_1)(dH/dt)$. Then,

$$z = -\exp\left(-i\gamma H_1\int_{-\infty}^{t}\sqrt{1+k^2t'^2}\,dt'\right)\int_{-\infty}^{t} i\gamma H_1\sqrt{1+k^2t'^2}\,\text{arc cot } kt' \cdot\exp\left(i\gamma H_1\int_{-\infty}^{t'}\sqrt{1+k^2t''^2}\,dt''\right)dt'.$$

Since $x_0 = \theta = -arc\ \cot\ \delta$, where the branch of the *arc* cot function used throughout this calculation is the one for which *arc* cot $(-\infty) = 0$, then *arc* cot $(\infty) = -\pi$.

The "susceptibilities" are:

$$\chi' = \frac{1}{2}\frac{\omega\chi_0}{\gamma H_1}\sin(\text{Re } z), \qquad \chi'' = \frac{1}{2}\frac{\omega\chi_0}{\gamma H_1}\text{Im } z$$

in our approximation [(Im z) $\ll 1$, if the sphere is the unit sphere].

Integrating by parts,

$$\begin{aligned} z &= -\exp\left(-i\gamma H_1\int^{t}\sqrt{1+k^2t'^2}\,dt'\right) \\ &\quad\cdot\int_{-\infty}^{t} i\gamma H_1\sqrt{1+k^2t'^2}\,\text{arc cot } kt'\exp\left(i\gamma H_1\int^{t}\sqrt{1+k^2t''^2}\,dt''\right)dt' \\ &= -\left[\text{arc cot } kt'\exp\left(-i\gamma H_1\int_{t'}^{t}\sqrt{1+k^2t''^2}\,dt''\right)\right]_{t''=-\infty}^{t''=t} \\ &\quad -\int_{-\infty}^{t}\frac{k}{1+k^2t'^2}\exp\left(-\gamma H_1\int_{t'}^{t}\sqrt{1+k^2t''^2}\,dt''\right)dt' \\ &= -\text{arc cot } kt - \exp\left(-i\gamma H_1\int^{t}\sqrt{1+k^2t'^2}\,dt'\right) \\ &\quad\cdot\int_{-\infty}^{t}\frac{k}{1+k^2t'^2}\exp\left(i\gamma H_1\int^{t'}\sqrt{1+k^2t''^2}\,dt''\right)dt'. \end{aligned}$$

If $k/(\gamma H_1) \ll 1$, the exponential will be roughly $e^{i\gamma H_1 t'}$, and the integral will oscillate fast and average out to zero, leaving us with $z \approx -arc \cot kt$, corresponding to the adiabatic rapid passage case.

The sudden case is

$$\gamma H_1 \ll k \equiv \frac{1}{H_1}\frac{dH_0}{dt}.$$

If $\gamma H_1 \ll k$, kt must be large compared with unity before the exponential starts differing considerably from unity. Using the approximation $1 + k^2t^2 \approx k^2t^2$, it can be easily seen that

$$z(t) = i\sqrt{\frac{2\gamma H_1}{k}}\, e^{i\gamma H_1 k(t^2/2)} \int_{-\infty}^{\sqrt{(\gamma H_1 k)/2}\, t} e^{-iw^2}\, dw$$

This result agrees, with the results of Jacobsohn and Wangness[3] and Salpeter.[4]

Physically, **S** initially starts out from the north pole along the $\varphi = 0$ meridan, and eventually turns around in a circle of radius

$$\sqrt{\frac{\pi 2\gamma H_1}{k}} = \sqrt{\frac{2\pi\gamma H_1^2}{\frac{dH}{dt}}},$$

i.e., one that is smaller as the sudden approximation works better (see Figs. 10 and 49).

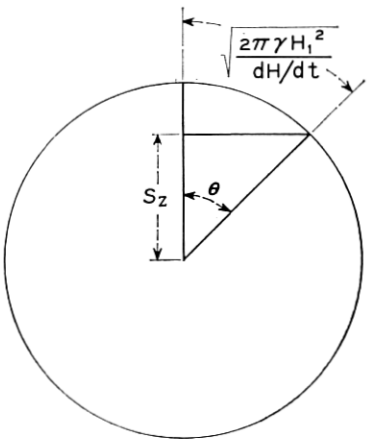

Fig. 49 — The loss of magnetization during an almost sudden passage.

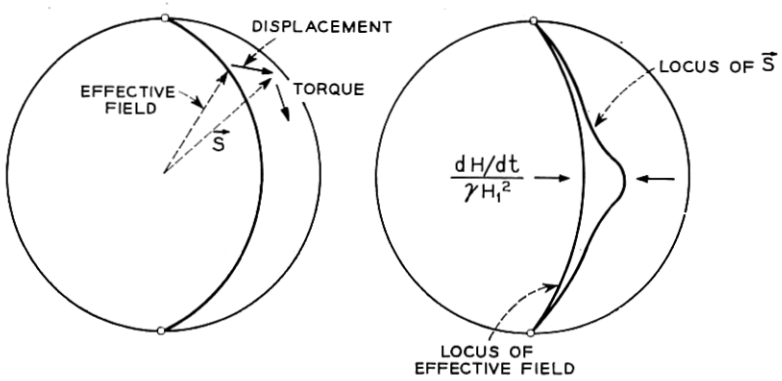

Fig. 50 — The locus of the magnetization vector for an almost adiabatic rapid passage.

If $\sqrt{(\pi 2\gamma H_1)/k} \ll 1$ for the movement along that circle,

$$S_z = S_0 \cos\theta \approx S_0\left(1 - \frac{\theta^2}{2}\right) = S_0\left(1 - \frac{\pi\gamma H_1}{k}\right);$$

i.e., the fractional loss of magnetization is $(\pi\gamma H_1^2)/(dH/dt)$, again a well-known result.

Note that the precession in the rotating frame taking place for large t is actually a rotation at a rate ω_0 in the fixed frame, i.e., the free induction tail. However, because the amplitude of our microwave signal at frequency ω is large compared with that of the free induction signal, one must consider the signal with respect to it, i.e., the beats of **S** with it.

A.2 *The Adiabatic Case*

The χ' and χ'' signals for a nonperfect adiabatic passage have been calculated by Salpeter.[4]

Physically, the occurrence of a nonvanishing χ'' can be seen as follows: If **S** is parallel to the effective field all the time, there is no torque on it. Thus, it cannot move. If we want it to move "longitudinally," we must displace it "laterally" by some small amount (see Fig. 50).

If the displacement is *small*, S can be assumed to move practically parallel to the effective field and

$$\frac{d\mathbf{S}}{dt} \approx \frac{d}{dt}\left(\frac{\mathbf{k} + \delta\mathbf{i}}{\sqrt{1+\delta^2}}\right) S = \frac{\mathbf{k} - \mathbf{i}\delta}{(\sqrt{1+\delta^2})}\,\dot{\delta}\,|\,S\,|.$$

Let $S = x\mathbf{i} + y\mathbf{j} + z\mathbf{k}$. From the differential equation

$$\frac{d\mathbf{S}}{dt} = -\gamma H_1 \sqrt{1+\delta^2}\left(\frac{\mathbf{i}+\delta\mathbf{k}}{\sqrt{1+\delta^2}} \times \mathbf{S}\right)$$

and our approximation for $d\mathbf{S}/dt$, it follows that

$$\frac{\mathbf{k}-\mathbf{i}\delta}{(\sqrt{1+\delta^2})^3}\dot{\delta}\,|\,S\,| = -\gamma H_1(\delta \times \mathbf{j} - Sy\mathbf{i} + y\mathbf{k} - z\mathbf{j}),$$

$$y = -\frac{\dot{\delta}}{\delta H_1}\frac{1}{(1+\delta^2)^{\frac{1}{2}}}S,$$

$$\chi'' = \frac{\frac{dH}{dt}}{\gamma H_1^2}\frac{1}{\left[1+\left(\frac{H-H_0}{H_1}\right)^2\right]^{\frac{1}{2}}}\left(\tfrac{1}{2}\frac{\chi_0\omega}{\gamma H_1}\right).$$

This χ'' satisfies the conservation of energy theorem:

$$E = M_z H_0 = \frac{\chi_0\omega}{\gamma} H_0 \frac{\delta}{\sqrt{(1+\delta^2)^2}},$$

$$\frac{dE}{dt} = \chi_0 H_0^2 \frac{\dot{\delta}}{(1+\delta^2)^{\frac{1}{2}}} = 2H_1^2\omega\chi'',$$

$$\chi'' = \frac{\chi_0 H_0^2 \frac{1}{H_1}\frac{dH}{dt}}{\left[1+\left(\frac{H-H_0}{H_1}\right)^2\right]^{\frac{1}{2}}}\left(\frac{1}{2H_1^2\gamma H_0}\right)$$

$$= \frac{\frac{dH}{dt}}{\gamma H_1^2}\frac{1}{\left[1+\left(\frac{H-H_0}{H_1}\right)^2\right]^{\frac{1}{2}}}\left(\frac{1}{2}\frac{\chi_0\omega}{\gamma H_1}\right).$$

For χ' and χ'' signals, see Figs. 2 and 42.

Note that, although $\chi' > \chi''$, if phase-sensitive detection is used, χ' may average out by the phase sensitive detector while χ'' does not. It tends to produce a signal at 90° with the modulating field. However, any "burning out" of the magnetization will produce a χ' signal much stronger than χ'' (see Section 6.6).

The loss of S_z due to nonadiabaticity has been estimated, in the general case, by Zener[13] to be $e^{-2\pi\gamma'}$, where

$$\gamma' = \frac{{E_{12}}^2}{\hbar\left[\frac{d(E_1 - E_2)}{dt}\right]},$$

and E_1, E_2, E_{12} are defined by

$$\mathcal{H}\Phi_1 = E_1\Phi_1 + E_{12}\Phi_2,$$

$$\mathcal{H}\Phi_2 = E_{12}\Phi_1 + E_2\Phi_2,$$

where

Φ_1 = "spin up" wave function,

Φ_2 = "spin down" wave function, and

$\mathcal{H}$ = the Hamiltonian of the system.

Here, $\mathcal{H} = \hbar\gamma(H - H_0)S_z + \hbar\gamma H_1 S_x$ in the rotating frame. Thus, say, for $S = \frac{1}{2}$

$$E_1 = \hbar\gamma(H - H_0)S,$$

$$E_2 = \hbar\gamma(H_0 - H)S,$$

$$E_{12} = \hbar\gamma H_1 S.$$

Therefore,

$$\gamma' = \frac{\gamma {H_1}^2}{4\frac{dH}{dt}} \qquad (S = \tfrac{1}{2}),$$

and the fractional loss is

$$\exp\left(-\frac{\pi}{2}\frac{\gamma {H_1}^2}{\frac{dH}{dt}}\right).$$

A.3 *Conclusion*

Within the adiabatic region, the loss of magnetization due to nonadiabaticity is negligible.

APPENDIX B

χ' and χ'' for an Almost Sudden Passage of an Inhomogeneously Broadened Line, Employing a System with a Bandwidth Narrow Compared with the Line Width

The susceptibility of an individual spin packet for an almost sudden passage ($dH/dt \gg \gamma H_1^2$) is

$$\chi'(t') + i\chi''(t') = \chi_0 \frac{H_0}{2H_1} i \sqrt{\frac{2\gamma H_1}{k}} e^{i\gamma H_1 k(t^2/2)} \int_{-\infty}^{\sqrt{(\gamma H_1 k)/2}\, t'} e^{-iw^2}\, dw$$

as derived by Salpeter[4] (or see Appendix A). Here $k = (1/H_1)(dH/dt)$ is assumed to be constant, and it is assumed that the magnetic field sweeps through resonance at $t' = 0$.

For spin packets swept through resonance at a time t', the susceptibility at time t is

$$\chi'(t,t') + i\chi''(t,t') = \chi_0 \frac{H_0}{2H_1} i \sqrt{\frac{2\gamma H_1}{k}} \exp\left[i\gamma H_1 b \frac{(t - t'^2)}{2}\right] \int_{-\infty}^{\sqrt{(\gamma H_1 k)/2}(-t')} e^{-iw^2}\, dw.$$

At a time t' the magnetic field is:

$$H(t') = H(t) - \frac{dH}{dt}(t - t') = H(t) - H_1 k(t - t').$$

The susceptibility due to spin packets resonating at fields between $H - H_1 k(t - t')$ and $H - H_1 k(t - t' + dt')$ is

$$h[H - H_0' - H_1 k(t - t')] H_1 k\, dt' [\chi'(t,t') + i\chi''(t,t')].$$

Superimposing the signals due to the various packets,

$$\chi'(t) + i\chi''(t) = \int_{-\infty}^{\infty} dt'\, h[H - H_0' - H_1 k(t - t')] H_1 k \chi_0 \frac{H}{2H_1} \cdot i \sqrt{\frac{2\gamma H_1}{k}} \exp\left[i\gamma H_1 k \frac{(t - t')^2}{2}\right] \int_{-\infty}^{\sqrt{(\gamma H_1 k)/2}(t - t')} e^{-iw^2}\, dw.$$

Let $t'' = t - t'$ and $H = H_0' + H_1 k t$. Then,

$$\chi'(t) + i\chi''(t) = \int_{-\infty}^{\infty} dt''\, h[H_1 k(t - t'')] \frac{\chi_0 H_0'}{2} i\sqrt{2\gamma H_1 k} \cdot \exp\left(i\gamma H_1 k \frac{t''^2}{2}\right) \int_{-\infty}^{\sqrt{(\gamma H_1 k)/2}\, t''} e^{-iw^2}\, dw.$$

For a gaussian line,

$$h[H_1k(t - t'')] = \frac{1}{\sqrt{2\pi}\Delta H} \exp\left\{-\frac{[H_1k(t - t'')]^2}{2\Delta H^2}\right\}.$$

So that

$$\chi'(t) + i\chi''(t) = \frac{\chi_0 H_0'}{2\Delta H} i \sqrt{\frac{\gamma H_1 k}{\pi}} \int_{-\infty}^{\infty} dt'' \exp\left\{-\frac{[H_1k(t - t'')]^2}{2\Delta H^2}\right\}$$
$$\cdot \exp\left(i\gamma H_1 k \frac{t''^2}{2}\right) \int_{-\infty}^{\sqrt{(\gamma H_1 k/2)}\, t'''} e^{-iw^2}\, dw.$$

Let

$$\sqrt{\frac{\gamma H_1 k}{2}}\, t'' = u, \qquad \sqrt{\frac{\gamma H_1 k}{2}}\, t = u_0.$$

Then

$$\chi'(t) + i\chi''(t) = \frac{\chi_0 H_0'}{2\Delta H} i \sqrt{\frac{\gamma H k_1}{\pi}} \sqrt{\frac{2}{\gamma H_1 k}}$$
$$\cdot \int_{-\infty}^{\infty} du \exp\left[-\frac{H_1 k}{\gamma \Delta H^2}\,(u - u_0)^2\right] e^{iu^2} \int_{-\infty}^{u} dw\, e^{-iw^2}.$$

If $H_1k/\gamma\Delta H^2 \ll 1$, the first term in the integrand may be assumed to be unity, and the integral is

$$\int_{-\infty}^{\infty} du\, e^{iu^2} \int_{-\infty}^{u} dw\, e^{-iw^2}.$$

This integral is the integral of $e^{i(u^2-w^2)}$ over the half of the u–w plane for which $u > w$ (see Fig. 51).

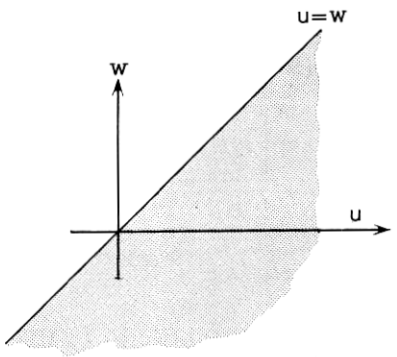

Fig. 51 — The half-plane over which integration of Appendix B is carried out.

This integral equals

$$\int_{-\infty}^{\infty} dw \int_{w}^{\infty} du\, e^{i(u^2-w^2)}.$$

In this integral, u and w may be renamed so that

$$\int_{-\infty}^{\infty} du \int_{-\infty}^{\infty} dw\, e^{i(u^2-w^2)} = \int_{-\infty}^{\infty} du \int_{u}^{\infty} dw\, e^{i(w^2-u^2)}.$$

Therefore

$$(\chi' + i\chi'') - (\chi' + i\chi'')^* = 2i\chi'' = \frac{\chi_0 H_0'}{\sqrt{2\pi}\Delta H}\, i \int_{-\infty}^{\infty} du \int_{-\infty}^{\infty} dw\, e^{i(u^2-w^2)},$$

$$\int_{-\infty}^{\infty} e^{iu^2}\, du = (1 + i)\sqrt{\frac{\pi}{2}},$$

$$\int e^{-iw^2}\, dw = (1 - i)\sqrt{\frac{\pi}{2}}.$$

Thus,

$$\chi'' = \frac{\pi}{2} \frac{\chi_0 H_0'}{\sqrt{2\pi}\Delta H},$$

for an "infinitely" wide line. For a finite line, we evidently have

$$\chi'' = \frac{\pi}{2} \chi_0 H h(H - H_0')$$

approximately, where $h(H - H_0')$ is the line shape, normalized to unity, and the approximation is certainly good if $dH/dt \ll \gamma \Delta H^2$.

When the direction of sweep is reversed, χ'' does not change sign, and it is independent of dH/dt and H_1. [However, the area, or integrated signal, is proportional to $1/(dH/dt)$.]

For an "infinitely" wide line, χ' is zero, since the equation

$$\int du \int dw\, e^{i(u^2-w^2)} = \int du \int dw\, e^{i(w^2-u^2)}$$

indicates that the imaginary component of this integral vanishes, and χ' is proportional to this component. Thus, the χ' "wiggles" tend to *cancel* each other. A nonvanishing χ' is due to the fact that the line is not infinitely wide.

As derived before, for a gaussian line

$$\chi'(t) + i\chi''(t) = \frac{\chi_0 H}{\sqrt{2\pi}\Delta H}\, i \int_{-\infty}^{\infty} du \exp\left[- \frac{H_1 k}{\gamma \Delta H^2} (u - u_0)^2 \right] \cdot e^{iu^2} \int_{-\infty}^{u} e^{-iw^2}\, dw.$$

Differentiating with respect to t, at $t = 0$

$$\frac{d}{dt}[\chi'(0) + i\chi''(0)] = \frac{\chi_0 H}{\sqrt{2\pi}\Delta H}\, i \frac{2H_1 k}{\gamma \Delta H^2} \sqrt{\frac{\gamma H_1 k}{2}} \cdot \int_{-\infty}^{\infty} du\, u \exp\left(- \frac{H_1 k}{\gamma \Delta H^2} u^2 \right) e^{iu^2} \int_{-\infty}^{u} e^{-iw^2}\, dw.$$

Now,

$$\begin{aligned} &\int_{-\infty}^{\infty} du \int_{-\infty}^{u} dw\, u \exp\left(- \frac{H_1 k}{\gamma \Delta H^2} u^2 + iu^2 - iw^2 \right) \\ &= \int_{-\infty}^{\infty} dw \int_{w}^{\infty} du\, u \exp\left(- \frac{H_1 k}{\gamma \Delta H^2} u^2 + iu^2 - iw^2 \right) \\ &= \frac{-1}{2\left(i - \frac{H_1 k}{\gamma \Delta H^2} \right)} \int_{-\infty}^{\infty} dw \exp\left(- \frac{H_1 k}{\gamma \Delta H^2} w^2 + iw^2 - iw^2 \right) \\ &= \frac{-1}{2\left(i - \frac{H_1 k}{\gamma \Delta H^2} \right)} \sqrt{\frac{\pi \gamma \Delta H^2}{H_1 k}}. \end{aligned}$$

If $dH/dt \ll \gamma \Delta H^2$, $H_1 k/\gamma \Delta H^2$ can be neglected when compared with unity, and we have

$$\left(\frac{d\chi'}{dt} \right)_{H = H_0'} = - \frac{\chi_0 H}{\sqrt{2\pi}\Delta H} \frac{2dH/dt}{\gamma \Delta H^2} \sqrt{\frac{\gamma dH/dt}{2}} \left(\frac{1}{2} \sqrt{\frac{\pi \gamma \Delta H^2}{dH/dt}} \right)$$

or, since $H = H_0 + (dH/dt)t$,

$$\left(\frac{d\chi'}{dH} \right)_{H = H_0'} = - \frac{H_0 \chi_0}{2\Delta H} \frac{1}{\Delta H}.$$

At $H = H_0' + \Delta H$,

$$\chi' \approx \chi'(H_0') + \left(\frac{d\chi'}{dH} \right)_{H = H_0'} \Delta H = - \frac{\chi_0 H}{2\Delta H} = - \frac{1}{\sqrt{2\pi}} \chi_0 H h(H_0' + \Delta H),$$

which is of the same order as χ''.

We have calculated χ'' only at the center (of a very wide) line, and, as to χ', only $d\chi'/dH$ has been calculated at the center of a gaussian line. However, for a microwave spectrometer the bandwidth of which is *small* compared with the line width, these results can be used to calculate χ' and χ'' for any part on any line, since the higher-order terms are due to spin packets off resonance, and these tend to produce high-frequency beats with the microwave signal. If the bandwidth of the system is small, these beats are not observed.

Let

$$\chi'(H) = ah(H - H_0') + b\frac{dh(H - H_0')}{dH} + c\frac{d^2h(H - H_0')}{dH^2} + \cdots,$$

and introduce a similar expression for χ''.

The first term in the above expression is the susceptibility of an infinitely wide line. This vanishes for χ', and has been calculated for χ''. Thus, the second term must be considered in the expression for χ', but not in that for χ''. So, let

$$\chi' = b\left[\frac{dh(H - H_0')}{dH}\right],$$

Then

$$\left(\frac{d\chi'}{dH}\right)_{H=H_0'} = b\left(\frac{d^2h(H - H_0')}{dH^2}\right)_{H_0'} = b\frac{1}{\sqrt{2\pi}\Delta H}\frac{1}{\Delta H^2}$$

at the center of a gaussian line. But, in this case,

$$\frac{d\chi'}{dH} = -\frac{\chi_0 H}{2\Delta H}\frac{1}{\Delta H},$$

so

$$b = -\Delta H \chi_0 H \sqrt{\frac{\pi}{2}},$$

$$\chi' = -\sqrt{\frac{\pi}{2}}\,\chi_0 H \frac{dh(H - H_0')}{dH}\Delta H,$$

$$\chi'_{\max} = \tfrac{1}{2}\chi_0 \frac{H}{\Delta H}\frac{1}{\sqrt{e}},$$

while

$$\chi''_{\max} = \tfrac{1}{2}\chi_0 \frac{H}{\Delta H}\sqrt{\frac{\pi}{2}}.$$

The difference between electron spin resonance and nuclear magnetic resonance may be noted. (The NMR case has been treated by Gabillard.[14])

With common NMR systems, the bandwidth may be large compared with the line widths, and the "beats" far off the line can be observed — and they yield the Fourier transform of the line. {Since the superposition $\int h(H - H_0') \exp [i\gamma(H - H_0')t]d(\gamma H)$ is essentially a Fourier transform of $h(H - H_0')$}. This is the signal observed in region III (see Section IV). The signal of region I is at the microwave frequency, but weak.

The agreement between the above calculations and experiment is excellent.

Fig. 12 confirms the following features:

i. *Shapes* of the signals are "dispersion" for χ', "absorption" for χ''.
ii. χ' and χ'' are of about the same strength.
iii. The signals are independent of dH_0/dt.

APPENDIX C

χ' and χ'' for a Nonadiabatic Passage, Nonuniform Rate of Sweep

C.1 χ' and χ'' for a Triangular Wave and Almost Sudden Transition of an Inhomogeneously Broadened Line

The general solution of the first differential equation of Appendix A is

$$z(t'') = \exp\left(i\frac{\gamma H_1 k}{2} t''^2\right) \int_{t_0}^{t''} i\gamma H_1 S_z \exp\left(-i\frac{\gamma H_1 k}{2} t'^2\right) dt' + \exp\left[i\frac{\gamma H_1 k}{2}(t''^2 - t_0^2)\right] z(t_0).$$

This solution corresponds to the signal from a spin packet swept through resonance at $t'' = 0$. t_0 may be any arbitrary time. Let

$$H = \begin{cases} H_0 + H_1 kt & t < 0, \\ H_0 - H_1 kt & t > 0. \end{cases}$$

At $t = 0$, the signal due to a packet swept through at $t = -t_0$ is

$$z(0, -t_0) = \exp\left(i\frac{\gamma H_1 k}{2} t_0^2\right) \int_{-\infty}^{t_0} i\gamma H_1 S_z \exp\left(-i\frac{\gamma H_1 k}{2} t''^2\right) dt''.$$

This packet will again resonate at $t = t_0$. For $t > 0$,

$$z(t) = \exp\left[-i\frac{\gamma H_1 k}{2}(t-t_0)^2\right] i\gamma H_1 \int_0^t S_z \exp\left[i\frac{\gamma H_1 k}{2}(t'-t_0)^2\right]dt'$$

$$+ \exp\left[-i\frac{\gamma H_1 k}{2}t(t-2t_0)\right]\exp\left(i\frac{\gamma H k}{2}t_0^2\right)$$

$$\cdot \int_{-\infty}^{t_0} i\gamma H_1 S_z \exp\left(-i\frac{\gamma H_1 k}{2}t'^2\right)dt'.$$

Superimposing the signals due to the various spin packets, as in Appendix B, we have, assuming $S_z = S_0$,

$$\chi'(t) + i\chi''(t) = \int_{-\infty}^{\infty} dt_0 h(H(t) - H_0' - H_1 k(t-t_0))H_1 k\chi_0 \frac{H}{2H_1}$$

$$\cdot i\gamma H_1 \left(\exp\left[-i\frac{\gamma H_1 k}{2}(t-t_0)^2\right]\int_0^t \exp\left[i\frac{\gamma H_1 k}{2}(t'-t_0)^2\right]dt'\right.$$

$$\left. + \exp\left\{-i\frac{\gamma H_1 k}{2}[t(t-2t_0) - t_0^2]\right\}\int_{-\infty}^{t_0}\exp\left(-i\frac{\gamma H_1 k}{2}t'^2\right)dt'\right).$$

For an "infinitely" wide line, let $h(H - H_0') = 1/(\sqrt{2\pi}\Delta H)$:

$$\chi'(t) + i\chi''(t) = \frac{i}{\sqrt{2\pi}}\frac{H}{\Delta H}\chi_0\left[\int_{-\infty}^{\infty} du\, e^{-iu^2}\int_{(u-\sqrt{(\gamma H_1 k)/2})t}^{u} e^{iw^2}\,dw\right.$$

$$\left. + e^{-\gamma H_1 k t^2}\int_{-\infty}^{\infty} du\, e^{+iu^2}\int_{-\infty}^{(u-\sqrt{(\gamma H_1 k)/2})t} e^{-iw^2}\,dw\right].$$

To evaluate the above integrals, we may employ the transformation

$$p = \frac{u+w}{\sqrt{2}}, \qquad q = \frac{u-w}{\sqrt{2}}.$$

Then

$$\frac{\partial(q,p)}{\partial(u,w)} = 1,$$

$$u^2 - w^2 = 2pq$$

and

$$\int_{-\infty}^{\infty} du \int_{(u-\sqrt{(\gamma H_1 k)/2})t}^{u} dw\, e^{-i(u^2-w^2)}$$

$$= \int_{-\infty}^{\infty} dp \int_{0}^{(\sqrt{(\gamma H_1 k t)/2})t} dq\, e^{-2ipq}$$

$$= \int_{-\infty}^{\infty} dp \left(-\frac{1}{2ip}\right) (\cos p\sqrt{\gamma H_1 k}\, t - i \sin p\sqrt{\gamma H_1 k}\, t - 1)$$

$$= \frac{1}{2}\int_{-\infty}^{\infty} dp\, \frac{\sin \sqrt{\gamma H_1 k}\, pt}{p} = \begin{cases} \frac{\pi}{2} & \text{for} \quad t = 0 \\ 0 & \text{for} \quad t = 0, \dagger \end{cases}$$

$$\int_{-\infty}^{\infty} du \int_{-\infty}^{u-\sqrt{(\gamma H_1 k)/2t}} dw\, e^{i(u^2-w^2)}\, dw$$

$$= \int_{-\infty}^{\infty} dp \int_{\sqrt{(\gamma H_1 k)/2t}}^{\infty} dq\, e^{2ipq}$$

$$= \int_{-\infty}^{\infty} dp\, \frac{1}{2ip} (e^{i\infty} - e^{i\sqrt{\gamma H_1 k}\, pt})$$

$$= -\frac{1}{2}\int_{-\infty}^{\infty} dp\, \frac{\sin \sqrt{\gamma H_1 k}\, pt}{p} = -\frac{\pi}{2}, \ddagger$$

$$\chi'(t) + i\chi''(t) = \frac{i}{\sqrt{2\pi}}\frac{H}{\Delta H}\chi_0 \frac{\pi}{2}(1 - e^{i\gamma H_1 k t^2}),$$

$$\chi''(H) = \frac{\pi}{2}\chi_0 H h(H - H_0')(1 - \cos \gamma H_1 k t^2),$$

$$\chi'(H) = \frac{\pi}{2}\chi_0 H h(H - H_0') \sin \gamma H_1 k t^2.$$

The assumptions are the same as those discussed in Appendix B.

† The integral

$$\int_{-\infty}^{\infty} du\, e^{-iu^2} \int_{u-\sqrt{(\gamma H_1 k)/2t}}^{u} dw\, e^{iw^2}$$

seems to be a discontinuous function of t. It obviously vanishes for $t = 0$, and equals $\pi/2$ for $t < 0$. This may be due to the nonphysical assumption of an infinite linewidth. However, practically, dH/dt cannot change abruptly. For a sinusoidal sweep, with its smooth change of dH/dt, no discontinuity is expected even for an infinitely wide line.

‡ The term $e^{i\infty}$ presents no difficulties. Mathematically, it can be removed by a slight generalization of the concept of convergence. Physically it can be removed by considering any amount of relaxation.

We have a steady χ'' equal to that due to a sweep at a constant rate, and additional oscillations at a frequency $\omega' = 2\gamma H_1 kt = 2\gamma(dH/dt)t$. (At $t = 0$, H is at the peak of the triangular waveform.) The χ' and χ'' to be expected are shown in Fig. 52.

The experimental trace on Fig. 53(a) resembles the expected trace. However, the magnetization under the experimental conditions was not uniform, so a very close agreement between the preceding theory and this experiment cannot be expected.

c.2 *Some Additional Considerations Concerning Case 6.11*

Consider the extreme nonadiabatic case ($\gamma H_1^2 \lll \omega_m H_m$). Let the width of the "unburnt" region of spins, [within the range $H_0 + (dH_0/dt)\ t \pm H_m$, see Fig. 38] be H'. Then, we may consider the following cases:

i. $H' < H_1$; i.e., all spin packets that are more than H_1 away from the extremum of the modulation cycles are saturated and "destroyed."

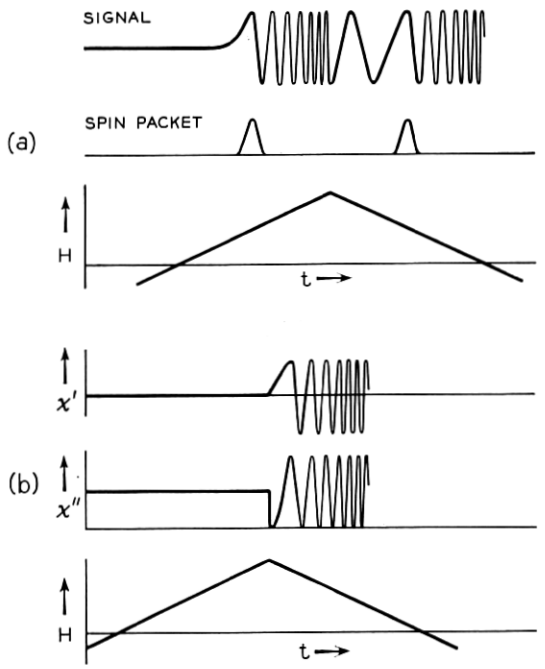

Fig. 52 — Illustration of the signal resulting from a triangular field modulation (almost sudden passage): (a) individual spin packet; (b) inhomogeneously broadened line.

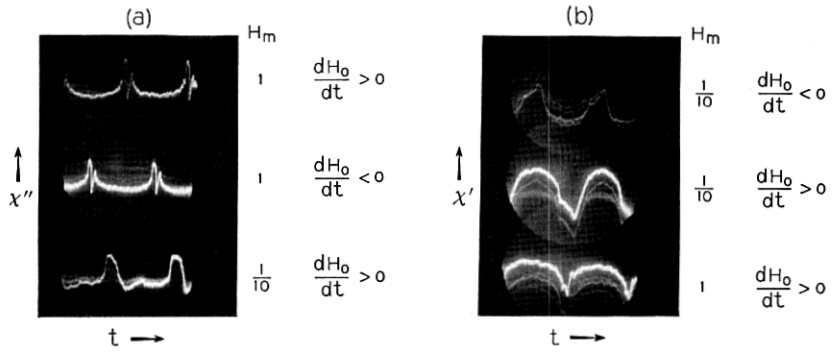

Fig. 53 — (a) χ'' scope trace of an extremely nonadiabatic passage. Data: $H_1 \approx 1/1000$ gauss; $\omega_m = 2\pi \times 100$ rad/second; $T = 1.2°K$; concentration, 6.5×10^{16} phosphorus atoms/cc. Top and center traces, $H_m = 1$ gauss, opposite senses of dH_0/dt; bottom trace, $H_m = 1/10$ gauss. The "wiggles" are probably damped at a rate determined by the T_2 of the sample, which is roughly of order 10^{-4} second (see Gordon and Bowers[15]); note, however, that the average of the 'wiggles' does not vanish, but seems to be proportional to $|S_z|$ (this is in agreement with the calculations of Appendix C); note also the sudden drop of χ'' when $dH/dt = 0$, predicted there (see Fig. 52). (b) χ' scope trace of an extremely nonadiabatic passage. Data: $H_1 = 1/1000$ gauss; $\omega_m = 2\pi \times 100$ rad/second; $T = 1.2°K$; concentration, 6.5×10^{16} phosphorus atom/cc. Top and center traces: $H_m = 1/10$ gauss, opposite senses of dH/dt; bottom trace: $H_m = 1$ gauss.

ii. $H' \gg H_1$, $\gamma H' > \Delta\omega_{sys}$, where $\Delta\omega_{sys}$ is the bandwidth of system.
iii. $H' \gg H_1$, $\gamma H' < \Delta\omega_{sys}$.

In all cases, it is assumed that most of the contribution is due to spin packets swept through *suddenly* (otherwise, we have the "moderate" nonadiabatic case, which is essentially the same as case 8).

In case i it can be assumed that we have only one spin packet, which, however, is not swept through at a uniform rate ($\delta = kt$), but at approximately $\delta = at^2$, with $a = (H_m/H_1)(\omega_m^2/2)$. Repeating the calculation of Appendix A for a general δ, for $\gamma H_1^2 \ll dH/dt$, we have

$$z = -i\gamma H_1 \int_{-\infty}^{t} \exp\left[i\gamma H_1 \int_{t'}^{t} \delta(t'')\, dt'' \right] dt'$$

as before. With our δ,

$$z \approx -i\gamma H_1 \int_{-\infty}^{t} \exp\left(-i\gamma H_1 a\, \frac{t^3 - t'^3}{3} \right) dt' .$$

Let

$$w \equiv \frac{a\gamma H_1}{3}\, t'^3 .$$

Then

$$z(t) = -i \sqrt[3]{\frac{(3\gamma H_1)^2}{a}} \exp\left(-i \frac{a\gamma H_1}{3} t^3\right) \int_{-\infty}^{\sqrt[3]{(a\gamma H_1)/3}} \frac{e^{iw}}{w^{\frac{2}{3}}}\, dw$$

(the integral can, if desired, be expressed in terms of the incomplete Γ function of a complex argument). At $t = 0$,

$$z(t) = -i \sqrt[3]{\frac{(\gamma H_1)^2}{9 \dfrac{H_m}{H_1} \dfrac{\omega_m^2}{2}}} \int_{-\infty}^{0} \frac{e^{iw}}{w^{\frac{2}{3}}}\, dw,$$

and the amount burnt per cycle is

$$2\left(\frac{2}{9} \frac{\gamma H_1^2}{H_m \omega_m} \frac{\gamma H_1}{\omega_m}\right)^{\frac{1}{3}} \left(\int_0^{\infty} \frac{\cos w}{w^{\frac{2}{3}}}\, dw\right)^2 .\dagger$$

Due to the slow rate of change of H near the extrema of the modulating cycle, there is a strong burnout, although $(\gamma H_1^2)/(H_m\omega_m)$ is small.‡

The amplitude of the signal should be of the order of $z(0)$ multiplied by the width of the region — which is of the order H_1 ; that is, the signal is roughly

$$\frac{1}{2} \frac{\chi_0 H_0}{\Delta H} \sqrt[3]{\frac{\gamma H_1^2}{H_m \omega_m} \frac{\gamma H_1}{\omega_m}} \frac{H_1}{H_m}.$$

Actually, for lower dH/dt than that indicated in the footnote ‡ below, the signal will be weaker. The signal in this case is very small, and this case is very inefficient. It is worthwhile to *increase* dH_0/dt to get a bigger signal.

Note that, for the passage to be sudden, we must have

$$\frac{dH}{dt} \approx H_m \omega_m \sqrt{2 \frac{H'}{H_m}} \approx H_m \omega_m \sqrt{2 \frac{H'}{H_m}} \gg \gamma H_1^2$$

that is,

$$\frac{\gamma H_1^2}{\omega_m H_m} \frac{\gamma H_1}{\omega_m} \ll 1$$

in addition to the condition on dH_0/dt given in the footnote‡.

† The definite integral here equals $(3\sqrt{3/2})(1/3!) = 2.32$ (see Jahnke and Emde[17]). For a power of 40 db below 10 milliwatts ($H_1 \approx \frac{1}{100}$ gauss), 1000 cps, $H_m = 1$ gauss the loss of magnetization per cycle is approximately

$$2\left(\frac{2}{9}\right)\left(\frac{17.6}{6280}\right)\left(\frac{17600}{6280}\right)^{\frac{1}{3}} (2.32)^2 = \frac{1}{6}.$$

‡ For this case to apply under the above experimental conditions, dH_0/dt should not sweep more than H_1 in about 6 cycles; i.e., $dH_0/dt < (\omega_m/2\pi)(H_1)(\frac{1}{6})$ or $dH_0/dt < \frac{1}{6}$ gauss second.

In case ii, we may use the "superposition of wiggles" calculated in Appendix B, and use the estimate of Section IV for the burnout rate:

$$\alpha = \frac{\pi\gamma H_1^2}{\frac{dH}{dt}}, \qquad \frac{dH}{dt} \approx \frac{\pi}{2}\frac{H'}{H_m}\omega_m H_m$$

near the extrema of the modulation cycle. The distance that H progresses in $N/2$ modulation cycles is

$$H' = \frac{dH_0}{dt}\frac{2\pi}{\omega_m}\frac{N}{2}.$$

Thus,

$$\frac{dH}{dt} \approx \frac{\pi}{2}\frac{H'}{H_m}\omega_m H_m \approx \frac{\pi}{2}\frac{dH_0}{dt}\frac{2\pi}{\omega_m}\frac{N}{2}\omega_m = \frac{\pi^2}{2}N\frac{dH_0}{dt},$$

$$\alpha(N) = \frac{2\gamma H_1^2}{\pi N\frac{dH_0}{dt}}.$$

This is the loss of a spin packet during the Nth sweep through it. This formula holds for the case when dH_0/dt is not so small that, for $N = 1$, $H' < H_1$; i.e., this only holds for: $dH_0/dt > (\omega_m H_1)/\pi$ or, say, $dH_0/dt >$ 2 gauss/second at 40 db and 1000 cps. Otherwise, the loss during those cycles for which $H' < H_1$ should better be approximated as in case i.

The total loss is estimated as follows:

$$\ln \prod_N [1 - \alpha(N)] = \sum_N \ln [1 - \alpha(N)] \approx -\sum \alpha(N)$$

$$\approx -\frac{2\gamma H_1^2}{\pi dH_0/dt}\ln N$$

for small $\alpha(N)$. Thus

$$S_N \approx S_0 \exp\left(-\ln N\frac{2\gamma H_1^2}{\pi dH_0/dt}\right)$$

and

$$\frac{S_N}{S_0} = \frac{1}{e} \qquad \text{for} \quad N \approx \exp\left(\frac{\pi dH_0/dt}{2\gamma H_1^2}\right).$$

This width will be appreciable if $dH_0/dt > \gamma H_1^2$. (This condition is

usually more exacting than $dH_0/dt > (\omega_m/\pi)H_1$, since $\gamma H_1 > \omega_m$ except at very low powers.) For this N,

$$H' \approx \frac{dH_0}{dt}\left(\frac{2\pi}{\omega_m}\right)^{\frac{1}{2}} \exp\left(\frac{\pi dH_0/dt}{2\gamma H_1^2}\right),$$

and this gives the width of the nonburnt region.

Note that, if $dH_0/dt > \omega_m H_m$, the direction of sweep of field will not reverse itself at all. Then we shall have (if $dH_0/dt - \omega_m H_m \gg \gamma H_1^2$) very little burnout, and case 9 applies.

Here, T_2 has been assumed to be small compared with $2\pi/\omega_m$. At these low powers, $H_1 < H_{\text{loc}}$, and the "zero field" value of T_2 can be employed.† For different T_2, see the discussion of Section 6.9.

This calculation gives $|S|$ for both cases ii and iii, essentially. The χ' and χ'' signals are calculated as in Section 6.8. (In case iii there will be some additional "wiggles".) Note that the expressions for χ' and χ'' apply not only for the natural line shape $h(H - H_0')$, but for any shape — such as the one we have here, which is determined by burning. This also implies that χ' and χ'' are of the same order of magnitude. However, the components at the field modulation frequency need not be of the same order of magnitude.

Note that when $dH/dt > 0$, and $dh(H - H_0)/dH > 0$, on the one hand, and $dH/dt < 0$, and $dh(H - H_0)/dH < 0$, on the other hand, the sign of χ' is the *same*. Thus, the scope traces will be as shown in Fig. 54 and the recorder traces as in Fig. 55. Experimental traces are shown in Figs. 42 and 53.

APPENDIX D

Superposition of Adiabatic Fast Passage Lines

For adiabatic fast passage,

$$\chi' \propto \frac{1}{\sqrt{1+\delta^2}} \qquad \delta = \frac{H - H_0}{H_1}.$$

Thus, for large δ, χ' falls down like $1/\delta$, and the superposition of signals due to packets of an infinitely broad line will yield an infinite result. Under actual physical conditions, there will be always something to limit χ': a finitely wide line, relaxation effects, etc. However, the calcu-

† This value has been measured by Gordon and Bower[15] and is approximately 10^{-4} second for the sample employed here.

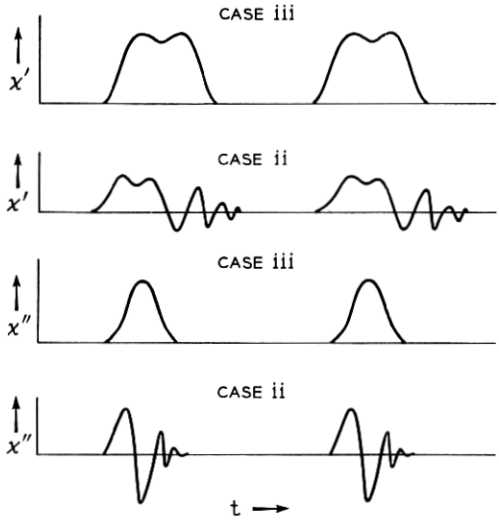

Fig. 54 — Expected χ' and χ'' scope traces of case 11; wiggles are observed when $\gamma H_1 \langle\langle\langle \omega_m H_m$, and $\omega_m T_2$ is not very small compared with unity.

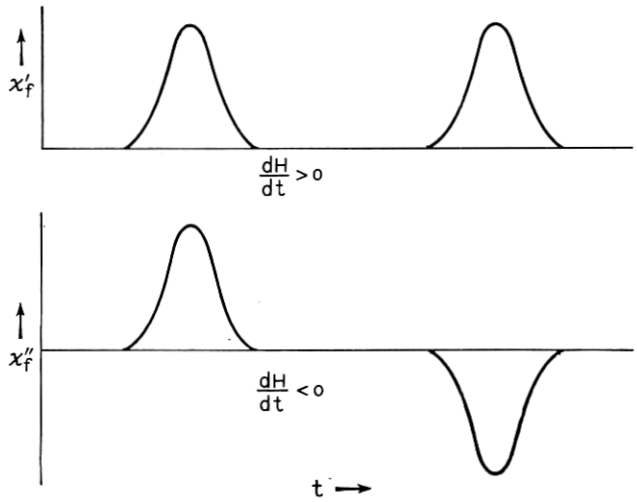

Fig. 55 — Expected recorder traces of case 11 (system relaxes between sweeps); the true line shape may be observed, sometimes even if H_m is *not* small compared with ΔH (the width of the nonburnt region must then be small). Compare with Figs. 42(a) and (b).

lation of the χ' signal involves integrals of the form

$$\int \frac{f(x)}{\sqrt{1+x^2}},$$

which are difficult to compute.

The case in which $f(x)$ is gaussian (i.e., a gaussian line, with relaxation neglected), has been treated by Feher[12] and Portis.[5] For it,

$$\int_{-\infty}^{\infty} \frac{h(H'-H_0)}{\sqrt{1+\delta^2}} \frac{dH'}{H_1} = \frac{1}{2\sqrt{2\pi}} \exp\left[-\left(\frac{H_1}{2\Delta H}\right)^2\right] K_0\left[\left(\frac{H_1}{2\Delta H}\right)^2\right]$$

for

$$h(H'-H_0) = \frac{1}{\sqrt{2\pi}\Delta H} \exp\left[-\frac{(H'-H_0)^2}{2\Delta H^2}\right],$$

and, for $H_1 \ll \Delta H$, this integral is, $(1/\sqrt{2\pi})\log(2\Delta H/H_1)$. This result will be of use for "plain" fast passage over a whole inhomogeneously broadened line, if

$$\frac{dH/dt}{\Delta H} \gg \frac{1}{\sqrt{T_1 T_2}}.$$

If field modulation is employed, this result does no longer apply (except in the "nonburnt" case 5). Practically, the width of the distribution of spins will be determined either by relaxation, or by the modulating field, H_m (or both).

The first case is difficult to treat. Portis[5] assumes an exponential distribution of packets,

$$\exp\left(-\left|\frac{H-H_0}{H_m\omega_m T_1}\right|\right),$$

where H is the magnetic field, H_0 is the resonant field of a packet and H_m is the peak modulating field.

This expression assumes that packets not yet swept over, are in a partly "relaxed" state given by this exponential; i.e., there is $t \to -t$ symmetry. As a matter of fact, the integral

$$\int \frac{e^{-|\alpha x|}}{\sqrt{1+x^2}}\, dx$$

is difficult to evaluate, so this approximation is not very helpful, practically.

The simplest approximation is, probably, to replace the actual $|S|$ distribution by a triangular one (see Fig. 56). In the case of an envelope

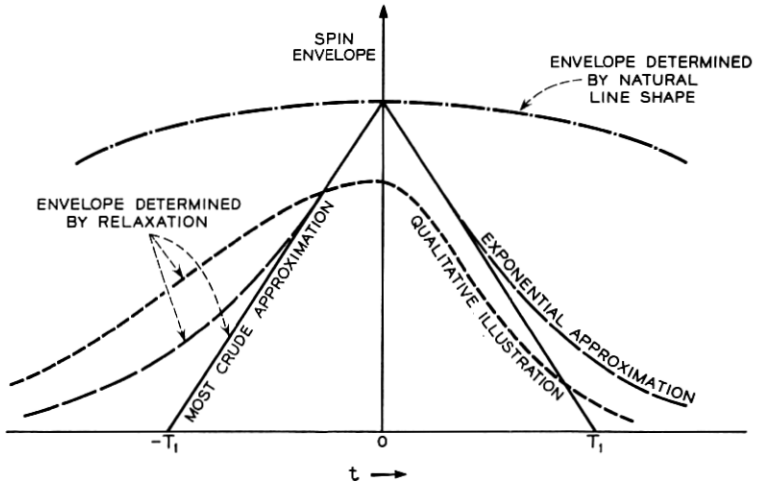

Fig. 56 — Envelope of the magnetization S_z, for an inhomogeneously broadened line under various experimental conditions.

determined by relaxation, it is reasonable to assume a width $t = T_1$, or

$$H' = \frac{dH}{dt} T_1 = \omega_m H_m T_1$$

in the center of the modulation cycle, for $T_1 = T_2$. (For $T_1 \neq T_2$, one might perhaps postulate a width $t = \sqrt{T_1 T_2}$.)

Thus,

$$\int_{-H_m\omega_m T_1}^{+H_m\omega_m T_1} \frac{1 - \left|\frac{H - H_0}{H_m\omega_m T_1}\right|}{\sqrt{1 + \left(\frac{H - H_0}{H_1}\right)^2}} \frac{d(H - H_0)}{H_1}$$

$$= 2 \log \frac{H_m\omega_m T_1 + \sqrt{H_1 + (H_m\omega_m T_1)^2}}{H_1}$$

$$- 2 \frac{1}{H_m\omega_m T_1} \left(\sqrt{H_1^2 + (H_m\omega_m T_1)^2} - H_1\right).$$

For adiabatic rapid passage, $H_1/(H_m\omega_m) \ll T_1$, so the integral is

$$\approx 2 \log \frac{2H_m\omega_m T_1}{H_1} - \left(\frac{H_1}{H_m\omega_m T_1}\right)^2 \approx 2 \ln \frac{2H_m\omega_m T_1}{H_1}.$$

Actually, since the integral $\int dx/\sqrt{1 + x^2}$ diverges only logarithmi-

cally, different shapes will change only the factor "2" in the logarithm, which has little effect on the amplitude and probably cannot be checked experimentally except with high-precision equipment.

If the width of the distribution is limited by H_m, it is reasonable to assume that the packets *outside* the interval $H_0 - H_m < H < H_0 + H_m$ do not yield any signal, particularly if $H_1 \ll H_m$.

APPENDIX E

Second-Order Effects Occurring When a Bridge Is Tuned to Observe χ' or χ'' Signals

When a "bridge" system is used in the detection of the microwave signal, it sometimes happens that the amplitude or phase unbalance of the bridge is not small, or that the changes in detected power are not small compared with the power itself. In these cases, the detected signals will not be pure χ' or χ'' signals, but rather will be distorted.

Consider a hybrid-T network (Fig. 57). The voltage in the receiving arm is:

$$\dot{V} = \dot{V}_1 + \dot{V}_2 ,$$

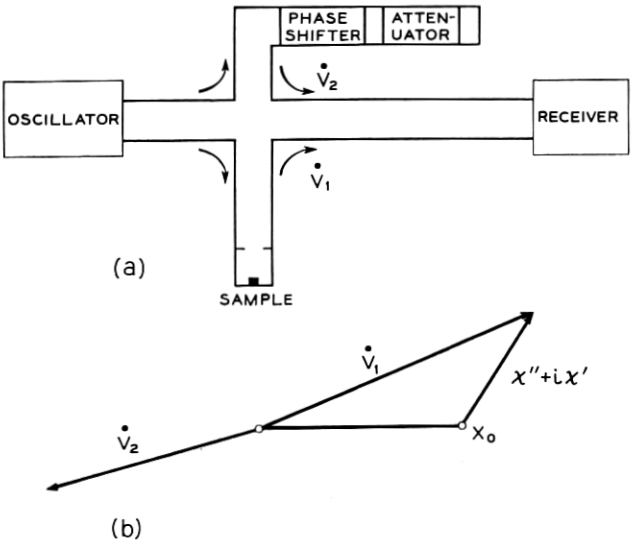

Fig. 57(a) — Outline of a hybrid bridge employed in electron spin resonance work; (b) vector diagram of the voltages entering the receiving arm of the bridge of (a).

where

$$\dot{V}_1 = x_0 + \chi'' + i\chi',\dagger$$

$$\dot{V}_2 = -x - iy,$$

with x_0, x, y, χ', χ'' being real numbers. (It is assumed that the cavity, or tuned circuit, is tuned to resonance.) Thus,

$$V = \sqrt{|\dot{V}_1 - \dot{V}_2|^2} = \sqrt{(x_0 + x + \chi'')^2 + (y + \chi')^2} \approx V_0 + \frac{x + x_0}{V_0}\chi'' + \frac{y}{V_0}\chi' + \frac{\chi''^2}{2V_0} + \frac{\chi'^2}{2V_0} - \frac{[(x + x_0)\chi'' + y\chi']^2}{2V_0^3} + \frac{[(x + x_0)\chi'' + y\chi']^3}{2V_0^5} + \cdots,$$

where

$$V_0 \equiv \sqrt{(x + x_0)^2 + y^2},$$

and it is assumed that

$$\chi'^2 + \chi''^2 < V_0^2.$$

Case 1

Let $x + x_0 = 0$. Then

$$V = V_0 + \chi' + \frac{\chi''^2}{2V_0} + \frac{\chi'^3}{2V_0^2},$$

$$\frac{dV}{dH} = \frac{d\chi'}{dH} + \frac{\chi''}{V_0}\frac{d\chi''}{dH} + \frac{3}{2}\left(\frac{\chi'}{V_0}\right)^2\frac{d\chi'}{dH}.$$

The main component of the signal is the χ' signal. The interference signal $(\chi''/V_0)(d\chi''/dH)$ is roughly of absorption-derivative shape, however, and is weaker at the shoulders. It can be reduced by slightly unbalancing the bridge ($x + x_0 \neq 0$). This will introduce a slight amount of $d\chi''/dH$ signal, which can be adjusted to be of opposite phase to $(\chi''/V_0)(d\chi''/dH)$. However, the absorption derivative component cannot be eliminated altogether. Thus, if χ' and χ'' have a definite parity, the observed signal will not.

In practice, this case occurs if the following steps are taken:

(a) The bridge is balanced; the reading of the attenuator, α db, is noted.

(b) The phase of V_2 is changed.

† Actually, the voltage is of course not equal to $\chi'' + i\chi'$, but only approximately proportional to it. For the other factors affecting it, see Ref. 6.

(c) The amplitude of V_2 is changed, so that a minimum detector output is observed, and the reading of the attenuator, β db, is noted.

(d) The amplitude of V_2 is changed by setting the attenuator at $2\alpha - \beta$ db. From Fig. 58, it is evident that, after step (a), $\dot{V}_2 = \mathbf{OA}$; after step (b), $\dot{V}_2 = \mathbf{OB}$; after step (c), $\dot{V}_2 = \mathbf{OC}$; and after step (d), $\dot{V}_2 = \mathbf{OD}$. From the geometry, $\overline{OB} = \overline{OA} = \sqrt{\overline{OC}\,\overline{OD}}$. Thus, $\log \overline{OD} = 2 \log \overline{OB} - \log \overline{OC}$, yielding our result.

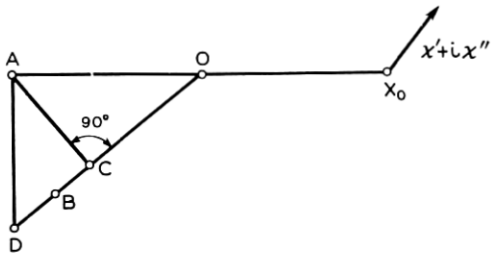

Fig. 58 — Vector diagram illustration of the voltages corresponding to cases (i), (iii) and (iv).

Case 2

Let $y = 0$. Then

$$V = V_0 + \chi'' + \frac{\chi'^2}{2V_0} + \frac{\chi''^3}{2V_0^2},$$

$$\frac{dV}{dH} = \frac{d\chi''}{dH} + \frac{\chi'}{V_0}\frac{d\chi'}{dH} + \frac{3}{2}\left(\frac{\chi''}{V_0}\right)^2 \frac{d\chi''}{dV_0}.$$

The main component of the signal is a χ'' signal. Again, there is an interference which can be reduced by slightly unbalancing the bridge ($y \neq 0$), but not eliminated. In practice, this case occurs if the bridge is balanced, and then the amplitude of V_2 is changed, without changing its phase.

Case 3

Let $x^2 + y^2 = x_0^2$, and say that

$$x = -x_0 \cos \varphi_0 ,$$

$$y = x_0 \sin \varphi_0 .$$

If φ_0 is small, to the first order in φ_0, then

$$V \approx V_0 + \chi' + \tfrac{1}{2}\varphi_0\chi'' + \frac{\chi''^2}{2V_0} - \frac{\chi'\chi''}{4V_0} + \frac{\chi'^3}{2V_0^2}.$$

This case is obtained when the bridge is balanced, and then the phase of V_2 is changed, but not its amplitude. We have a "χ'" signal, with some "χ''" admixed.

Case 4

Let

$$x = -r \cos \varphi_0 ,$$

$$y = r \sin \varphi_0 .$$

Let φ_0 be constant and r satisfy $\partial V_0/\partial r = 0$. Then, again to the first order in φ_0,

$$V \approx V_0 + \chi' + \varphi_0 \chi'' + \frac{\chi''^2}{2V_0} - \frac{\chi'\chi''}{V_0} + \frac{\chi'^3}{2V_0^2} .$$

This case is obtained when the bridge is balanced, then the phase of V_2 is changed, and then the amplitude of V_2 is changed so that minimum microwave power is detected. Again, we have a χ' signal with a small admixture of χ''.

We see that the distortions of the χ' and χ'' signals are of two kinds:

i. Those due to a nonvanishing φ_0, i.e., to a large unbalance of the bridge.

ii. Those due to nonvanishing χ'/V_0, χ''/V_0, i.e., to "strong" signals.

The distortions of the first kind can be removed altogether by proper adjustment of the bridge. (If $V_0 \gg \chi', \chi''$, Case 1 above will yield a pure χ' signal; while Case 2 will yield a pure χ'' signal.)

The distortions of the second kind cannot be removed by any adjustment of the bridge. They will give rise to errors in measurements of the center of the line, its width and its intensity.

Therefore, if V_0 is not large compared with χ', χ'' (a condition that is indicated by a change in detector crystal current on passing through line), it is recommended to *increase* the detuning of the bridge, and if a χ' signal is desired, manipulate it as described in Case 1 of this Appendix. (It may then be necessary to introduce attenuation in the bridge output arm to avoid overloading the detector.)

An experiment was carried out to check these calculations, employing as bridge elements a Hewlett-Packard X885A phase shifter and a Hewlett-Packard X382A attenuator. The sample used was D.P.P.H., and the experiments were performed at room temperature.

The experimental results agree with these calculations, and indicate that the above bridge elements can be assumed to be ideal. A quite pure χ' signal could be obtained by the method indicated in Case 1, even for a phase shift $\varphi_0 = 60°$.

APPENDIX F

A Particular χ' Trace Observed at High Powers

A peculiar trace was observed at high powers and small dH/dt with the 0.37 ohm-cm sample. The trace (as observed at the output of the IF amplifier, with no phase sensitive detector used) is shown in Fig. 59. It looks like a "slow passage" trace (Fig. 2) but, after passing the line once, it is saturated and on the next sweep no signal whatsoever is seen. If the trace were due to slow passage, it should not depend upon the history of the system, and thus should not saturate.

A possible explanation for this phenomenon is as follows: At high powers, forbidden lines are excited. These forbidden lines correspond to a simultaneous flip of an electron and a Si^{29} nucleus interacting with it. These forbidden lines have been observed directly and are discussed in a separate paper. Now, each donor interacts with many Si^{29} nuclei and thus gives rise to many forbidden lines. Under the given experimental conditions each forbidden line is traversed "almost suddenly." Thus, the superposition of these lines should give rise to a dispersion signal (Appendix B). The probability of a donor to flip during the passage of each forbidden line is small, since the passage is almost sudden. But, since there are many forbidden line in which each donor participates, the over-all probability to flip may be considerable, and we may obtain saturation.

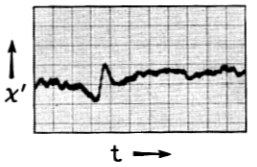

Fig. 59 — χ' of the bound donor electron line in phosphorus doped silicon, under strong microwave power, with no phase sensitive detector (or magnetic field modulation) present. The shape of the line resembles that of Bloch's "slow passage" case; however, the line saturates after a single passage through it. Data: Sample, phosphorus-doped silicon; impurity concentration, 1.7×10^{16} atoms cc; $T = 1.25°K$; $T_1 \approx T_2 \approx 20$ seconds; $H \approx 3200$ gauss; $H_1 \approx 1/30$ gauss; $dH/dt = 3$ gauss/second.

REFERENCES

1. Bloch, F., Phys. Rev., **70,** 1946, p. 460.
2. Bloembergen, N., Purcell, E. M. and Pound, R. V., Phys. Rev., **73,** 1948, p. 679.
3. Jacobsohn, B. A. and Wangness, R. K., Phys. Rev., **73,** 1948, p. 942.
4. Salpeter, E. E., Proc. Phys. Soc., **63A,** 1950, p. 337.
5. Portis, A. M., *Magnetic Resonance in Systems with Spectral Distributions*, A.R.D.C., 1955.
6. Feher, G., B.S.T.J., **36,** 1957, p. 449.
7. Redfield, A. G., Phys. Rev., **98,** 1955, p. 1787.
8. Wangness, R. K. and Bloch, F., Phys. Rev., **89,** 1953, p. 728.
9. Bloembergen, N., Shapiro, S., Pershan, P. S. and Artman, J. O., Phys. Rev., **114,** 1959, p. 445.
10. Pines, D., Bardeen, J. and Slichter, C. P., Phys. Rev., **106,** 1957, p. 489.
11. Portis, A. M., Phys. Rev., **91,** 1953, p. 1071.
12. Feher, G., Phys. Rev., **114,** 1959, p. 1219; Feher, G. and Gere, E. A., Phys. Rev., **114,** 1959, p. 1245.
13. Zener, C., Proc. Roy. Soc., **A137,** 1932, p. 696.
14. Gabillard, R., Comp. rend., **233,** 1951, p. 33.
15. Gordon, J. P. and Bowers, K. D., Phys. Rev. Letters, **1,** 1958, p. 368.
16. Abragam, A., to be published.
17. Jahnke, E. and Emde, F., *Tables of Functions*, Dover Publications, New York, 1945, p. 20.